Master's thesis

NTNU
Norwegian University of Science and Technology
Faculty of Engineering
Department of Marine Technology

Jon Magnus Moen

Automatic control with risk contingencies for autonomous passenger ferry

Master's thesis in Marine Technology
Supervisor: Roger Skjetne
Co-supervisor: Mathias Marley
June 2021

NTNU
Norwegian University of
Science and Technology

Jon Magnus Moen

Automatic control with risk contingencies for autonomous passenger ferry

Master's thesis in Marine Technology
Supervisor: Roger Skjetne
Co-supervisor: Mathias Marley
June 2021

Norwegian University of Science and Technology
Faculty of Engineering
Department of Marine Technology

NTNU
Norwegian University of
Science and Technology

NTNU Trondheim
Norwegian University of Science and Technology
Department of Marine Technology

MASTER OF TECHNOLOGY THESIS DEFINITION (30 SP)

Name of the candidate:	Moen, Jon Magnus
Field of study:	Marine cybernetics
Thesis title (Norwegian):	Automatisk styring med risikohåndtering for autonom passasjerferje
Thesis title (English):	Automatic control with risk contingencies for autonomous passenger ferry

Background

The milliAmpere demonstrator addresses development of novel methods to enable autonomous passenger transport in city water channels. This requires a high level of safety, including safe and comfortable vessel responses and anti-collision in a possibly crowded water channel. Hence, the ability to safely maneuver in a harbor is especially critical and involve complex maneuvering skills as well as contingency control modes in cases of emergency or conflict resolution.

When designing the control hierarchy of an autonomous passenger ferry, the designer must design based on a philosophy that worst case failures (WCFs) do happen. Software weaknesses and bugs will always exist, and faults and conflicting objectives will always occur. This can be solved by two methods: 1) designing with enough active redundancy to ensure that loss of active operating mode cannot happen for the defined WCFs, or 2) designing relevant submodes, called Minimum Risk Conditions (MRCs) that the autonomous vessel control system enter when exceeding its safe operating envelope.

In this project, we aim to describe the control system architecture, on a high level, for the milliAmpere application, define its normal autonomous control modes, and then also define a set of relevant MRCs. The MRCs should map events in the external environment (e.g. complex traffic situation) and/or events in the control system (e.g. failure of some function) to minimum risk contingency objectives. We consider then some of these MRCs to be realized as active safety control modes that the autonomous control system will enter if some supervisory function demands it.

The candidate should first propose an autonomous control system abstraction for milliAmpere, specifying the control system architecture (main subsystems and components – both shipboard and external functions), defining a set of normal control modes (NCMs), and finally defining and describing a set of relevant MRCs. Then the candidate should formulate a control problem involving some NCMs with some MRCs for a realistic operation. Based on this, the candidate should implement the NCMs and MRCs as separate control objectives, a mode-transition mechanism, and a supervisory function that commands transitions between the control modes. The results should be demonstrated by simulation for the milliAmpere vessel, where transitions from NCMs to MRCs occur with acceptable performance.

Scope of Work

1. Perform a background and literature review to provide information and relevant references on:
   - Autoferry project and milliAmpere demonstrator, incl. relevant situation awareness functions.
   - Autonomous ships and relevant specifications of Minimum Risk Conditions.
   - IMO and/or ISO standards or guidelines for autonomous ships.
   - Maneuvering control design for path-following.
   - COLREGs, and Control barrier Functions (CBFs) for collision avoidance.

   Write a list with abbreviations and definitions of terms and symbols, relevant to the literature study and project report.
2. Describe the autonomous control system architecture for milliAmpere, specifying the main subsystems and components of the autonomous control system, the software topology, and the communication channels for signals between the subsystems/components, considering both shipboard and external functions.
3. Propose relevant sets of NCMs and MRCs for milliAmpere. Perform a mapping, under each NCM, of (high-level) events in vessel systems or external conditions to activation of the MRCs.

4. Formulate a control problem involving some NCMs with some MRCs for a realistic operation, e.g. CBF-based auto-crossing with anticollision, and MRCs as contingency control modes due to CBF conflicts. Design and implement the NCMs and MRCs, a mode-transition mechanism, and a supervisory function that commands transitions between the control modes.
5. Using the milliAmpere simulation model as a case study, implement and demonstrate your solution, discuss resulting performance for various scenarios, and make conclusions.

Specifications

Every weekend throughout the project period, the candidate shall send a status email to the supervisor and co-advisors, providing two brief bulleted lists: 1) work done recent week, and 2) work planned to be done next week.

The scope of work may prove to be larger than initially anticipated. By the approval from the supervisor, described topics may be deleted or reduced in extent without consequences with regard to grading.

The candidate shall present personal contribution to the resolution of problems within the scope of work. Theories and conclusions should be based on mathematical derivations and logic reasoning identifying the steps in the deduction.

The report shall be organized in a logical structure to give a clear exposition of background, problem/research statement, design/method, analysis, and results. The text should be brief and to the point, with a clear language. Rigorous mathematical deductions and illustrating figures are preferred over lengthy textual descriptions. The report shall have font size 11 pts., and it is not expected to be longer than 70 A4-pages, 100 B5-pages, from introduction to conclusion, unless otherwise agreed. It shall be written in English (preferably US) and contain the elements: Title page, abstract, preface (incl. description of help, resources, and internal and external factors that have affected the project process), acknowledgement, project definition, list of symbols and acronyms, table of contents, introduction (project background/motivation, objectives, scope and delimitations, and contributions), technical background and literature review, problem formulation, method, results and analysis, conclusions with recommendations for further work, references, and optional appendices. Figures, tables, and equations shall be numerated. The original contribution of the candidate and material taken from other sources shall be clearly identified. Work from other sources shall be properly acknowledged using quotations and a Harvard citation style (e.g. natbib Latex package). The work is expected to be conducted in an honest and ethical manner, without any sort of plagiarism and misconduct, which is taken very seriously by the university and will result in consequences. NTNU can use the results freely in research and teaching by proper referencing, unless otherwise agreed.

The thesis shall be submitted with an electronic copy to the main supervisor and department according to NTNU administrative procedures. The final revised version of this thesis definition shall be included after the title page. Computer code, pictures, videos, dataseries, etc., shall be included electronically with the report.

Start date: 15 January, 2021 **Due date:** As specified by the administration.

Supervisor: Roger Skjetne
Co-advisor(s): Mathias Marley (on CBF theory in particular)

Signatures:

Roger Skjetne

Digitally signed by Roger Skjetne
Date: 2021.05.03 13:59:11
+02'00'

Preface

This thesis concludes my master's degree in marine cybernetics at the Norwegian University of Science and Technology (NTNU), and is written during the spring of 2021. It is the result of five years of studies that have given me knowledge within marine technology in general and especially marine cybernetics. The subject of research is the automatic control of an autonomous passenger ferry with risk contingencies, which make the system able to handle situations outside normal operation.

The work has been performed in the following way. Firstly, necessary background knowledge was acquired. This was partly done through the work with my project thesis (Moen, 2020). Then, a basic control system for an autonomous passenger ferry was developed, together with a simulator for testing. This platform was developed further during the first months of the master thesis period. In parallel, research was done on the state of risk-mitigating control systems, and ideas for minimum risk conditions for milliAmpere were formulated. After a nominal control system with satisfactory performance was completed, the work continued with theoretical design and implementation of a supervisory switching algorithm to mitigate risk in emergency scenarios. Multiple alternatives were explored before the most promising were tested through simulations. This produced the results shown at the end of this thesis.

I would not have been able to achieve the results presented here by myself. The nominal control system has been developed in collaboration with both my co-supervisor Mathias Marley and Nora Åsheim, who has more competence within this field than I. This made me able to focus more on the main part of my thesis: control in emergency situations. When it comes to the supervisory switching algorithm for selecting which mode to operate in, the ideas have come through good discussions with my supervisors Roger Skjetne and Mathias Marley.

Jon Magnus Moen
Trondheim, June 9, 2021

Acknowledgments

My supervisor Professor Roger Skjetne and co-supervisor Mathias Marley have provided valuable guidance during the work with this thesis. Roger has been of great help with understanding the problem at hand, and Mathias has given good, detailed help when required. I want to thank them for their guidance and contributions through the whole period. Additionally, I would like to thank Nora Åsheim for her help and good discussions regarding obstacle avoidance in control systems. Thanks also to my friend Brynhild Igland for help with proofreading the thesis and valuable input on structuring.

This work has been performed on campus Tyholt on NTNU, where I have shared an office with four fellow students. This has been a productive environment for me and helped me keep my spirits high when the work was difficult. I would therefore like to thank the boys of office C1.062 for the good discussions, pool matches, and long days of work. It is always easier to do things together, and this has shown to be true also for writing a master thesis. I am also very grateful for all the friends I have gotten through my 5 years at NTNU. Lastly, I would like to thank my family for the support which has made me able to complete this degree.

Abstract

The development of autonomous ships has accelerated in the last years, with multiple trials of such vessels underway. A relevant application for this technology is passenger ferries used for crossing urban waterways. This thesis proposes an automatic control system with risk contingencies for use on an autonomous passenger ferry. This includes guidance and control modes for all phases of nominal operation, as well as for emergency modes. Minimum risk conditions (MRCs) are used to mitigate risk in emergencies. A mode supervisor is used for determining which mode to operate in.

The case study in this thesis is the milliAmpere experimental platform, a prototype of an autonomous, all-electric passenger ferry. A set of MRCs is proposed for the operation of such a ferry, together with relevant causes for the use of these. Additionally, risk-influencing factors are discussed to give an impression of what may introduce risk into the operation of a ferry like milliAmpere. To be able to develop a sufficiently detailed control system, two MRCs are selected for detailed implementation in a simulation study: crash stop and evasive maneuver. The functionality of the total system is tested through a series of simulations. The simulations show satisfactory performance of both the nominal control system, as well as the mode supervisor including selection of the best MRC mode.

To be able to operate autonomously, the system must have a method of deciding which mode is best suited given the circumstances. This is solved through a mode supervisor. It takes in all available information and decides which mode is the best based on certain criteria. For emergency situations where collision is imminent, two indicator functions for selecting the best MRC are proposed. The first compares the necessary maneuver with the limitations of the vessel to find the mode that is most probable of success. The second utilizes a new way of quantifying an estimate of collision risk through a risk function to determine which mode is the safest. Alternative methods that are not studied in detail in this thesis are also discussed, to provide a perspective on other solutions to the supervising problem.

Furthermore, all modes are detailed into guidance- and control laws. In nominal operation, a two-parameter guidance function is used in the undocking- and crossing modes. Here, a control barrier function (CBF) is used to ensure that the path is safe, and make alternations to the path to avoid obstacles. The docking mode is divided into two phases where the first take the vessel to a point outside the docking location while ensuring that the heading is normal to the dock. Then the second phase consists of moving the vessel in a slow, controlled manner toward the dock before arriving at a docked position. For all modes of nominal operation, a backstepping controller is used to control the vessel according to the desired position and heading.

For the two MRC-modes selected for implementation in the simulation study, guidance and control have been implemented in a simple manner to show how such modes would work. Here, PID controllers are used to achieve the desired position and heading. In crash stop, the objective is to stop as soon as possible while keeping the heading constant. During an evasive maneuver, the guidance function provides a heading and speed reference signal that takes the vessel into a hard turn and reduces the speed such that the vessel is at rest at the end of the maneuver. After completion of the two MRCs considered for imminent collision (crash stop /evasive manuever), the system enters another MRC; dynamic positioning mode. The vessel then maintains its position until operation can be restarted.

Sammendrag

Utviklingen av autonome skip har skutt fart de siste årene, med flere prøveprosjekter for slike skip på vei. Et relevant bruksområde for denne teknologien er passasjerferger for bruk til kryssing av urbane vannveier som kanaler og elver. Denne oppgaven foreslår et automatisk kontrollsystem med risikohåndtering for bruk på en autonom passasjerferge. Dette inkluderer funksjoner for guiding og kontroll for alle faser av normal operasjon, i tillegg til nødmoduser. Minste-risiko-tilstander (MRT-er) er brukt for å minimere risikoen i nødstilfeller. En modusveileder brukes for å bestemme hvilken modus som skal brukes.

Eksempelstudiet i denne oppgaven er milliAmpere, som er en prototype av en autonom, elektrisk passasjerferge. Denne brukes som eksperimentell plattform for forskning på denne typen fartøy. Et sett med MRT-er er foreslått for operasjonen av en slik ferge, sammen med relevante årsaker til bruk av disse. I tillegg, så er risikopåvirkende faktorer diskutert for å gi et inntrykk av hva som kan introdusere risiko i operasjonen av en ferge som milliAmpere. For å være i stand til å utvikle et detaljert nok kontrollsystem, så er to MRT-er er valgt ut for detaljert implementasjon og testing i en simuleringsstudie: full stopp og unnamanøver. Funksjonaliteten til det totale systemet er testet i en rekke simuleringer. Simuleringene viser tilfredsstillende ytelse for både det nominelle kontrollsystemet, og modusveilederen som velger den beste MRT-modusen.

For å være i stand til å operere autonomt så må systemet være i stand til å bestemme hvilken modus som passer best, gitt omstendighetene. Dette er løst gjennom en modusveileder. Dette er en funksjon som tar in all tilgjengelig informasjon og bestemmer hvilken modus som er best basert på visse kriterier. For nødstilfeller der kollisjon er nært forestående så er det foreslått to indikatorfunksjoner for å velge den beste MRT-modusen. Den første sammenligner den nødvendige manøveren med begrensningene til fartøyet for å finne modusen som har størst sannsynlighet for å lykkes. Den andre bruker en ny måte å kvantifisere et estimat av kollisjonsrisiko ved bruk av en risikofunksjon til å bestemme hvilken modus som er sikrest. Alternative metoder som ikke er undersøkt nærmere er også diskutert, for å gi et perspektiv på andre mulige løsninger.

Alle moduser er spesifisert og implementert til guiding- og kontrollfunksjoner. I normal operasjon ved kryssing og avgang fra kai, så brukes en guidefunksjon der banen er parametrisert av to parametere. Her blir en kontrollbarrierefunksjon brukt til å forsikre at banen er sikker, og gjøre endringer på banen for å unngå hindre. Kaileggingsfasen er delt inn i to faser der den første tar fartøyet til et punkt utenfor kaien mens fartøyet har kurs normalt på kaien. Den andre fasen består da av å flytte fartøyet sakte og kontrollert mot kaien før det stopper en bestemt avstand fra kaikanten. I alle de tre fasene av normal operasjon så benyttes en *backstepping*-kontroller til å styre fartøyet i henhold til ønsket posisjon og kurs.

For de to MRT-modusene som er valgt til implementasjon i simuleringsstudiene, så har guiding- og kontrollfunksjonene blitt implementert på en enkel måte for å vise hvordan disse modusene vil være. Her brukes en PID-kontroller til å oppnå ønsket posisjon og kurs. I en full stopp-manøver så er målet å stoppe så fort som mulig mens kursen holdes konstant. Under en unnamanøver så kalkulerer guidingsfunksjonen en kurs- og hastighetsreferanse som endres slik at fartøyet tar en hard sving og senker farten slik at det står stille ved endt manøver. Etter begge de to MRT-modusene så går systemet inn i en ny MRT; dynamisk posisjonering. Fartøyet holder da posisjonen til operasjonen kan startes på nytt.

Contents

List of Tables

List of Figures

Abbreviations

ASV	=	autonomous surface vessel
CBF	=	control barrier functions
CLF	=	control Lyapunov function
COLAV	=	collision avoidance
COLREG	=	Convention on the International Regulations for Preventing Collisions at Sea
DOF	=	degree of freedom
DP	=	dynamic positioning
FTC	=	fault-tolerant control
GNC	=	guidance, navigation and control
GNSS	=	global navigation satellite system
IMO	=	International Maritime Organization
IMU	=	inertial measurement unit
LIDAR	=	light detection and ranging
MASS	=	maritime autonomous surface ships
MRC	=	minimum risk condition
NCM	=	normal control mode
NED	=	north-east-down
NTNU	=	Norwegian University of Science and Technology
OS	=	own ship
P	=	port
PID	=	proportional-integral-derivative
QP	=	quadratic programming
RF	=	risk function
RIF	=	risk influencing factor
RoRo	=	roll on, roll off
SA	=	situational awareness
SB	=	starboard
TS	=	target ship
WCF	=	worst case failure
WP	=	waypoint

Chapter 1

Introduction

This chapter presents the motivation for the thesis in light of recent developments in the field of autonomy. The objective, scope, contributions and outline of the thesis is also defined.

1.1 Motivation

In the last decade, a lot of attention has been directed to the advent of autonomous ships. For a while, it was only the subject of researchers, but in recent years a couple of commercial projects have been launched. An example is the *Yara Birkeland*, which is intended to be an autonomous container feeder vessel traveling autonomously between two ports in Eastern Norway. The vessel has finished construction, but it is still unclear when it will be put into autonomous operation as the project has experienced some challenges and delays. Additionally, similar projects as ASKOs RoRo (roll-on, roll-off) drones which will carry semi-trailers across the Oslofjord have been launched. The concept for these can be seen in Figure 1.1b.

Autonomous vessels might have even bigger potential at a smaller scale, with shorter distances and more specialized operation patterns. This is the basis of *Zeabuz*, a start-up from the Norwegian University of science and technology (NTNU) research community that aims to make emission-free, autonomous passenger ferries a reality. These will be operated in urban waterways and thus provide a less intrusive and cheaper alternative to building bridges (Zeabuz, N.D.a). A concept drawing is shown in Figure 1.1a. The concept has been researched by the Autoferry project[1] at NTNU, which will be introduced more thoroughly in Section 2.11. Here, real-world experiments have been performed on a 5-meter long concept vessel named *milliAmpere*. Last December, this research community performed a 3-hour experiment where the ferry operated autonomously for the whole experiment (Zeabuz, 2020). Various obstacles were introduced, and the system performed well. Zeabuz will design and launch the first ferry system in 2022 (Zeabuz, N.D.b).

Although the development of autonomous ships and passenger ferries is well underway, there are still areas where more research is needed. An example of this is safety and safety assurance. Up until now, most research has been directed to nominal operation, e.g. docking, crossing, collision avoidance, etc. However, an aspect that is proving to be very important as well, is the safety of these systems

[1] https://www.ntnu.edu/autoferry

(a) Zeabuz' concept for urban passenger ferry. Courtesy of Zeabuz

(b) Asko's autonomous ferry for fjord crossings. Courtesy of Asko

Figure 1.1: Autonomous concepts

when unforeseen events, faults, and failures occur. That autonomous systems perform well in these kinds of situations is extremely crucial if the adoption of autonomous vessels is to be widespread. The autonomous control systems must perform as well as conventional ship systems with a captain at the wheel. The hope is that they will be even better, such that the number of accidents is reduced. To reach this point, two main things must be accomplished:

- Technical safety must be ensured. This means developing the algorithms and methods that will ensure the safety of the system at all times.
- Perceived safety must be ensured. This means convincing users, authorities, and other stakeholders that the system is indeed safe. This might be harder to solve.

1.2 Objective

This master thesis aims to contribute to reaching technical safety of autonomous vessels. The objective is to develop, implement and test a control system for an autonomous passenger ferry. This control system should incorporate both normal operation modes and emergency modes through the use of minimum risk conditions (MRCs). The nominal control system should be able to perform a nominal operation from start to finish with sufficient performance. This includes collision avoidance functionality. In emergency modes, the control system should be able to reach the control objective of the MRC that is specified, such that risk is minimized. The system must have a good method of choosing which MRC to enter, based on the current state of the vessel and surroundings. Furthermore, the system should be tested through appropriate simulations to assure that the behavior is as intended. Finally, the thesis aims to provide a good discussion regarding the implementation of MRCs in control systems - both on the solutions chosen here, but also other possible solutions that are not pursued further.

1.3 Scope

The scope of work in the thesis is to:

- Perform a background and literature review on:
  - Autoferry and milliAmpere

  - Autonomous ships and minimum risk conditions
  - Standards and guidelines for autonomous ships
  - Maneuvering control and guidance designs
  - Collision regulations and collision avoidance methods
- Describe the control system for the case study vessel milliAmpere
- Propose nominal and emergency modes for milliAmpere and describe the scenarios where these are used
- Formulate a control problem for a realistic operation of milliAmpere which includes collision avoidance and contingency handling functionality
- Design and implement a control system that solves the control problem. When feasible, base this existing work done by others
- Show the performance of the system through simulation of different scenarios.

1.4 Contributions

As far as the author is aware, this is the first publication that details the use of MRCs in a control system for ships together with autonomous switching to these. The novelty includes a method of selecting the best MRC of the ones available, given a situation where an autonomous surface vessel (ASV) is about to collide with a stationary obstacle. Additionally, the selected MRCs are detailed into guidance and control modes, which are implemented. The functionality is verified through simulations in MATLAB. The novel supervisor algorithm is used together with a nominal control system based on control barrier functions. A set of MRCs suitable for the operation of an autonomous passenger ferry is also proposed, followed by a discussion on risk influencing factors that may lead to activation of MRCs.

1.5 Thesis outline

The structure of the thesis is as follows. Chapter 2 contains the theoretical background of the work in this thesis, along with a literature review of existing work relevant to this thesis. Chapter 3 contains a definition of different control modes relevant to the operation of milliAmpere, along with a discussion of when each mode is suitable, together with a disucssion on risk influencing factors for the operation. Then, Chapter 4 is a formulation of the control problem to be solved by the autonomous control system. Chapters 5, 6 and 7 contains detailed descriptions of the proposed mode supervisor, guidance system, and control system, respectively. Together, the proposed system should solve the control problem that is stated. Following up on this, simulation scenarios to show this are presented in Chapter 8, together with the simulation setup. The results from these simulations are in Chapter 9. Lastly, the results are discussed in Chapter 10, before a conclusion is made in Chapter 11. Proposals for further work are also given here.

Chapter 2

Technical background and literature review

This chapter provides background information and relevant references on subjects important to the subject of an autonomus passenger ferry. This includes: guidance and control functions for autonomous ships, rules and regulations, collision avoidance, minimum risk condition, fault-tolerant control, and the Autoferry project.

2.1 Vessel model

In this section, a vessel model for a 3 degrees-of-freedom (DOF) surface ship will be defined. Here, the DOFs considered are surge, say and yaw. Before this is done, some notations have to be defined. In this thesis, two reference frames are used. The North-East-Down (NED) frame and the BODY frame. For a 3DOF model, the notation follows what is common in the literature, as defined in SNAME (1950). The definition can be found in Table 2.1. Following this definition, the position and velocity vectors are defined as $\boldsymbol{\eta} = \begin{bmatrix} x & y & \psi \end{bmatrix}^\top$ and $\boldsymbol{\nu} = \begin{bmatrix} u & v & r \end{bmatrix}^\top$, respectively.

Table 2.1: Notation, as defined by SNAME (1950)

DOF	Velocities (BODY)	Forces and moments (BODY)	Position (NED)
Surge	u	X	x
Sway	v	Y	y
Yaw	r	N	ψ

Then, a control design model can be defined. The following model is a simplified model defined by Fossen (2021) and is a good representation of the equations of motion of a 3DOF marine craft that is not affected by environmental forces:

$$\begin{aligned} \dot{\boldsymbol{\eta}} &= \mathbf{R}(\psi)\boldsymbol{\nu} \\ \mathbf{M}\dot{\boldsymbol{\nu}} + (\mathbf{C} + \mathbf{D})\boldsymbol{\nu} &= \boldsymbol{\tau}. \end{aligned} \tag{2.1}$$

Here, the following matrices and vectors are used:

- **M** is the inertia matrix

$$\mathbf{M} = \begin{bmatrix} m - X_{\dot{u}} & 0 & 0 \\ 0 & m - Y_{\dot{v}} & -Y_{\dot{r}} \\ 0 & -Y_{\dot{r}} & I_z - N_{\dot{r}} \end{bmatrix} \tag{2.2}$$

- **C** is the Coriolis matrix

$$\mathbf{C} = \begin{bmatrix} 0 & 0 & Y_{\dot{v}} v + Y_{\dot{r}} r \\ 0 & 0 & -X_{\dot{u}} \\ -Y_{\dot{v}} v - Y_{\dot{r}} r & X_{\dot{u}} u & 0 \end{bmatrix} \tag{2.3}$$

- **D** is the damping matrix

$$\mathbf{D} = -\begin{bmatrix} X_u & 0 & 0 \\ 0 & Y_v & Y_r \\ 0 & N_v & N_r \end{bmatrix} \tag{2.4}$$

- $\mathbf{R}(\psi)$ is the rotation matrix

$$\mathbf{R}(\psi) = \begin{bmatrix} \cos\psi & -\sin\psi & 0 \\ \sin\psi & \cos\psi & 0 \\ 0 & 0 & 1 \end{bmatrix} \tag{2.5}$$

- $\boldsymbol{\tau} = \begin{bmatrix} X & Y & N \end{bmatrix}^\top$ is the forces and moment acting on the vessel.

The hydrodynamic parameters that are the elements of these matrices will be presented later. For starboard-port symmetrical vessels such as the one considered in this thesis, the symmetry leads to a decoupling of DOFs such that surge is uncoupled with sway and yaw motion.

2.2 Maneuvering control designs

For maneuvering operations, several different control designs are used. For this literature review, a couple of them will be summarized in short.

2.2.1 PID-controllers

The proportional–integral–derivative (PID) controller is one of the classic controllers, and still in use in many applications. It was proposed in 1922 by Nicholas Minorsky and was adopted for applications in the 1930s and -40s (Bennett, 1996). PID controllers were also used in the first maritime control systems, the early versions of dynamic positioning (DP) systems that were tested in the 1960s (Paulsen, 2019). With a control design model as in equation 2.1, the generalized control forces can be computed as (Fossen, 2021):

$$\boldsymbol{\tau}_{PID} = -\mathbf{K}_p \tilde{\boldsymbol{\eta}} - \mathbf{K}_d \dot{\boldsymbol{\eta}} - \mathbf{K}_i \int_0^t \tilde{\boldsymbol{\eta}}(\tau) d\tau. \tag{2.6}$$

Here $\tilde{\boldsymbol{\eta}} = \boldsymbol{\eta} - \boldsymbol{\eta}_d$ is the position deviation. The controller gains $\mathbf{K}_p, \mathbf{K}_d, \mathbf{K}_i > \mathbf{0}$ are gain matrices that decide the weighting of the different terms for each DOF. They can be computed by pole-placement algorithms, (for details, refer to Fossen (2021)) or tuned manually. Among the relevant controller designs for marine applications, PID controllers are the easiest to tune.

2.2.2 Backstepping-controllers

Another control design used for maneuvering purposes is backstepping controllers. This is done by recursive construction of a control Lyapunov function (CLF). It is related to the method of feedback linearization but more flexible. It allows the designer to exploit some linearities while canceling others, thus leading to more robustness in the controller. This is, for example, presented in Fossen (2021) and Skjetne (2020c). However, backstepping controllers need a relatively precise model of the system to effectively cancel out unwanted nonlinearities. A cascaded backstepping design such as the one presented in Skjetne (2020c) is applied for docking in Gauslaa (2020) and maneuvering in Jensen (2020). Here, the control is designed for two subsystems: $\eta \to \eta_d$ and $\nu \to \alpha_1$, where α_1 is a virtual control in the first subsystem. To prove stability, this method relies on cascaded systems theory. The design can be applied to desired paths parametrized by one or two path variables, and the controller is tuned by two gain matrices, $\mathbf{K}_1$ and $\mathbf{K}_2$.

2.3 Maneuvering guidance designs

The following section presents guidance function designs relevant to the application in this thesis. Here, it is assumed that the objective is to create a path between two or more waypoints (WPs) $\mathbf{p}_1, \mathbf{p}_2, \ldots, \mathbf{p}_n$.

2.3.1 One-variable parametrization

To create a straight line between the two points, the desired position can be expressed using a scalar path variable $s_1 \in [0, 1]$ (Marley, 2021):

$$\mathbf{p}_d(s_1) := (1 - s_1)\,\mathbf{p}_1 + s_1 \mathbf{p}_2. \tag{2.7}$$

Then, the speed along the path can be controlled by a speed assignment $v_1(s_1)$, and setting $\dot{s_1} = v_1(s_1)$. This can for example be set to a constant reference speed, or to use a hyperbolic tangent function to create a smooth increase and decrease in speed at the beginning and end of the path.

2.3.2 Two-variable parametrization

When it is desirable to leave the straight line between the path, another path parameter $s_2 \in \mathbb{R}$ can be used. The path parameter vector is $\mathbf{s} = \begin{bmatrix} s_1 & s_2 \end{bmatrix}^\top$. Then, by using the tangent vector $\mathbf{T}$ between the points and the normal vector $\mathbf{N}$, the desired path can be expressed as Marley (2021):

$$\mathbf{p}_d(\mathbf{s}) := \mathbf{p}_1 + L\left(s_1 \mathbf{T} + s_2 \mathbf{N}\right), \tag{2.8}$$

where $\mathbf{L} := |\mathbf{p}_2 - \mathbf{p}_1|$. For $s_2 = 0$, this gives the same result as Equation 2.7. For other cases, the value of s_2 determines how far from the straight-line path the desired path is. The geometry of this parametrization is shown in Figure 2.1. A speed assignment is used also for the normal path variable, such that $\dot{s}_2 = v_2(\cdot)$. This can for example be determined based on if there are obstacles in the way such that the straight-line path is not feasible.

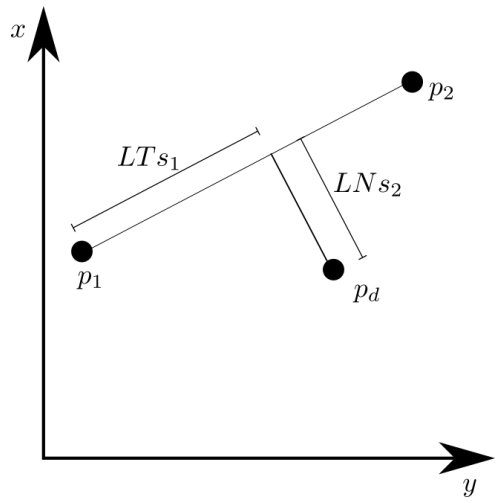

Figure 2.1: Construction of the desired position based on two path parameters

2.3.3 Path generation

In many situations, there are more than two WPs, and it is desired to create a smooth path between these. Chapter 12.3 in Fossen (2021) summarizes how to use straight lines together with inscribed circles. This is relatively simple to do but results in a jump in the desired yaw rate during the transition from line to arc. The shortest way between two poses was proved by Dubins (1957), which in summary means that: "The shortest path (minimum time) between two poses (x_i^n, y_i^n, ψ_i) and $(x_{i+1}^n, y_{i+1}^n, \psi_{i+1})$ of a craft moving at constant speed U is a path formed by straight lines and circular arc segments" (Fossen, 2021, p. 329).

To ensure continuity also in the desired heading (and higher-order derivatives), spline interpolation can be used. For example, Knædal (2020) uses a septic Bézier curve to interpolate the path, which results in $\mathcal{C}^3$ continuity. It is also possible to use cubic interpolation techniques, as shown by for example Lekkas (2014). However, this does not achieve as high a degree of continuity as with the septic Bézier curve and lacks continuity in curvature. A hybrid path parametrization can also be used, as presented in Skjetne (2005). This divides the overall path into path segments between each of the WPs. These segments are constructed as polynomials of a desired order r, where demands for the values at each WP where the segments are concatenated give a set of equations to find the overall coefficients.

2.4 Autonomous docking and departure

This section is adapted from Moen (2020). When docking with ships, two main methods are common when not assisted by tugs and anchors (Murdoch et al., 2012): port side docking and docking with thrusters. Port side docking uses only the rudder and main propeller to approach the quay at an angle and stop while simultaneously using the astern force from slowing down to rotate the ship parallel to the dock. Docking with thrusters is done by moving the ship to a position just outside the quay, with heading parallel to the quay. Then, thrusters are used to produce a lateral force and move the ship in sway towards the dock.

An additional and somewhat specialized case is that of a docking car ferry. RoRo ferries, such as the ones common in Norwegian fjords, have specialized docks, called linkspans, with a ramp in the front for

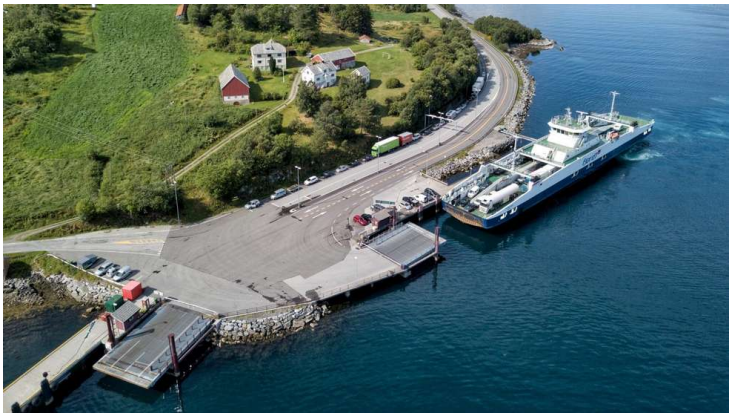

Figure 2.2: Example of a ferry linkspan. Image courtesy of Møre-Nytt.

cars and a quay on one of the sides. An example of this can be seen in Figure 2.2. The car ferry is in other words docking with the bow/stern and one of the sides simultaneously. This method is also used by many passenger ferries and other vessels where the berthing period is short.

Independent of the docking method, some principles are important. Murdoch et al. (2012) defines the most important rules as:

- Slow speed
- Controlled approach
- Planning
- Teamwork
- Checking equipment

For an ASV, the two first are the most important to follow, and the third is a prerequisite for autonomous operation. The desired behavior must be implemented in a control system to ensure that it is slow and controlled. This might require some different parameters compared to other operating phases, such as maneuvering.

2.4.1 Relevant environmental effects

When docking a vessel, multiple environmental effects can impact the operation. Firstly, wind forces may cause the vessel to drift, especially in beam wind. It can also affect the heading of the vessel, depending on the wind direction. A robust controller for autonomous docking should therefore take wind forces into account. Secondly, current can affect docking in various ways. Current from ahead slows the ship down while current from aft can increase the speed, making it harder to slow down and decrease the effect of rudders/thrusters. Side currents can cause the vessel to drift out of course.

Additionally, hydrodynamic effects because of the proximity to land and harbor structures, as well as shallow water depth and varying bottom conditions are also factors. In shallow water, the resistance on a ship increases due to changes in the wave pattern (Koushan, 2017). Additionally, the maneuverability and turning ability can be reduced, according to Murdoch et al. (2012). In channels and canals, the water depth may also vary. There are often banks so that the water is shallow in some places and deeper in others. This makes the aforementioned effects vary during the crossing and thus harder to account for.

2.4.2 Docking with thrusters

The master thesis of Gauslaa (2020) proposes a guidance-, navigation- and control (GNC)-system for the docking of a ship. Here, a docking in sway is used, where the ship moves to a position a bit outside the quay and uses the thrusters to move sideways to the dock. The method consists of two phases:

- **Phase 1:** Bring the ship from its initial position in proximity of the dock to a position aligned outside its designated docking spot, parallel to the dock.
- **Phase 2:** Bring the ship in sway towards the quay in a controlled fashion, stopping at a desired distance from the dock. This should be done at low speed and with a heading parallel to the quay.

For Phase 1, path planning is done by placing 4 waypoints (WPs) in addition to the initial position, according to following expressions:

$$p_4 = p_{dock} + \mathbf{R}_2^\top(\phi_{dock}) \begin{bmatrix} 0 \\ d_{ph1} \end{bmatrix}, \tag{2.9a}$$

$$p_3 = p_4 + \mathbf{R}_2^\top(\phi_{dock}) \begin{bmatrix} d_{tang} \\ 0 \end{bmatrix}, \tag{2.9b}$$

$$p_2 = p_3 + \mathbf{R}_2^\top(\phi_{dock}) \begin{bmatrix} c_{2,x}\Delta_x \\ c_{2,y}\Delta_y \end{bmatrix}, \tag{2.9c}$$

$$p_1 = p_3 + \mathbf{R}_2^\top(\phi_{dock}) \begin{bmatrix} c_{1,x}\Delta_x \\ c_{1,y}\Delta_y \end{bmatrix}, \tag{2.9d}$$

$$p_0 = \begin{bmatrix} x_0 \\ y_0 \end{bmatrix}. \tag{2.9e}$$

The symbols are as defined in Table 2.2 with values proposed in Gauslaa (2020). The procedure ensures a path that in the last waypoint has a normal vector perpendicular to the dock by placing p_3 the same distance from the dock as p_4. The two other waypoints, p_1 and p_2, are placed using coefficients $c_{i,x}$ and $c_{i,y}$ that are multiplied by longitudinal and lateral distance between initial and final position, Δx and Δy. These are defined in the local coordinate system where the x-axis is parallel to the dock. The rotational matrix $\mathbf{R}_2^\top$ ensures that the path planning also works if the dock has an angle offset ϕ_{dock} relative to the global coordinate system. An example of a path planned by the proposed algorithm is shown in Figure 2.3. In Gauslaa (2020), this path planning algorithm is combined with a hybrid path parametrization for path generation. This ensures a smooth path is produced from the waypoints.

2.4.3 Ferry docking

In recent years, more and more automatic functions have been built into ferries, as with other types of vessels. Ferries typically traffic the same waters every time and are therefore suitable for automation of the operation. At the time of writing, both Wärtsilä and Kongsberg have shown successful trials of

Table 2.2: Definition of symbols

Parameter	Definition	Value
d_{ph1}	Distance from dock to p_4	$3B$
d_{tang}	Distance from p_3 to p_4	$0.75L$
$c_{1,x}$	Distance coefficient in x for p_1	0.66
$c_{1,y}$	Distance coefficient in y for p_1	0.33
$c_{2,x}$	Distance coefficient in x for p_2	0.66
$c_{2,y}$	Distance coefficient in y for p_2	0.10

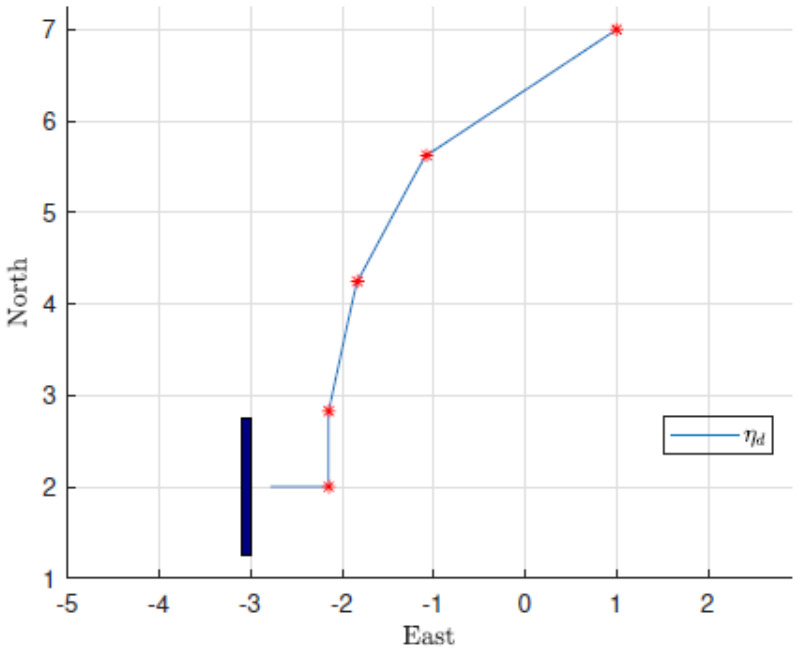

Figure 2.3: Path planned by the proposed path planning algorithm. Courtesy of Gauslaa (2020)

full-scale ferries docking automatically (Austin (2020); Wärtsilä (2018)). Additionally, experiments and research have been conducted in the Autoferry project with milliAmpere as the experimental platform.

For example, Bitar et al. (2020) proposes an optimal control problem (OCP)-based trajectory planner tested on milliAmpere, specialized in the docking phase. This means formulating the trajectory planning as an optimization problem. The trajectory is planned with a horizon of 120 seconds. Here, the trajectory planner works together with a PID controller for DP in a hybrid structure. This makes it possible to run the trajectory planner at a low rate, and let the controller handle the dynamics in between planning steps. The results of the experiments are promising, but it is concluded that the controller does not behave optimally, and thus the result could be better with a controller tuned and designed for the purpose. In this paper, the vessel is docked only with the bow, thus neglecting the effect of the side quay. This is sufficient as the speed during the docking phase is so low that the risk for a hard collision can be considered low. However, this should be investigated further to ensure passenger safety.

2.4.4 Undocking/departure

When a vessel shall embark on a journey from a docked position, it is departing. This can be seen as the opposite of the docking operation. It is also performed in the same surroundings. Therefore, the environmental effects can be assumed to be the same. The undocking phase is not discussed much in literature, but it is common to apply the same principles as when docking. The motion shall be in a slow, controlled manner until the vessel is sufficiently clear of the dock and other obstructions.

2.5 Fault-tolerant control

When designing a control system for use in real life, it is important to assure that the system is fault-tolerant. On this subject, a few definitions are necessary.

Definition 2.1. ***Fault - (Blanke et al., 2016).*** *A fault is something that changes the behavior of a system such that the system no longer satisfies its purpose.*

This is in everyday language and the literature used interchangeably with failure. In this thesis, the two are differentiated. A failure is defined as:

Definition 2.2. ***Failure - (Blanke et al., 2016).*** *A failure describes the inability of a system or component to accomplish its function. The system or component has to be shut off because the failure is an irrecoverable event.*

These two definitions are further used to define fault-tolerant control (FTC) as follows:

Definition 2.3. ***Fault-tolerant control - (Blanke et al., 2016).*** *To avoid production deterioration or damage to machines and humans, faults have to be found as quickly as possible and decisions that stop the propagation of their effects have to be made. These measures should be carried out by the control equipment to make the system fault-tolerant. If they are successful, the system function is satisfied also after the appearance of a fault, possibly after a short time of degraded performance in which the control algorithm adapts to the faulty plant. Thus, the fault-tolerant control has to prevent a component fault from causing a failure at the system level.*

Within the literature, fault-tolerant control is studied to increase the safety, availability, and reliability of systems. Blanke et al. (2016) gives an in-depth description of all parts of FTC, including analysis of systems, fault diagnosis, fault accommodation, and reconfiguration methods. Here, different types of fault tolerance are defined:

- *Passive fault tolerance* means making the control law fulfill the objective even when faults occur. This is usually associated with a very low level of performance and is a conservative approach.
- *Active fault tolerance* is divided into *fault accommodation* and *system reconfiguration*. Fault accommodation is used when some knowledge of the fault impact is available, so a set of constraints can be computed to solve the control problem. The objective is the same as for the healthy system. System reconfiguration is used when the faulty system is unknown, so the only solution is to switch off faulty components and try to achieve the objectives using the healthy components.

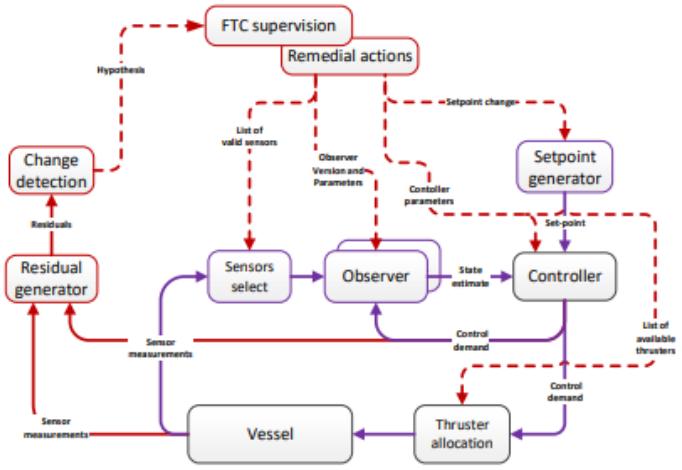

Figure 2.4: Fault tolerant control architecture as presented in Blanke and Nguyen (2018).

- *Supervision* can be used when no solution exists for other methods, such that the original objective can not be achieved. Supervision means changing the objective for the system. This can either be chosen from a set of objectives based on the system properties or decided by operators.

The type of fault tolerance to be used depends on the system. Passive fault tolerance is used where robustness is very important, and performance is of lower priority. If performance is more important, the two other methods are preferable.

The application of fault-tolerant control is presented in various papers. For example, Blanke and Nguyen (2018) presents a fault-tolerant position mooring control for offshore vessels. This is based on a control architecture which in addition to the traditional blocks for such a guidance, navigation and control (GNC) system also contains a setpoint generator, a residual generator, a change detector, an FTC supervisor, and a remedial actions function block. This architecture is shown in Figure 2.4. The FTC supervisor is the center of this architecture, and it is an example of fault tolerance through supervision. It keeps an account of the state of sensors, actuators, and system parameters. Based on this information it can ensure that only components and signals that are healthy are used in the control of the vessel. The system is tested by simulations and experiments where the following cases were tested: line breakage, slow drift in measurements, measurement jumps, and thruster failures. For all cases, the results show improvement over the system without FTC.

In Yang et al. (2012), an architecture without the supervisor to find the correct controller is proposed. Instead, a switching algorithm is used to sequentially switch controllers. This way, a series of unstable modes are activated one by one until a stable mode is activated. This introduces instability in the system, but overall stability is guaranteed if the activation periods of the stable modes are long enough compared to those of unstable modes. It is also preferable to go through as few unstable modes as possible. Therefore, the optimal switching sequence is calculated based on a control cost function to minimize the number of unstable controllers to be activated. The method used in this paper eliminates the need for individual fault detection and isolation, although to the cost of periods of instability in the transient phase where the controllers are switched. This a type of active fault tolerance, where the system is changed after an unstable mode has been encountered, to arrive at a stable mode again.

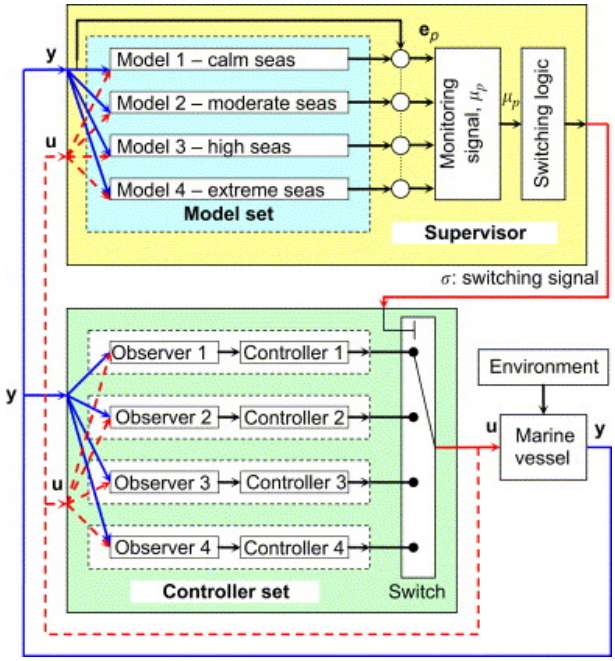

.

Figure 2.5: Concept of hybrid control system, courtesy of Nguyen et al. (2007)

2.6 Hybrid control

The idea of hybrid control is to be able to switch between controllers automatically. Also here, a supervisor is needed to determine which controller is used. Additionally, a set of controllers, also called the controller bank is included in the system. This type of system can be seen in Figure 2.5. In Nguyen et al. (2007), this principle is used to design a hybrid controller for calm to extreme sea conditions. Two different PID controllers are used, made for calm/moderate seas and extreme seas, respectively. In the transition between moderate and extreme seas (high seas), the two are combined through a weighting function such that:

$$\widehat{\boldsymbol{\tau}}_{q3} = \alpha_1 \left(\widehat{\omega}_p\right) \widehat{\boldsymbol{\tau}}_{q2} + \alpha_2 \left(\widehat{\omega}_p\right) \widehat{\boldsymbol{\tau}}_{q4}, \tag{2.10}$$

where $\widehat{\boldsymbol{\tau}}_{qi}$, is the control force from each controller while α_i is the weighting functions as functions of the estimated peak frequency of waves $\widehat{\omega}_p$. The weighting functions are chosen to ensure a smooth transition in the control loads. Testing of this architecture shows a performance improvement compared to a single controller architecture when the conditions are changing. Hybrid control systems can contribute to both fault tolerance and better performance. Fault tolerance is achieved through system reconfiguration, where one of the controllers is designed to handle a certain fault, with sufficient performance. To improve performance, hybrid control can be used as shown in the article, where several controllers and observers with specific operational areas are used together. This makes it possible to design these with better performance, instead of designing a robust controller that can achieve the objective in all conditions.

2.7 Minimum risk conditions

An important task to overcome before the adoption of autonomous ships can become widespread is that they must be sufficiently safe to ensure that neither lives nor the environment is put in unnecessary

harm, meaning that operating these vessels comes with low risk. A starting point to identify risk has typically been to describe a large number of scenarios where things can go wrong. This is often done by brainstorming and checklists. A large challenge with this method is that it is impossible to foresee everything that can occur, especially when the system complexity is increasing (Utne et al., 2017). Such events are called *black swans* and are outliers/hazardous events with extreme consequences, that can not be expected based on available experience. This concept is relevant for autonomous systems, due to the novelty and complexity of the systems. This underlines the need for thorough testing without consequences such as simulations and model tests.

To tackle abnormal situations outside the normal operation, the concept of minimum risk conditions (MRCs) is widely used The notion of MRCs has been used in the development of safe autonomous vehicles, both on cars (NHTSA, N.D.) and ships (DNV-GL, 2018). For this thesis, the following definition is used.

Definition 2.4. ***Minimum risk condition - (DNV-GL, 2018).*** *A minimum risk condition is a state that the ship should enter when the autonomous systems encounter situations outside of those in which it can operate normally, but still should be able to handle somehow.*

The transition from normal operation to MRC usually happens because of a failure or abnormal situation. This can be caused by external effects (e.g. weather change, interference from other ships) or internal incidents (e.g. failure of sensor system). After being put in an MRC, events may occur that make it possible to restore normal operation (e.g. better weather or restored sensor system). It is important to underline the difference between an MRC and the "fail to safe" which are used in some regulations and guidelines today. On this, Rødseth (2018) specifies that MRC differs from these in the sense that one cannot define a completely safe state for a ship and all external factors. Therefore, the term minimum risk is used instead, to indicate that it is a state of minimum risk, but that total safety is not guaranteed.

MRCs are dependent on the vessel operation mode, location, and operating environment. Additionally, there may be several possible MRCs for any given situation. This demands that the autonomous system decides in real-time which MRC is the most relevant. When hazardous or unwanted events have occurred, MRCs can be a means of minimizing risk until the situation is recovered. The set of conditions can vary from system to system, depending on the capabilities of the system. For a ship (autonomous or remotely operated), an example of an MRC might be to stop and keep the position (DNV-GL, 2018).

2.8 Guidelines for autonomous ships

While the development of autonomous ships is happening in research and industry, the regulatory side of the maritime industry has struggled to keep up. For example, DNV-GL stated that "The instruments in use by the International Maritime Organization (IMO), governing the safety of commercial shipping do not provide any regulations for such novel technologies and operational concepts"(DNV-GL, 2018, p. 7). This was also recognized by the IMO and its member states. A scoping exercise has been underway since 2017, "to determine how the safe, secure and environmentally sound operation of Maritime Autonomous Surface Ships (MASS) may be introduced in IMO instruments"(IMO, 2020). At the time of writing, IMO's websites still state that the aim is to complete this exercise by 2020. However, the COVID-19 pandemic has suspended IMOs meetings so it is unknown when this scoping exercise will be concluded. This section will discuss the regulations and guidelines that exist at the time of writing.

First, a definition of the different levels of autonomy is necessary. For the development of MASS, the International Maritime Organization (IMO) has defined four levels of autonomy:

Definition 2.5. ***Degrees of autonomy - (IMO, 2020).***

The four degrees of autonomy identified are:

- ***Degree one:*** *Ship with automated processes and decision support: Seafarers are on board to operate and control shipboard systems and functions. Some operations may be automated and at times be unsupervised but with seafarers on board ready to take control.*
- ***Degree two:*** *Remotely controlled ship with seafarers on board: The ship is controlled and operated from another location. Seafarers are available on board to take control and to operate the shipboard systems and functions.*
- ***Degree three:*** *Remotely controlled ship without seafarers on board: The ship is controlled and operated from another location. There are no seafarers on board.*
- ***Degree four:*** *Fully autonomous ship: The operating system of the ship can make decisions and determine actions by itself.*

Today, some systems on ships might operate in degree one, for example, DP-systems, autopilots, etc. These are often specialized in one particular operation. Then, as the degree of autonomy increases, there is less and less human interaction in the control loop. Trials are underway for ships of degrees two and three. For this purpose, IMO has released interim guidelines for MASS trials (IMO, 2019). This document lacks any concrete guidelines, but focuses on that such trials should be sufficiently safe. Formulations like "Trials should address the risks to safety, security, and protection of the environment." and "Appropriate steps should be taken .." are used. This leaves it up to state authorities and other stakeholders to ensure that necessary measures are taken.

Norway has been leading the development towards autonomous ships and has developed more detailed guidelines for such trials. In Norwegian Maritime Authority (2020), it is described which demands that have to be met for ships that are intended to be autonomous or remotely operated. Here, it is stated that a model test (either physical or simulation) should be used to verify the control system. This should verify the defined MRC scenarios, compliance with collision regulations, and a test of all aspects of the vessel's operation. The vessel shall also go through a testing period in full scale before it is put into normal operation. Since the autonomous systems in question are so new, it is hard to make guidelines more specific than this. The bottom line when it comes to regulations on autonomous ships is that the system will need to go through thorough testing to ensure that the system can operate safely under the given circumstances. The specifics of the testing will vary depending on vessel type, degree of autonomy, operational area, etc. Nevertheless, it is safe to assume that the system will need to pass rigorous simulator testing before testing on water. The procedures for this will likely be more standardized in the coming years, as ship owners, class societies and governing bodies gain more experience on the subject.

MRCs are also incorporated in their preliminary guidelines. There, it is specified that in a concept of operations (CONOPS), the operator/owner shall specify the MRCs available to a vessel in normal operation. This means that these conditions have to be incorporated from the start of the design phase. It is stated that at least two MRCs shall be available under normal operation and that at least one shall be available after a fire. A failure mode and effect analysis (FMEA) and a model or simulation test, shall document that these requirements are met.

2.9 Control barrier functions

The development of control barrier functions (CBFs) is motivated by an increasing focus on safety for modern control systems and autonomous systems. Ames et al. (2019, p. 1) states that CBFs "play a role equivalent to Lyapunov functions in the study of liveness properties." This means that CBFs can be used to guarantee the safety of control systems. This section introduces the theory of CBFs. For this, nonlinear control affine systems on the form

$$\dot{\boldsymbol{x}} = \boldsymbol{f}(\boldsymbol{x}) + \boldsymbol{g}(\boldsymbol{x})\boldsymbol{u}, \quad \boldsymbol{x}(0) = \boldsymbol{x}_0, \tag{2.11}$$

are considered. Here $\boldsymbol{f} : \mathbb{R}^n \to \mathbb{R}^n$ and $\boldsymbol{g} : \mathbb{R}^n \to \mathbb{R}^m$ are locally Lipschitz. $\mathbf{x} \in \mathbb{R}^n$ is the state vector and $\mathbf{u} \in \mathbb{R}^m$ is the control input vector. This formulation can be used to describe a lot of different autonomus systems, for example an ASV like *milliAmpere*, described by a model like in Equation 2.1. It is assumed that there exists a set $\mathcal{C}$ that is a safe set. Safety is then ensured by making sure that system is not leaving $\mathcal{C}$, i.e. enforcing invariance on the set. Then a barrier function can be defined as a continuously differentiable function $h : \mathbb{R}^n \to \mathbb{R}$, such that:

$$\begin{aligned} \mathcal{C} &= \{x \in \mathbb{R}^n : h(x) \geq 0\} \\ \partial\mathcal{C} &= \{x \in \mathbb{R}^n : h(x) = 0\} \\ \mathrm{Int}(\mathcal{C}) &= \{x \in \mathbb{R}^n : h(x) > 0\}\,. \end{aligned} \tag{2.12}$$

where $\mathrm{Int}(\mathcal{C})$ is the interior of $\mathcal{C}$. In other words, the barrier function is positive in the interior of the safe set. Thus, safety can be guaranteed by keeping $h(\mathbf{x}) > 0$. Thus, a CBF gives a method to quantify the set of control inputs at a point $\mathbf{x}$ that keeps the system safe. The next section will present examples of how this is exploited to make collision avoidance systems.

2.10 Collision avoidance

Some of the content in this section is from Moen (2020). The Convention on the International Regulations for Preventing Collisions at Sea (COLREGs) is important when it comes to autonomously operating ships. They are international navigation rules which are to be followed by all vessels at sea to avoid collisions. Although the current regulations are written to be followed by humans commanding ships, autonomous ships must likely follow the same rules to avoid confusion as it is the only available framework at the time being and in the near future (Porathe, 2019). Porathe also highlights the importance of predictable behavior by autonomous ships, such that human operators on other ships can plan accordingly. Therefore, in this thesis, it will be assumed that an ASV will have to follow the COLREGs defined in Definition 2.6. Some other rules are, as stated in Porathe (2019), very qualitative in nature and hard to implement in a software system. The different situations of overtaking (OT), head-on (HO), stand-on (SO), and give-way (GW) are displayed graphically in Figure 2.6.

Definition 2.6. ***Relevant COLREGs - (IMO, 1972).***

- ***Rule 13, overtaking:*** *A vessel is deemed to be overtaking when coming up on another vessel from a direction more than 22,5°abaft of her beam. Any vessel overtaking any other should keep out of the way of the vessel being overtaking.*

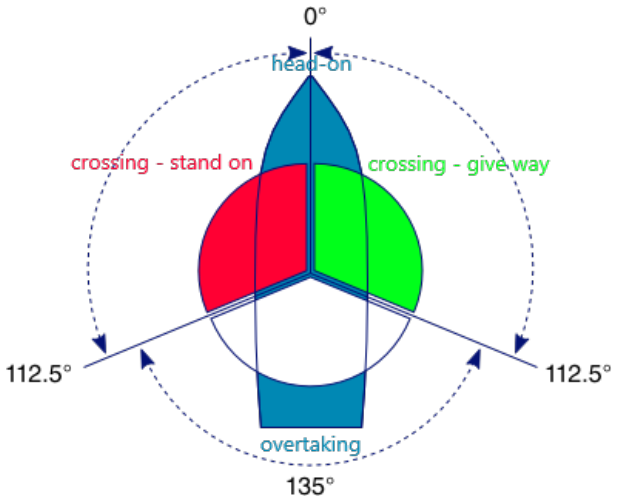

Figure 2.6: Graphical display of COLREGs

- ***Rule 14, head-on situation:*** *When two power-driven vessels are meeting on reciprocal or nearly reciprocal courses to involve risk of collision each shall pass on the port side of the other.*
- ***Rule 15, crossing situation:*** *When two power-driven vessels are crossing to involve risk of a collision the vessel which has the other on her own starboard side shall keep out of the way and shall, if the circumstances of the case admit, avoid crossing ahead of the other vessel.*
- ***Rule 16, action by give-way vessel:*** *Every vessel which is directed to keep out of the way of another vessel shall, so far as possible, take early and substantial action to keep well clear.*
- ***Rule 17, action by stand-on vessel:*** *Where one of two vessels is to keep out of the way the other shall keep her course and speed. The stand-on vessel may, however, take action to avoid collision by her maneuver alone, as soon as it becomes apparent to her that the vessel required to keep out of the way is not taking appropriate action in compliance with the rules. This rule does not relieve the give-way vessel of her obligations.*

Since it is a prerequisite for autonomous ships to be able to operate safely in an environment containing other ships (both controlled by humans and autonomous), many have studied the implementation of collision avoidance (COLAV) into the control software of an ASV. Several different methods have been tried. For example in Fleischer (2020), COLAV is done by using a bio-inspired neural network to perform the path-planning. Other ships are accounted for in the path-planning algorithm proposed by defining forbidden regions with very high costs, making the neural network guidance model discard the possible routes through obstacles. The forbidden regions span an area wider than the vessel, to ensure that the encounter between the two ships is done correctly (i.e., the ship passes at the correct side). The results are very good, and the algorithm produces compliant behavior for all scenarios tested.

In Jensen (2020), collision avoidance is performed with a method using two path parameters, as the one presented in Subsection 2.3.2. If an obstacle region overlaps with the nominal path, then the second path parameter is updated to make the vessel deviate from the nominal path and avoid the obstacle, with a given safety distance between own ship (OS) and target ship (TS). This is implemented into the speed assignment on s_2, with a $\tanh$-function to ensure a smooth transition from the nominal path to avoiding the TS and a smooth return to the nominal path. Simulations show that this method was able to handle COLAV situations in accordance with COLREGs 14 and 15. However, it should be noted that these simulations only assume one obstacle.

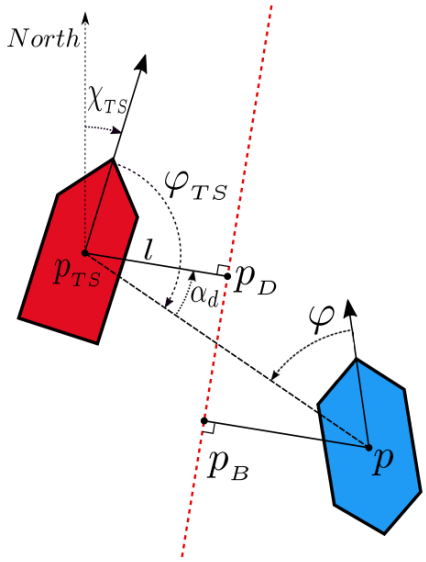

Figure 2.7: Partitioning of North-East plane. Courtesy of Thyri (2019).

Thyri (2019) uses yet another method, called path velocity decomposition. Here, the objects are transformed onto a two-dimensional $path \times time$ space. The advantage of this is that the objects are represented by their position in both space and time. Therefore, a path created in $path \times time$ will be collision-free, assuming the objects keep constant speed and course. To find the optimal path, a set of collision-free vertices are created, where each vertex has costs based on velocity, risk, and time used. Dijkstra's minimum cost path algorithm is used to find an optimal path. The path is then transformed into waypoints in North-East-Down (NED)-frame. The proposed COLAV system also continuously monitors if the planned path is feasible, and replans accordingly. In the thesis, the system is tested both in simulations and onboard the milliAmpere, with good results. The ferry can safely avoid up to 4 objects on a $100\,\mathrm{m}$ transit.

The concept of CBFs can be used for collision avoidance purposes. This is done through simulations with milliAmpere as the case study by Thyri et al. (2020). Here, the CBF is used at the kinetic level and included in a CLF-based quadratic programming (QP) controller. The CBF is based on a partitioning of the North-East plane into two, such that the OS and the TS are in separate parts. The partitioning is done such that the border is a length $l > 0$ from the TS. See Figure 2.7 for graphical representation of the domain partitioning. Based on this, the CBF is formulated such that the OS does not enter the TS domain, which takes both position and velocity relative to the TS domain into account. This makes the vessel respect the COLREGs presented in Definition 2.6. Simulations show that the system can act according to COLREG rules 13, 14, 15, and 17.

An alternative method is to utilize a CBF at the kinematic level, i.e. in the guidance function. In Marley (2021) it is explained how this can be used together with a two-parameter guidance function to plan a collision-free path. In Marley et al. (2020), a CBF is combined with a hybrid feedback controller for heading control. The CBF used is

$$B(p) := \|p - p_o\| - r_o, \tag{2.13}$$

where p is the OS position, p_o is the position of the obstacle, and r_o is the radius of the obstacle region. This function is negative when the vessel is in the interior of the obstacle region. By enforcing $\dot{B} \geq -\frac{1}{T_b}B$, safety is ensured. Here, T_b is a time constant dependent on the vessel properties. The obstacle avoidance abilities are tested by simulation of an underactuated ship. The obstacle is a circular obstacle placed such the nominal vessel path is blocked. The proposed controller structure shows satisfactory

performance and can avoid the obstacle in a consistent manner.

2.11 Autoferry project and milliAmpere demonstrator

This section is partly based on Moen (2020). The case study which will be used in this thesis is milliAmpere. milliAmpere is an experimental platform used in the Autoferry project at NTNU, which is a digital transformation project at NTNU focused on autonomous, all-electric passenger ferries for urban water transport (NTNU, N.D.). milliAmpere is built as an experimental platform to test GNC systems by students and researchers at NTNU. It is a prototype of an autonomous passenger ferry that may replace pedestrian bridges on some short crossings in urban areas.

Figure 2.8: The milliAmpere. Courtesy of Kai Dragland

The vessel is displayed in Figure 2.8. It is $5\,\mathrm{m}$ long has a beam of $2.8\,\mathrm{m}$ and weighs $1670\,\mathrm{kg}$. It is fore-aft and port-starboard symmetrical with a flat bottom and no keel. It is equipped with sensors for navigation; including GNSS, LIDAR, Radar, cameras, IMU, and ultrasonic distance sensors. For propulsion, milliAmpere is equipped with two $2\,\mathrm{kW}$ azimuth thrusters. They each have a maximum thrust of $500\,\mathrm{N}$, and are located at the centerline, $L_x = 1.8\,\mathrm{m}$ from CO. See Figure 2.9. Here, it can be seen how the thrusters are placed and how the thrust F_i depends on the azimuth angle α_i. Combined, the thrusters can produce a maximum force of $1000\,\mathrm{N}$ and a maximum moment about CO of $1800\,\mathrm{N\,m}$.

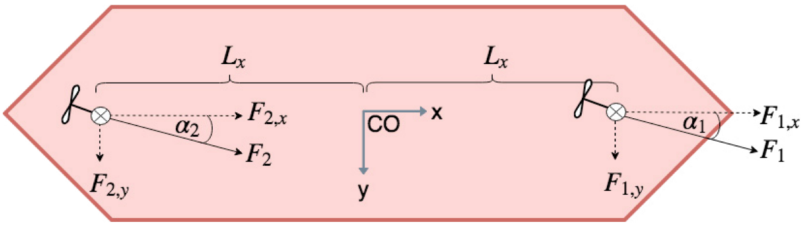

Figure 2.9: Thrust configuration of a double-ended ferry such as the milliAmpere. Courtesy of Torben et al. (2019)

2.11.1 Operational area

The area considered for the operation of milliAmpere during the Autoferry project has been the crossing of *Kanalen*, a channel in downtown Trondheim. This is the area intended for the final iteration of the ferry (Sæther, 2019), and is representative for the type of crossings where autonomous passenger ferries will be applicable. The crossing is approximately 100 m long. The area is relatively shielded from wind and waves. The traffic in the channel is mainly leisure craft - sailboats, motorboats, kayaks, etc. The operating pattern of such a ferry would typically be that it crosses back and forth over the canal. This could follow a set timetable or be on demand such that passengers call the ferry when needed, similar to a pedestrian road crossing.

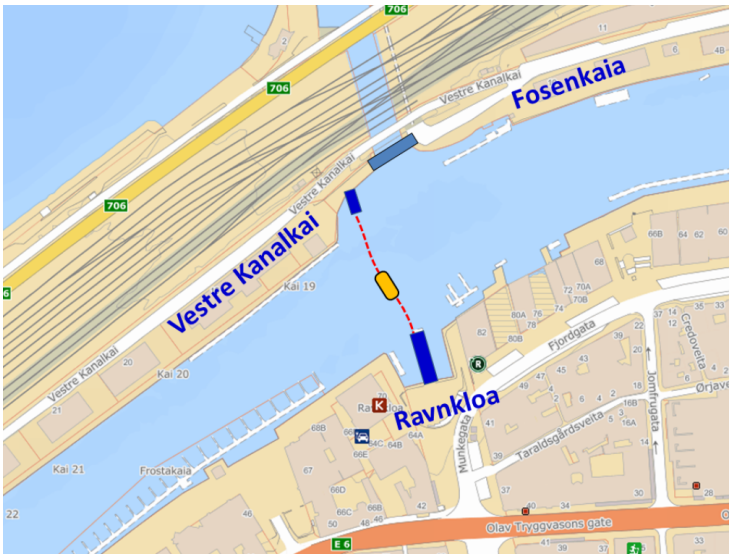

Figure 2.10: Intended operational area. Courtesy of Egil Eide.

Chapter 3

Control modes and minimum risk conditions

Before presenting the problem formulation and the control system to solve this, the control modes for an autonomous passenger ferry like milliAmpere will be defined in this chapter. These will be used as a basis to design the automatic control system in this thesis. Both normal control modes to be used in nominal operation, together with a set of minimum risk conditions that can ensure safety of the vessel in various abnormal situations will be presented. Various causes for the use of MRCs are also listed. Furthermore, different risk influencing factors that can lead to such situations are discussed in Section 3.3. For each normal control mode, specific events that demand the use of MRCs are presented in Section 3.4. To ensure that a sufficient level of detail is achieved for the rest of the work, two of these minimum risk conditions are chosen to develop further. They are presented in Section 3.5.

3.1 Normal control modes

When the ferry is in normal operation, it switches between three normal control modes (NCMs). Those three are here defined as:

Definition 3.1. ***Operating modes of an autonomous passenger ferry:***

- ***Undocking/takeoff:*** *the phase where the vessel moves from a moored position to a position with a safe distance to the dock where crossing can commence.*
- ***Crossing:*** *from the position outside the origin dock, the vessel crosses the canal and arrives at a position by the target dock, where docking can begin.*
- ***Docking:*** *from a position in proximity to the target dock, the vessel moves in a controlled manner to arrive moored at its target dock.*

When combined with a bumpless transfer between the modes, these three modes ensure a successful autonomous crossing from origin to destination. It is convenient to divide the operation into different modes because the control objectives differ between these modes, and it is desirable to have different guidance methods as well. For example, in the docking phase, it is critical to maintain low speed and have a controlled approach, as mentioned in Section 2.4. One would also like to have control over the

path-planning in the guidance layer to ensure that the docking position is correct. A method for this was proposed in Moen (2020). When dividing the operation into different phases, it is necessary to have a sort of supervisor that determines which mode that should be used. A method for this will be proposed in Chapter 5. It is worth noting that Definition 3.1 is made for the operation of a small passenger ferry with a short crossing. For a larger ferry crossing a fjord, a harbor maneuvering phase between crossing and docking might be relevant.

3.2 Minimum risk conditions

To handle situations where normal operation is not possible or safe, the system should incorporate MRCs, as defined in Definition 2.4. These should be used in situations outside normal operation to ensure that minimum risk is imposed on the vessel, the people on board, and the environment. For the case study of milliAmpere with the operational pattern and -area as specified in Subsection 2.11.1, the following MRCs are proposed and will be used throughout the thesis:

1. **Stay moored:** if a fault or failure is detected while the vessel is still at quay, then a suitable response is to stay moored until the failure is properly handled.
2. **Move away from quay:** relevant if, for instance, the vessel itself has caught fire or there is a fire nearby. The vessel should then move to a safe distance, but not too far such that it is impossible to extinguish the fire on the vessel from shore. Before this is done, it must be certain that no humans are on board, so evacuation of these is not made harder.
3. **Return to origin/continue to destination:** applicable for the failure of a secondary or non-critical system. Then it is not critical to assess it right away, but the vessel can return to port or continue to the destination, depending on which is closest. This might be done with limited speed, depending on the status of the propulsion system.
4. **Stop and keep position:** if the situation exceeds the complexity that the system can handle, e.g. with high traffic or bad weather, this MRC can be used. The position is kept until normal operation can resume.
5. **Call for assistance:** if a failure occurs that is so critical that the vessel can not move safely on its own, then assistance is needed. This might be combined with the previous MRC to keep position while waiting, or the vessel might be adrift for the wait. Alternatively, an emergency anchor can be dropped.
6. **Drop anchor:** this condition is especially relevant in the case of thruster failures leading to little or no propulsion. Then an anchor can be used to keep the position. This is, of course, only relevant if an anchor is available. The depth at the location must also be considered to ensure that anchoring is possible.
7. **Evasive maneuver:** although collision avoidance is a part of nominal operation, faults can happen. Then it might be necessary to perform an emergency evasive maneuver to avoid collision with vessels or other obstructions. Evasive maneuvers can of course be executed in both directions, therefore this condition is divided into:
    7.1. Starboard maneuver
    7.2. Port maneuver

8. **Crash stop:** if the vessel is on a collision course, on course to enter a dangerous area, or in a critical navigation conflict requiring to come to a full stop as soon as possible, then the most sensible action might be a crash stop. This means stopping as fast as possible, by using maximum reverse thrust.
9. **Rescue turn:** if a passenger falls overboard, the ship should handle this by positioning itself in proximity to where the passenger fell off. To do this, for example, an Anderson or Williamson turn can be used (Formela et al., 2015). Since the ferry is double-ended, it is also possible to just reverse. This MRC must be activated either by a button or similar for other passengers to use (this must be weighed against issues with potential abuse), or if the system in some way could detect if a passenger falls off.

Together, these MRCs will be sufficient to handle a wide range of possible situations. In some scenarios, multiple MRCs might be suitable. This must be taken into consideration when developing the switching method. The causes for entering MRC can be diverse, but in general, two main categories with corresponding subcategories can be specified:

- **Faults & failures:** some component is not functioning properly. Examples are listed below.
  - **Faults in navigational sensors:** this is challenging because it can result in insufficient situational awareness (SA) and cause dangerous situations.
  - **Faults and failures in power and propulsion system:** power loss can lead to thruster failure, where propulsion is lost. Thruster faults can also yield a thruster unresponsive, such that thrust or azimuth angle is constant.
  - **Faults in maneuvering control system:** as with any software/control system, the maneuvering control system is subject to bugs and programming errors. This can cause unexpected behavior and may lead to situations which the nominal control system is unable to handle properly.
  - **Faults in auxiliary systems:** in addition to the faults already mentioned, there are additional systems that are important to the functionality of the vessel. An example is a fault in the fire suppression system, which should lead to a pause in operation until resolved.
  - **Failure in non-redundant component:** for non-redundant components, there are no extra components available. An example is the battery. If the battery and power supply fail, this will cripple the overall system.
- **Capacity exceeded:** situations where the system can not find a safe way to reach the objective. Examples are:
  - **Navigational conflicts:** the overall traffic situation with high traffic or many obstacles makes it impossible to plan and execute safe maneuvering.
  - **Exceeded capability:** Too much payload and/or harsh weather with large environmental loads possibly exceeding limits of propulsion system. This makes it difficult to maintain safety margins, thus maneuvering can be unsafe.

Here, the first category represents physical events limiting the capacity of the system, while the second represent limitations in the propulsion, sensor, and control systems. This is not necessarily a failure, but a limitation in design. It is impossible to design for all possible situations, so the system must have a solution when the complexity is too high to handle. The next section will give some examples of which events that can lead to these faults and failures.

Table 3.1: Relevant MRCs for each operating mode

MRC / NCM	1	2	3	4	5	6	7	8	9
Undocking	YES	YES	NO	YES	YES	YES	NO	YES	YES
Crossing	NO	NO	YES	YES	YES	YES	YES	YES	YES
Docking	YES	YES	NO	YES	YES	YES	NO	YES	YES

Table 3.1 sums up which MRCs are available in each NCM. Here, MRC3 is not included in the docking and undocking phase since the vessel already is in the dock area. MRC7 is not included in these phases either, because an evasive maneuver might be risky when space is limited. MRC 1 and 2 are not relevant in the crossing phase because it only applies when the vessel is close to the dock.

3.3 Risk influencing factors

The two main groups of causes for MRCs presented in the last section can be influenced by various external factors. Therefore, this section will present various risk influencing factors (RIFs), and what faults or failures this can cause. For each category of RIFs, the best mitigating actions will be discussed. The discussion will be based on the operation of a small passenger ferry like milliAmpere operating in the area as defined in Subsection 2.11.1. The work presented is based on Moen (2020).

3.3.1 Environmental effects

The location of the canal crossing is quite shielded from the rest of the Trondheim Fjord by the island and breakwater outside. Additionally, the waves in the Trondheim Fjord are seldom very big, so the effects of waves will be limited. However, wind may influence more. milliAmpere has a relatively large projected area and no keel, so beam wind may introduce significant forces on the vessel. This should be compensated for in the control system, but may still have an effect. Since this is a canal, current will be present. The current velocity can vary but should be manageable for the control system to counteract. The effect of wind and current together may in some cases be so large that the control system is not able to follow the desired position. This is then an example of when the capability of the system is exceeded. In this case, stationkeeping should be used as mitigating action. This ensures that all available force goes to counteracting the environmental forces.

Weather can affect the system's ability to observe its surroundings. Fog, rain, snow, and hail can obstruct the sensors onboard completely, and/or lead to erroneous measurements. This is an example of faults in navigational sensors and can lead to insufficient SA. Camera, LIDAR, and Radar systems may be affected by this (Zang et al., 2019). If the SA is deemed insufficient, then stationkeeping should be used until it is sufficient again. This reduces the risk of collisions.

3.3.2 Human interference

When operating in an urban waterway such as the Trondheim harbor, human interference is the largest risk factor. It is also highly unpredictable and can be difficult to measure/detect. Therefore, a conservative approach must be taken when considering these risks, for example by implementing the system in such

a way that the ferry stops if there is uncertainty whether there is a human in the canal or not. The list of situations that follows is a non-exhaustive list of situations with potential risks caused by human interference.

- Boats in the way: there might be boats in the canal, obstructing the path of the ferry.
- Kayaks in the way: leisure craft without an engine such as kayaks may obstruct the path.
- People in the water: people can be in the water around the docks.
- Objects between ferry and dock: floating objects between the ferry and the dock can interfere with the docking process.
- Movement on board: if the passengers move very much around or are placed very unevenly, it might affect the hydrodynamic properties of the ferry.
- Passenger overboard: when on a boat in motion, the possibility that a passenger falls overboard will always be present.

The RIFs discussed here do not cause any faults, and are thus categorized under the "capacity exceeded" category. Some of these risks should be avoided by the COLAV system, but if this fails and collision is imminent or it is uncertain if a risky situation is about to happen, a crash stop or evasive maneuver will be the best risk-mitigating action in these situations. For the case where a passenger falls overboard, MRC9 representing a rescue turn will be the best.

3.3.3 Fire hazard

The milliAmpere and later versions of the same type are small and relatively simple vessels, without too much equipment on board. Anyhow, there is still a risk of fire on board. Batteries, electrical wiring, computer equipment, electrical propulsion, and so on can in a worst-case scenario catch fire. Additionally, parts of the surroundings might catch fire, for example on a nearby leisure vessel or in a building on shore. This must be regarded as a real possibility, to be accounted for with MRCs. These are categorized under "faults and failures", and the severity of the fire, as well as the vessel's position, will influence which action is best suited to minimize the risk. MRCs 2, 3, 4, and 5 are relevant in these cases.

3.3.4 Technical problems

A final category of risk influencing factors is technical problems. The list of causes for MRCs in Section 3.2 discusses a lot of the technical problems that can happen. For some faults and failures, the system may be able to keep operation going by fault accommodation or system reconfiguration. For others, an MRC must be used to minimize the risk. For the least critical situations where maneuverability is intact, MRC3, which takes the vessel to port might be used. For more critical faults, MRCs 4, 5, and 6 are likely to be better options.

3.4 Transitional events

This section builds upon the RIFs presented in the last section and will contain a mapping of events that can cause the activation of MRCs in each of the three NCMs. The list will not include all possible events,

but serve as illustrative examples and include the most probable scenarios. For each phase, a few events will be described, together with which MRCs can be activated to mitigate the situation.

3.4.1 Undocking

In the undocking phase, the vessel has low speed and is moving away from the quay. Then, the following scenarios are examples of events that need MRCs:

1. **Fault while docked:** if a fault in any part of the system decreases performance below a set threshold is detected, the ferry should abort the mission and enter MRC1 (stay moored).
2. **Fire nearby:** if a fire is detected nearby, the vessel should enter MRC2 (move away from quay) to ensure safety of the vessel and passengers.
3. **Obstacle detected:** if an obstacle is detected that can not be avoided by the nominal COLAV system, an MRC needs to be used. Due to the low speed and possible confined waters, MRC4 (stop and keep position) is the best choice in this situation.

3.4.2 Crossing

During crossing, the situation is a bit different than in undocking. The speed is higher, and the operational domain is bigger and farther from land. Examples of high-level events leading to activation of MRCs in this mode are:

1. **Collision imminent:** if the COLAV system fails or an obstacle is detected too late, MRC7 (evasive maneuver) or MRC8 (crash stop) has to be executed.
2. **Loss of propulsion:** if a loss of propulsion is detected, MRCs need to be entered. This can either be MRC6 (drop anchor), MRC4, or MRC3 (return to origin/continue to destination), depending on the amount of propulsion left.
3. **Navigational conflicts:** the situation, including traffic and weather conditions, makes it impossible to maneuver safely. Then, MRC4 might be used until the situation is manageable.

3.4.3 Docking

In the docking phase, the vessel has low speed and is located close to the dock, similar to the undocking phase. Therefore, the following are examples of high-level events that lead to the activation of MRCs:

1. **Fire nearby:** if a fire is detected nearby, the vessel should enter MRC2 to ensure safety of the vessel and passengers.
2. **Sudden obstacle:** if an obstacle is suddenly detected, for example, a swimming person, the system should enter MRC2 until the situation is cleared.

3.5 Selection of most relevant MRCs

Although a complete system will need to include enough MRCs to handle a lot of different situations, it is quite a lot of work. Therefore, to be able to detail each MRC and be able to incorporate these into a control system for testing, 2 MRCs are selected for further development. These are the following:

1. **Crash stop**
2. **Evasive maneuver:**
    2.1. Evasive maneuver starboard
    2.2. Evasive maneuver port

In this section, each MRC is detailed into functional demands for guidance and control. Relevant causes that trigger them are also given.

3.5.1 Crash stop

This MRC is activated when the situation demands that the vessel comes to a full stop as fast as possible. This can for example be activated if the vessel is on a collision course with another vessel or obstacle, and the guidance function cannot find a feasible path to avoid it. It should also be activated if the vessel is on course to enter a dangerous area. If the system encounters a navigational conflict such that no safe path to the destination can be planned, this should also be activated. This can for example happen if the traffic picture suddenly gets very busy. Lastly, a crash stop should be performed if the vessel deviates from the desired path by a distance larger than a set safety margin.

For a ship with azimuth propellers, a crash stop can be done by turning the propellers $180°$, or by reversing the rotation of the propellers. A third method is to point the azimuths $30°$ and reversing the propellers. This utilizes the drag of the azimuth unit in addition to the thrust produced by the propellers. The effectiveness of these procedures is investigated by Nowicki (2014) and Park et al. (2020). They find that turning the azimuths around and turning the azimuths outward is the most effective method, respectively. However, these experiments were done for large ships ($277\,\mathrm{m}$ and $70\,\mathrm{m}$) with two azimuths placed at the stern. For the smallest ship, reversing the propellers is almost as good as turning them outward (6% longer stopping length). Ultimately, the best solution is dependent on the specific vessel. Therefore, the method where the propeller revolutions are reversed is assumed to be sufficient here. This is relatively simple to implement and seems to be quite effective. Then it must be noted that for a vessel that will be put into operation, tests should be performed to find the best method.

For this mode, the guidance layer does not need to provide a desired position. The output of the controller block in this mode should then be full throttle in the opposite direction of the velocity as long as the vessel has a forward speed. After the vessel has come to a stop, the system can transition to station-keeping until the situation is cleared.

3.5.2 Evasive maneuver

An evasive maneuver should be performed when the nominal COLAV system has failed or an obstacle has not been detected in time to be avoided, such that a collision is imminent. The result should then be

a hard turn to either port or starboard. The new heading after the turn should be sufficient to avoid the obstacle. To relate this maneuver to classical ships, an evasive maneuver would entail that the captain turns the rudder hard to either port or starboard. milliAmpere does not have a rudder, so this behavior must be mimicked for the fully-actuated case. During the maneuver, the speed should be ramped to zero. The maneuver is complete when the vessel has obtained the new heading and stopped. Then the vessel can transition into stationkeeping until the situation is resolved.

To complete this task, the guidance function must provide a heading reference that takes the vessel into a turning circle maneuver, and keeps the heading constant when the heading has changed enough. Additionally, a reference speed must be provided, that gradually ramps to zero at the end of the maneuver. A controller must be in place to control the heading and speed to the desired references.

Chapter 4

Problem formulation

The overall goal of this thesis is to develop a control system capable of mode switching between nominal operation modes and emergency modes. In this chapter, the problem is formulated as functional demands for the subsystems that are treated in this thesis. Two subsystems are in focus; the mode supervisor and the motion control system. The proposed system architecture including these two systems can be seen in Figure 4.1. The details of the red blocks are not considered in this thesis, while the green boxes are in focus. Therefore, three subproblems are specified: the supervisor problem, the guidance problem and the control problem. At the end of the chapter, the limitations and assumptions used during the thesis work are given.

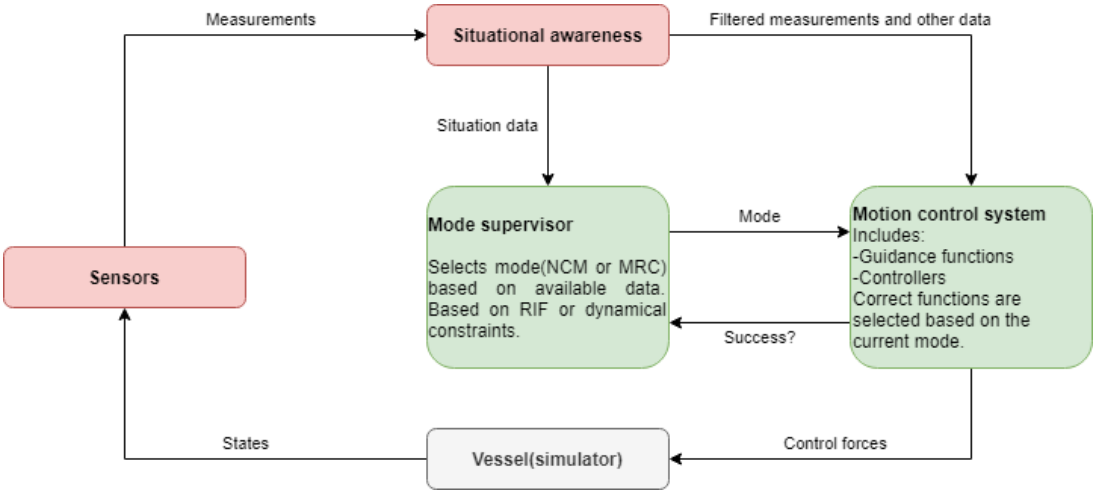

Figure 4.1: Proposed system architecture.

4.1 Mode supervisor problem

To switch between the modes described in Chapter 3, a mode supervisor is to be implemented. This will be integrated with the rest of a conventional GNC system as shown in Figure 4.1. As seen, the mode supervisor will interact with the rest of the GNC system. It will take input from the following modules:

- **Situational awareness**: from the situational awareness/sensor fusion module, information about the surroundings in terms of the traffic and weather situation.
- **Motion control system:** from the motion control system, the mode supervisor receives information on whether a collision-free path can be constructed or not.

Based on the information received, the mode supervisor should determine which mode that should be used. The alternatives are three NCMs (undocking, crossing, docking) or three MRCs (crash stop, evasive maneuver port, evasive maneuver starboard). The supervisor shall run continuously, but measures have to be taken to avoid *chattering*, which is the problem when a signal is switching back and forth rapidly. Therefore, when an MRC is entered and nominal operation is interrupted, the MRC should be finished before another switching is considered.

The output from the mode supervisor should be which mode the system should operate in. This signal is fed to the motion control system, which in turn will implement the corresponding changes. The working method of the affected subsystems in each mode will be formulated in the following sections.

4.2 Guidance problem

The guidance system is responsible for generating the desired path of the vessel. This will result in a reference signal that will be used by the control system. The reference signal is the desired position $\boldsymbol{\eta}_d = [x_d, y_d, \psi_d]^\top$. The guidance system is active in all phases of operation, so in the following, the methodology used in each phase will be described. Although the methodology is different, the objective is the same: to generate a safe and feasible path for the vessel to follow. This means ensuring that the path is collision-free, both regarding static and dynamic obstacles.

Collision avoidance is to be included through the use of CBFs. CBFs are described in Section 2.9, and relevant applications of CBFs are discussed in Section 2.10. The CBF should be formulated in a way such that the vessel keeps a safe distance from all obstacles. The CBF should be active in the undocking and docking phases. Although it is desirable to have collision avoidance that is COLREG-compliant, this is not an objective in this thesis as it is quite complicated. Instead, a simpler collision avoidance functionality will be implemented, which achieves the objective of simply avoiding any obstacle.

4.2.1 Undocking

In the undocking phase, the target is to move the vessel in a controlled manner from a moored position to a position outside the dock where crossing can commence. In this regard, a safe distance from the dock, d_{safe} must be defined so that a small passenger ferry like milliAmpere is clear of the dock and the hydrodynamic effects mentioned in Section 2.4.1. Furthermore, the vessel shall have a controlled behavior with low speed of maximum $u_{takeoff}$.

4.2.2 Crossing

After the undocking phase, the crossing phase follows. Here, the objective is to move from a position outside the origin dock to a position outside the target dock where auto-docking can commence. The vessel shall come to a complete outside the target dock. Since the crossing is short and relatively

uncomplicated, a straight line parametrization can be used as the base for path planning in this phase. This means that the nominal crossing path is a straight line between WPs outside the two docks. Then, alterations to this path can be made based on the CBF.

4.2.3 Docking

The docking guidance should be based on the method developed by Moen (2020), which is based on Gauslaa (2020). This divides the docking operation into two phases; approach and docking. The approach takes the vessel close to the dock with normal heading to the dock, while docking is the final meters of the operation. The final design should be better on the points of improvement mentioned in Moen (2020). This includes avoiding unnecessary S-turns and ensuring a smooth transition between approach and docking. The most important thing during docking is slow speed and a controlled approach, as mentioned in Section 2.4. The docking guidance shall plan a path from the starting position to a docked position. The maximum velocities will be defined as $u_{approach}$ and u_{dock}, in the approach to the dock, and the last meters of the docking, respectively.

4.2.4 MRC

In addition to guidance for the three NCMs, there should also be guidance functions for the selected MRCs, if such is necessary. Recalling the specification of MRC-modes in Section 3.5, this is not necessary for the crash stop mode. For the evasive maneuver, a guidance function is necessary. This should provide a desired heading to be used in a heading controller. This should lead to a maneuver that turns the vessel $90°$ as fast as possible. At the same time, it should provide a reference speed that gradually ramps to zero so the vessel is at rest when the maneuver is over.

When changing modes, the guidance function should assure a smooth transition and initialization of the new mode. This can be done by weighting the desired position for the old and new modes in a transition phase. However, the desire for a smooth transition must be weighed against the time used to make the transition. For some mode transitions, time is limited, so a smooth transition might not be prioritized.

4.3 Control problem

The control system shall determine the desired general force vector $\boldsymbol{\tau}_d$ that will result in the vessel following a desired path. This control problem is called *the maneuvering problem*, and was formulated mathematically as follows by Skjetne (2005). It is divided into two tasks:

1. **Geometric task** - for any continuous function $s(t)$, force the vessel position $\boldsymbol{\eta}$ to converge to the desired position $\boldsymbol{\eta}_d(s)$:
$$\lim_{t\to\infty} |\boldsymbol{\eta}(t) - \boldsymbol{\eta}_d(s(t))| = 0. \tag{4.1}$$

2. **Dynamic task** - satisfy the speed assignment - force the path speed $\dot{s}(t)$ to converge to a desired speed $v_s(s(t), t)$:
$$\lim_{t\to\infty} |\dot{s}(t) - v_s((s(t), t)| = 0. \tag{4.2}$$

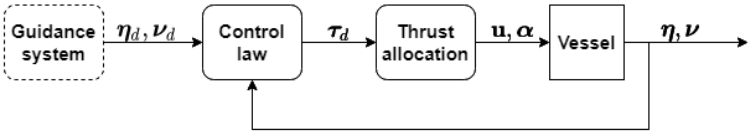

Figure 4.2: Subsystems of the control system and interaction with guidance system

The speed assignment is one of several possible dynamic tasks and is the most relevant for the application of an autonomous passenger ferry. When formulated this way, it is possible to treat the design of the path and the desired motion along the path separately. milliAmpere is fully actuated, so solving both tasks is feasible. The control system is made up of the submodules as shown in Figure 4.2. The desired position and velocity vectors $\boldsymbol{\eta}_d$ and $\boldsymbol{\nu}_d$ are fed into the *control law* from the guidance system. The control law computes the desired force vector $\boldsymbol{\tau}_d$. This is used directly as input to the vessel model. Thrust allocation is not considered. For the nominal control modes, a cascaded backstepping controller is chosen. The basis for this controller is presented in Skjetne (2020b).

In addition to solving the maneuvering problem when in nominal operation, the control system should be able to react adequately to changes in control objectives when an MRC is entered. This entails having a hybrid control structure with automatic switching between the controllers. This leads to a fault tolerance through supervision, where the mode supervisor provides the signals to determine which controller should be used. The controllers should be able to accomplish the new control objectives, based on input from the eventual guidance function. The new control objectives for the selected MRCs are:

- **Crash stop:** come to a stop as fast as possible.
- **Evasive maneuver**: control the heading of the vessel to the reference heading provided from the guidance system. At the same time, the vessel speed should be controlled to the reference speed.

4.4 Limitations and assumptions

To limit the workload of this thesis and ensuring that sufficient time has been available to work with the main objective of the thesis, some simplifications and assumptions have been made. The main objective and most central part of the problem faced in this thesis is to develop a mode supervisor that merges normal and emergency control modes into an autonomous control system with risk-mitigating capabilities. The following limitations and assumptions have been made during the thesis work:

- Necessary state estimates are assumed to be available from an observer. The implementation of the observer is not considered, neither is measurement noise.
- The movement of the vessel is restricted to the 3 horizontal DOFs surge, sway, and yaw, with a control design model as given in Section 2.1. The parameters of this model are assumed known.
- Thruster dynamics are not considered in the control problem.
- Obstacles are assumed to be stationary.
- COLREGs are not considered in the implementation of obstacle avoidance.
- Environmental forces are not included.

- The case study considered is milliAmpere, with an operational area crossing Kanalen in Trondheim. Both are presented in Section 2.11.
- Situational awareness and sensors fusion is not considered, but all necessary measurements are assumed available. This includes the position of obstacles.
- For simplicity, only the position of the center of the vessel is considered regarding obstacle avoidance.
- Here, all MRC modes are executed until they are finished, without reevaluating during the maneuver.

Chapter 5

Mode supervisor

In this chapter, the algorithm behind the mode supervisor will be explained thoroughly. The supervisor should solve the problem formulated in Section 4.1. First, a mapping of the modes used is presented. After this, the logic behind mode switching in nominal control is presented, before the same is done for switching to MRC control modes. Lastly, some alternative methods that are not pursued closer in this thesis are presented.

5.1 Mapping of modes

As previously stated, the system proposed in this thesis will consider six modes, where three are NCMs and three are MRCs. All modes are not available or suitable at all times. Table 5.1 summarizes the relationship between the seven modes. The rows represent the current mode, while the columns represent the mode to be switched to. The reasoning behind the table will follow.

Firstly, the switching between NCMs (represented by the first three columns of the first three rows) is treated. The nominal switching is dependent on the distance to the two docks. When undocking, crossing should be activated when the distance to the origin dock is over a threshold, and the distance to the target dock is over a threshold. If the target dock is closer, then the switching should go directly into docking mode. When crossing is active, docking mode should be activated when the distance to the target dock is low enough. In docking mode, undocking can be activated if a new trip is started after the docking is completer. Also, crossing mode can be activated if the destination is changed while docking. Details for the nominal switching are given in Section 5.2.

Secondly, the switching from NCM to MRC (represented by the three leftmost columns of the first three rows) is treated. In docking and undocking phases, the only MRC available is crash stop and should be used for whatever reason an MRC is activated. This is because an evasive maneuver is considered too abrupt and uncontrolled when operating in a restricted area close to shore. Also, the speed is low, so the stop length will be short when a crash stop is performed. In crossing mode, all three MRCs are available. Then, the system must decide which mode is best suited for the situation. The details for this are given in Section 5.3.

Thirdly, the switching from MRC back to NCM (the last three rows of the first three columns). When an MRC-mode is finished, the vessel is keeping its position in DP-mode. To go back to nominal operation,

Table 5.1: Switching table for modes

From \ To	Undocking	Crossing	Docking	Crash stop	Ev. maneuver SB	Ev. maneuver P
Undocking	-	Sufficient distance to dock	Closer to target dock	Collision imminent or other abnormal situation	N/A	N/A
Crossing	N/A	-	Within docking distance of target dock	Collision imminent or unable to follow desired position	Collision imminent, SB is shortest way	Collision imminent, P is shortest way
Docking	Activation of new trip	Changed destination	-	Abnormal situation	N/A	N/A
Crash stop	Navigational conflict/ collision is avoided			-		
Ev. port	Collision avoided &	Collision avoided &	Collision avoided &		-	
Ev. SB						-

it must be ensured that it is safe to resume operation and that the situation is resolved. For now, it is assumed that this is done by a human operator at a control center. Therefore, no functionality for resuming operation is implemented. It is safe to assume that the first autonomous vessel will have continuous contact with an operator at shore. In the future, autonomous systems might be able to assess if the operation should be resumed, but this is not considered here.

Lastly, the switching from MRC to MRC is represented by the lower right corner of the table. As seen, this is left blank. In this thesis, it is assumed that once in an MRC, this mode should be completed without switching to another mode. In a real implementation of a system like this, it might be necessary to assess the risk during the execution of an MRC-mode, to ensure that the selected mode is indeed the one with minimum risk. This can for example be relevant if the situation changes a lot during the execution or if faults occur during the maneuver. But based on the assumptions in Section 4.4, this is not necessary for this thesis.

5.2 Switching between nominal modes

In nominal operation, the vessel should switch from undocking to crossing, to docking and start over for a new trip. As seen in Table 5.1, this is mainly dependent on the vessel's position relative to the docks. For the undocking phase to be over and the crossing phase to begin, the vessel should have sufficient distance to the departure dock, such that it is safe to increase the velocity to crossing speed. This distance is called d_{undock}. If the distance from the vessel to the origin dock is larger than d_{undock}, then switching should commence. Additionally, to avoid unnecessary many switchings during one trip, it should also be checked that the distance to the target dock is larger than a specified distance $d_{dock,direct}$. If not, the switching should be directly from undocking to docking.

In crossing mode, the only available mode is docking. This should happen when the vessel has come

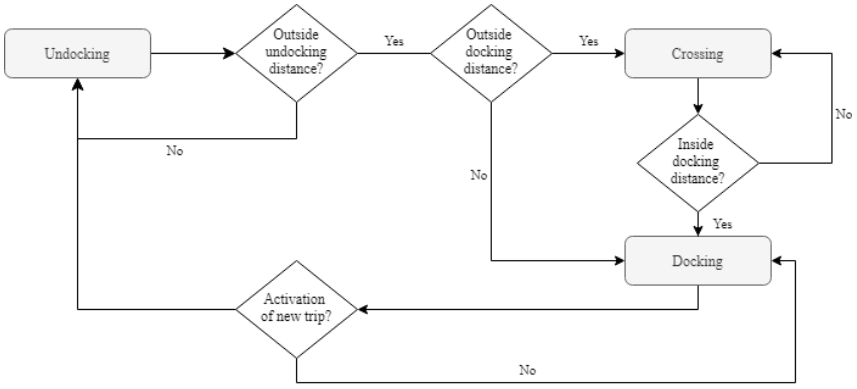

Figure 5.1: Flowchart for switching between nominal control modes.

sufficiently close to the target dock. I.e. the distance to the target dock is less than a specified docking distance d_{dock}. Finally, the transition from docking phase to undocking should happen when a new trip is activated through some sort of activation signal. The transition between nominal control modes is illustrated through the flowchart in Figure 5.1. The distances are given in Table 5.2.

Table 5.2: Distances for nominal switching

Symbol	Explanation	Value
d_{undock}	Distance from origin dock when crossing is entered.	$10\,\mathrm{m}$
$d_{dock,direct}$	Maximum distance from target dock to go directly from undocking to docking.	$25\,\mathrm{m}$
d_{dock}	Distance from target dock when docking mode is entered.	$15\,\mathrm{m}$

5.3 MRC-switching

Since the MRCs that are investigated in this thesis are related to unsafe situations where obstacles are involved, it is necessary to specify how an obstacle should be represented from the supervisor's point of view. In this context, it is assumed that the supervisor receives only the position of obstacle center, p_o. Based on this, three different regions are defined, representing the risk associated with being there:

- Red region: the red region is the most dangerous region and contains the obstacle itself and a small safety distance around. This region is associated with the most risk, as a collision is very likely in this region. This region must be avoided at all times.
- Yellow region: the yellow region is the limit of the nominal control system. The nominal COLAV system has the objective of keeping the vessel out of this region, as it is associated with a risk of collision. If the vessel enters this area despite this, then measures should be taken through an MRC.
- Green region: the green region represents the safe region and is the area of the action space that are not yellow or red. Here, nominal operation is executed, and the area is associated with low risk.

The simplest way of diving the action space into these regions is to use p_o and create two circles with radiuses r_r and r_y, where the inner circle is the red region and the space between the circles is the yellow

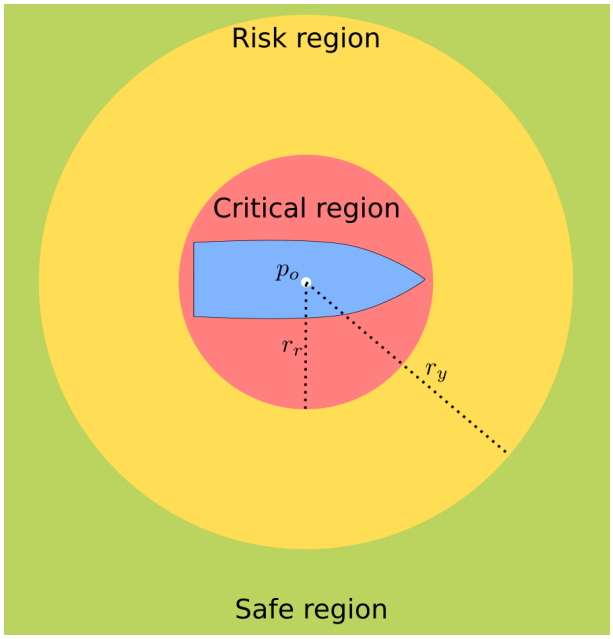

Figure 5.2: Illustration of regions around an obstacle

region. This is illustrated in Figure 5.2, for a general boat-shaped obstacle. When the action space is divided into these regions, it is possible to use this as a criterion to decide when to enter an MRC. The simplest is to say that an MRC should be entered when the vessel is located inside the yellow region. The vessel's course and velocity can also be used to say if the vessel is about to enter the yellow region.

When it is determined that an MRC should be used, the supervisor function must decide which MRC to enter. This is done through the use of an indicator function. It is assumed that such an indicator function can quantify the relative risk of performing a crash stop and evasive maneuver, respectively. This can for example be the risk of impact, the velocity at impact or impact energy, etc. This function is used to evaluate the available MRCs against each other, and then select the one with the lowest risk. In the following, two alternatives for such an indicator function are presented.

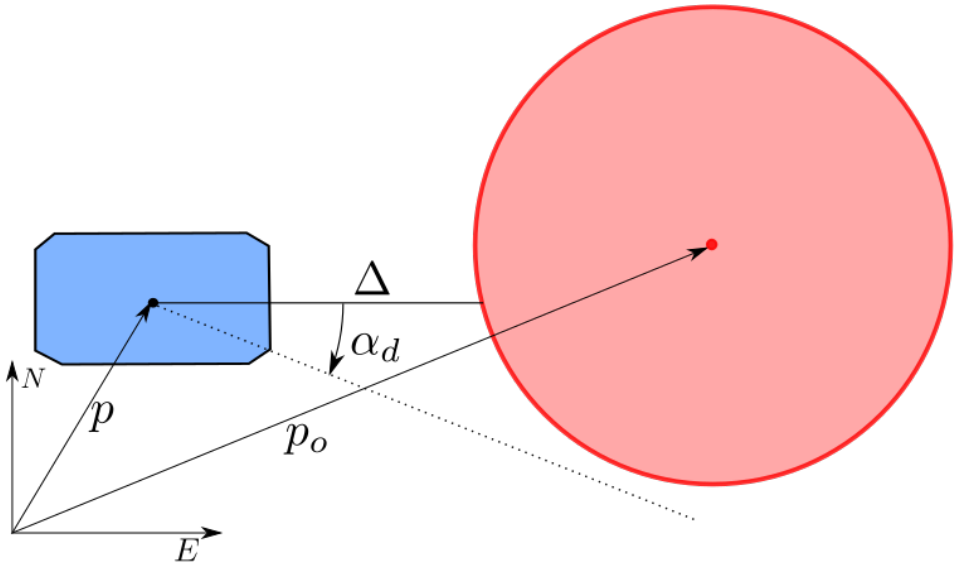

Figure 5.3: Parameters for collision indicator. Vessel in blue, obstacle in red

5.3.1 Indicator function based on dynamical constraints

An example of such an indicator function is now presented. This uses the position and velocity of the ship to determine the time to impact t_i. For the crash stop case, the necessary acceleration to stop in time a_{safe} can then be calculated. For the evasive maneuver, the necessary angular velocity ω_{safe} to rotate to a safe heading can be calculated, assuming the required heading change is known. First, the distance to the obstacle has to be calculated. This is taken as the intersection between the line extended from the vessel in the current heading direction, and the circular obstacle region. This distance is called Δ. A graphical representation of the problem can be seen in Figure 5.3. Using the distance, the time to collision assuming constant speed U can be calculated:

$$t_i = \frac{\Delta}{U}. \tag{5.1}$$

Then, the necessary acceleration to stop in time during a crash stop is found as

$$a_{safe} = \frac{U}{t_i}. \tag{5.2}$$

Correspondingly, the necessary angular velocity to obtain the new heading required for an evasive maneuver is

$$\omega_{safe} = \frac{\alpha_d}{t_i}, \tag{5.3}$$

where α_d is the required heading change. This is a simplification, as the vessel will continue forward while it changes heading. To compare the two maneuvers and decide which to use, the fractions

$$p_{cs} = \left|\frac{a_{safe}}{a_{max}}\right| \qquad , \qquad p_{em} = \left|\frac{\omega_{safe}}{\omega_{max}}\right| \tag{5.4}$$

are used. The mode with the lowest value is then selected. If an evasive maneuver is the best choice, then it is also necessary to determine if it goes to port or starboard. This is done simply by checking the sign of α_d. A positive sign gives a starboard maneuver, while a negative sign gives a maneuver to port.

5.3.2 Indicator function based on a risk index

Another possibility is to use a function that in some way quantifies the risk of a certain position and control input. Call this the risk function (RF) R. This can for example be formulated in the same fashion as a CBF. Here, the same formulation as in Marley et al. (2021) is used. Then R is:

$$R(p, z) := r_s - |\mathbf{p}| - t_o U \frac{\mathbf{p}^\top}{|\mathbf{p}|}\mathbf{z}, \tag{5.5}$$

where z is the angle vector corresponding to the ship course $\mathbf{z} = \begin{bmatrix}\cos\chi \\ \sin\chi\end{bmatrix}$ and $\mathbf{p}$ is the position of the vessel relative to the obstacle s.t $\mathbf{p} = \mathbf{p}_v - \mathbf{p}_o$. The vessel velocity is U, r_s is the safe radius and t_0 is a time constant. This gives an indication of the risk of the vessel given its position and velocity. Higher R means larger risk. The first two terms evaluate to the distance from vessel to obstacle, while the last term is the relative velocity between vessel and obstacle weighted by t_0. The derivative of R can be found, given a control input $\mathbf{u} = \begin{bmatrix}a & r\end{bmatrix}^\top$ where a is linear acceleration and r is yaw rate:

$$\dot{R} = L_f R + \mathbf{L_g R u}. \tag{5.6}$$

Table 5.3: Control input for MRCs

MRC	Control input $\mathbf{u}$
Crash stop	$\mathbf{u}_{cs} = \begin{bmatrix} -a_{max} & 0 \end{bmatrix}^\top$
Evasive maneuver starboard	$\mathbf{u}_{emsb} = \begin{bmatrix} 0 & r_{max} \end{bmatrix}^\top$
Evasive maneuver port	$\mathbf{u}_{emp} = \begin{bmatrix} 0 & -r_{max} \end{bmatrix}^\top$

The Lie derivatives are:

$$L_f R = -U\frac{\mathbf{p}^\top}{|\mathbf{p}|}\mathbf{z} - t_0\frac{U^2}{\mathbf{p}|}\left(\frac{\mathbf{p}^\top}{|\mathbf{p}|}\mathbf{S}^\top\mathbf{z}\right) \tag{5.7}$$

and

$$\mathbf{L_g R} = -\frac{\mathbf{p}^\top}{|\mathbf{p}|}\begin{bmatrix}\mathbf{z} & U\mathbf{S}\mathbf{z}\end{bmatrix}. \tag{5.8}$$

With the derivative of R, one can find the best control input to reduce the risk R. In this context, it is desirable to choose the MRC with the lowest $\dot{R}$ such that the risk is reduced the fastest. If a_{max} is the maximum linear acceleration achievable by the ship and r_{max} is the maximum yaw rate, then the control inputs corresponding to each of the MRCs are as presented in Table 5.3. Then the mode can be selected such that $\dot{R} = \min(\dot{R}(\mathbf{u}_{cs}), \dot{R}(\mathbf{u}_{emsb}), \dot{R}(\mathbf{u}_{emp}))$. This method then assumes that the crash stop and evasive maneuvers are implemented such that the resulting motion corresponds to maximum linear acceleration and yaw rate, respectively.

If multiple obstacles are present, the MRC selected should minimize the derivative of the risk index function regarding all obstacles, which corresponds to the most reduction in risk. This is done by calculating the risk derivative of each control input for each obstacle. If there are n obstacles present, this will result in a matrix $\dot{\mathbf{R}}$ corresponding to:

$$\dot{\mathbf{R}} = \begin{bmatrix} \dot{R}_1(\mathbf{u}_{cs}) & \dot{R}_2(\mathbf{u}_{cs}) & \dots & \dot{R}_n(\mathbf{u}_{cs}) \\ \dot{R}_1(\mathbf{u}_{emsb}) & \dot{R}_2(\mathbf{u}_{emsb}) & \dots & \dot{R}_n(\mathbf{u}_{emsb}) \\ \dot{R}_1(\mathbf{u}_{emp}) & \dot{R}_2(\mathbf{u}_{emp})) & \dots & \dot{R}_n(\mathbf{u}_{emp}) \end{bmatrix}, \tag{5.9}$$

where $\dot{R}_i$ is the derivative of the risk indicator function for obstacle i. Then, to decide which action is best based on all the obstacles, one needs to determine which row is best. Initially, this was done by taking the sum of each row and selecting the row with the lowest sum. However, this is problematic when the obstacles are at different distances from the vessel. To account for this, a weighing is proposed. If the distances to each obstacle d_i are in a diagonal distance matrix

$$\mathbf{D} = diag(d_1, d_2, \dots, d_n), \tag{5.10}$$

then a weighed version of $\dot{\mathbf{R}}$ can be calculated as:

$$\dot{\mathbf{R}}_w = \dot{\mathbf{R}}\mathbf{I}_n\mathbf{D}^{-1}, \tag{5.11}$$

where $\mathbf{I}_n$ is the identity matrix of size n. This means that every entry in $\dot{\mathbf{R}}$ is weighted by the inverse of the distance to the corresponding obstacle. Then, the best action can be selected by finding which row of $\dot{\mathbf{R}}_w$ that has the lowest sum. By doing it this way, obstacles far away contribute little to the sum, and the closest ones contribute the most. Since the distance is always positive, the signs of the derivatives are also preserved. The formulation in Equation 5.11 also works for one obstacle, as I_n and $\mathbf{D}$ become scalar. Other weight functions might also be possible, to shift the priority of which objects are most important.

Algorithm 1: Supervisor pseudocode

```
input : mode,position,velocity,obstacle position, α_d, dock position, initial position, COLAV
        index
output: new mode, waypoints
if not initialized then
    Calculate waypoints;
end
if undocking then
    if MRC activated then
        set mode to crash stop;
    else if sufficient distance to both docks then
        set mode to crossing;
        set new waypoints if necessary;
    else if sufficient distance to origin dock, but not target dock then
        set mode to docking;
    end
else if crossing then
    if distance from desired position too large then
        set mode to crash stop;
    else if within risk region then
        run indicator function to determine best mode, set mode to the result;
    else if within docking distance to target dock then
        set mode to docking;
    end
else if Crash stop then
    if velocity low enough then
        activate DP-mode;
    end
else if Evasive maneuver then
    if velocity low enough then
        activate DP-mode;
    end
end
```

5.3.3 Main algorithm

With the indicator functions in place, the main algorithm for the supervisor can be formulated. This is shown in Algorithm 1. Here, it is seen that the supervisor does a series of checks in each mode to determine the state of the system and which mode to go into next. Of course, if none of the if-sentences are true, then the system will just continue in the current mode. Both nominal modes and MRC modes are treated by this algorithm. The Matlab implementation of this can be seen in Appendix A.1.

The input to the supervisor function is the following:

- **Mode:** the current mode is needed to determine which checks to perform.
- **Position & velocity:** necessary as input to the indicator function.
- **Obstacle position:** also necessary as input to the indicator function.

- $\boldsymbol{\alpha_d}$: needed for the indicator function based on dynamical constraints.
- **Dock- and initial position:** for calculation of waypoints in the initialization phase.
- **COLAV-index:** this is an index that is set in the guidance layer. This is an integer that can have values:
  - -1: the vessel should crash stop. Usually because the vessel is too far from $\mathbf{p}_d$
  - 0: no problems detected, continue nominal operation.
  - $1, 2, \ldots, n$: the vessel is in the yellow region of an obstacle. The total number of obstacles is n, so the index then defines which obstacle it is close to.

This gives the necessary data to compute which mode should be executed. In Algorithm 1 it can be seen how this is done. The first level of if-sentence checks which mode is the current. Then, the next level of if-sentences contains checks applicable for that mode. The output is the mode that should be executed, together with the waypoints that should be used. To determine which numbers to use for max acceleration and max yaw rate, a small simulation was done. This resulted in $a_{max} = 0.42\,\mathrm{m\,s^{-2}}$ and $\omega_{max} = 1.2\,\mathrm{rad\,s^{-1}}$.

5.4 Alternative methods

During the work with this thesis, it has become quite apparent that the mode switching problem for a risk-mitigating mode supervisor can be solved in many different ways. Therefore, a few thoughts on alternative methods are presented in this section. These have not been pursued in this thesis because of time limitations but might be good solutions to the problem.

Firstly, an alternative is to use a simulator to predict the behavior of the vessel during execution of the available modes. If a simulator of sufficient fidelity is available and has a short enough run time such that results are quickly available, this is possible. One would then simulate each available mode, for example, crash stop, evasive maneuver starboard, and evasive maneuver port as used above. These simulations are then initialized with the current state of the ship and obstacles, current, waves, wind, etc., to best possible represent the current situation. Then, each simulation will simulate a given time ahead, large enough so that the result of each maneuver is clear. This will result in three different trajectories for the ship. These are then evaluated to see which performed best given certain criteria. An example of such criteria is for example the closest distance to the critical obstacle region. In this case, the best alternative is to choose the mode that keeps the largest distance to the obstacle. Otherwise, one can use a risk function as in Subsection 5.3.2 and choose the mode that has the lowest maximum risk during the maneuver.

Secondly, the obstacle representation can be different. Most obstacles relevant to this application (boats, kayaks, etc.) have a slender shape, and thus a critical region shaped like a circle might not be the optimal choice. For example, an ellipsis can be used to better represent the real shape of the obstacle. This will also likely improve the selection of MRC because the object is represented better. For example, an evasive maneuver will be more feasible when on course to colliding with another vessel head-on. Similarly, a crash stop might be more sensible when on a crossing collision course. This is because the TS will be wider on a crossing course than head-on. This is not accounted for with a circular critical region. However, this may complicate the indicator function when formulated as the RF presented here when the radius is not the same in every direction. That being said, there might exist alternative formulations that can more easily account for an elliptical area.

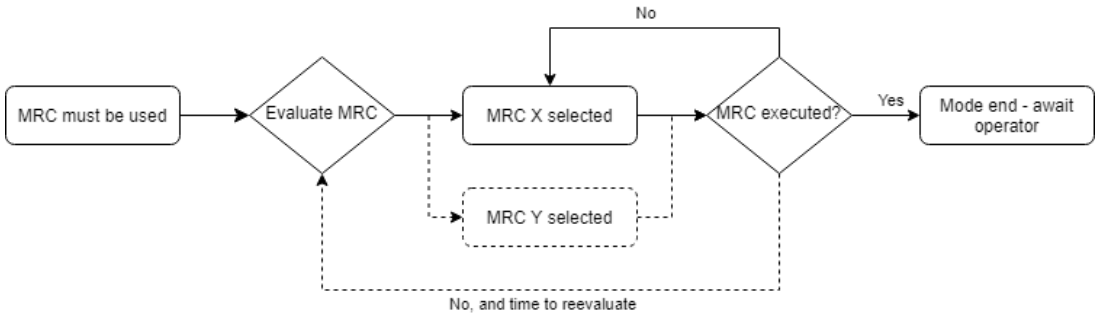

Figure 5.4: MRC switching flow. The dotted lines represent an alternative method with reevaluation, while the solid lines represent the proposed solution.

Thirdly, one can imagine more advanced forms of indicator functions. A method that is used for the identification of states that are not directly observable is hidden Markov models (HMM), as described in Reilly (2020). Here, one would define the different modes of the system as states Q and the information that is available from the SA system as observations O. To complete the model, one would need to quantify the transition probabilities of moving from one state to another, together with the probability of observing o_t when the system is in state q_i. Then, if all this data is supplied, the HMM can be used to determine the most probable state given the observations. However, quantifying the necessary data might be difficult when little knowledge about the system is available. A method to get this data might be to simulate a lot of situations with different parameters to get initial values of the probabilities which also can be improved using operational data during real operation. A challenge with this can be that nominal operation normally is overrepresented in data from real operation, as emergency situations are rare. Another challenge is that it is more of a black box than the methods proposed in this thesis, which might be a challenge regarding assurance of the system.

In this thesis, it is assumed that an MRC-mode is to be completed before new modes are considered. This then implicitly assumes that the mode that is selected as the best when the maneuver is initiated, remains the best mode for the duration of the maneuver. This is not necessarily true. During the maneuver, things can change, both external and internal factors. A result can then be that the MRC selected does not have the lowest risk anymore. To mitigate this, it is possible to reevaluate the risk while the MRC is executed. However, care must be taken to avoid that the mode is changed back and forth too much, as this might lead to risk in itself because of unpredictable behavior. A possibility is to reevaluate the mode at certain intervals. The difference between the proposed method and one with reevaluation is illustrated in Figure 5.4.

Chapter 6

Guidance system

The guidance system presented in this chapter aims to solve the guidance problem presented in Section 4.2. It will be a hybrid system, comprised of four guidance functions, depending on the mode. These are used for undocking/crossing, docking, evasive maneuvers, and DP, respectively. Each section will provide the equations and theory that go into the calculation of the necessary parameters.

6.1 Undocking and crossing

The guidance function in undocking and crossing is based on the same principle; guidance based on two path parameters. It is a design based on Skjetne (2020c), Marley (2021) and Åsheim (2021). Additionally, Jensen (2020) has used a similar method with two path parameters but with a different approach for obstacle avoidance. First, $\mathbf{p_0}$ and $\mathbf{p_t}$ is defined as the initial and final waypoints for the phase, respectively. These are assumed to be available from a high-level planner. Then the path parameters $s_1 \in [0, 1]$ and s_2 are used to continuously parametrize the desired path, according to (Marley, 2021):

$$\mathbf{p_d}(s) := \mathbf{p_0} + L(s_1\mathbf{T} + s_2\mathbf{N}), \tag{6.1}$$

where $L = |\mathbf{p_t} - \mathbf{p_0}|$ is the distance between the waypoints, $\mathbf{T}$ is the unit tangent vector along the straight line between the waypoints and $\mathbf{N}$ is the unit normal vector. These are defined as

$$\mathbf{T} := \frac{\mathbf{p}_2 - \mathbf{p}_1}{|\mathbf{p}_2 - \mathbf{p}_1|}, \quad \mathbf{N} := \begin{bmatrix} 0 & -1 \\ 1 & 0 \end{bmatrix} \frac{\mathbf{p}_2 - \mathbf{p}_1}{|\mathbf{p}_2 - \mathbf{p}_1|}. \tag{6.2}$$

With this parametrization, s_1 determines the position along the straight-line path, and s_2 determines the deviation from this path in the direction normal to the straight-line. The path parameter vector is $\mathbf{s} = \begin{bmatrix} s_1 & s_2 \end{bmatrix}^\top$. With $s_2 = 0$, the path is a straight line parametrization, and a non-zero s_2 is used for collision avoidance by increasing the deviation from the straight-line path in the normal direction. The speed assignment for s_1 is given as in Skjetne (2020c):

$$\dot{s}_1 = v_p\left(t, s_1\right) = \sigma_p(t)\frac{u_s\left(s_1\right)}{\left|\mathbf{p}_d^{s_1}\right| + \varepsilon}, \tag{6.3}$$

where $\sigma_p : \mathbb{R}_{\geq 0} \to \{0, 1\}$ is an activation signal of the motion and $\mathbf{p}_d^{s_1}$ is the derivative of the desired position with respect to s_1. $0 < \varepsilon \ll 1$ is a small number included to avoid division by zero if $\mathbf{p_0} = \mathbf{p_t}$

Table 6.1: Definition of parameters for speed profile

Parameter	Explanation	Value undocking	Value crossing
$\bar{u}_\beta$	Speed	0.8	0.5
$\bar{a}_\beta$	Acceleration	0.2	0.2
λ	Small number	0.0001	
Δ_{u_s}	Gain for slope at $s_1 = 1$	3	

and u_s is the speed profile. The speed profile from Skjetne (2020c) is altered a bit to give a smooth acceleration also in the transition between undocking and crossing. The following speed profile increases the speed up to max speed in undocking and then further up to max speed in crossing when this mode is entered, and then decreases down to zero speed towards then end of the crossing phase. Let $m = 1$ correspond to docking mode and $m = 2$ correspond to crossing mode. Then the speed profile is

$$u_s(s_1) = \begin{cases} \bar{u}_{\beta,d} \tanh\left(k_\beta (s_1 + \lambda)\right) & m = 1 \\ \bar{u}_{\beta,d} + \bar{u}_{\beta,c} \tanh\left(k_\beta (s_1 + \lambda)\right) & s_1 \in \left[-\lambda, \frac{1-\lambda}{2}\right), m = 2 \\ (\bar{u}_{\beta,d} + \bar{u}_{\beta,c}) \tanh\left(k_\beta \frac{(1+\lambda-s_1)}{\Delta_{u_s}}\right) & s_1 \in \left[\frac{1-\lambda}{2}, \infty\right), m = 2. \end{cases} \tag{6.4}$$

Here, the gain k_β is set to limit the desired acceleration. It is computed as

$$k_\beta = \frac{|\mathbf{p}_d(\mathbf{s})|}{\bar{u}_\beta^2} \bar{a}_\beta, \tag{6.5}$$

with parameters for the correct phase.

The parameters in the speed profile determine the behavior of the vessel and are defined in Table 6.1. Note that the speed parameters $u_{\beta,d}$ and $u_{\beta,c}$ are added together in Equation 6.4 such that the value in crossing is the sum of these. The tangential path parameter s_1 varies between 0 and 1 during each mode and is reset when crossing is initiated.

As a baseline, $s_2 = 0$, and

$$\dot{s}_2 = k \tanh \frac{s_2}{\Delta_{\dot{s}_2}}. \tag{6.6}$$

This expression for $\dot{s}_2$ is zero for $s_2 = 0$ and ensures that the value decreases to zero again when s_2 is nonzero. The gains k and $\Delta_{\dot{s}_2}$ decides the rate of decrease and the slope at $s_2 = 0$, respectively. This is to lead the vessel back on the straight line path after avoiding a obstacle. A CBF is used to check if the assigned path derivative vector $\dot{\mathbf{s}} = \begin{bmatrix} \dot{s}_1 & \dot{s}_2 \end{bmatrix}^\top$ are safe. If the result is that it is not safe, then $\dot{\mathbf{s}}$ is updated to achieve safety. The CBF is defined as

$$B(\mathbf{s}) := |\mathbf{p_d}(\mathbf{s}) - \mathbf{p_o}| - r_o, \tag{6.7}$$

where $\mathbf{p_o}$ is the position of the obstacle and r_o is the radius of the obstacle region. B is positive when the vessel is outside r_o and negative when inside. The time derivative of B is

$$\dot{B}(\mathbf{s}) = \frac{\mathbf{p}_d(\mathbf{s})^\top}{|\mathbf{p}_d(\mathbf{s}) - \mathbf{p}_o|} \mathbf{p}_d^s(\mathbf{s}) \dot{\mathbf{s}}. \tag{6.8}$$

Safe path parameters are found by ensuring that

$$\dot{B}(\mathbf{s}) \geq -\alpha(B(\mathbf{s})), \tag{6.9}$$

with α being a extended class-κ function. This is, as in Marley (2021), chosen to be:

$$\alpha(B(\mathbf{s})) = \frac{1}{T_b} B(\mathbf{s}). \tag{6.10}$$

$T_b > 0$ is a time constant dependent on the vessel's properties. The constraint on $\dot{B}(\mathbf{s})$ allows B to decrease when the vessel is far away from the obstacle region while forcing $\dot{B}(\mathbf{s})$ to be non-negative when the vessel is close to, and on the boundary of obstacle region. If the path derivatives are found to be unsafe, then a new pair of derivatives are found by minimizing the deviation from desired to safe path derivatives. This is done through a QP problem. For this purpose, the deviation between safe and desired derivatives is defined as $\mathbf{x} = \dot{\mathbf{s}}_s - \dot{\mathbf{s}}_d$. Then the QP problem

$$\begin{aligned} \min_{\mathbf{x}} \quad & \frac{1}{2}\mathbf{x}^\top \mathbf{Q}\mathbf{x} \\ \text{s.t.} \quad & \mathbf{A}\mathbf{x} \leq \mathbf{b} \end{aligned} \tag{6.11}$$

can be solved. Here, the constraint represent Equation 6.9. To find $\mathbf{A}$ and $\mathbf{b}$, Equations 6.8 and 6.10 are inserted into 6.9. In the following, it is left out that $\mathbf{p_d}$ is a function of $\mathbf{s}$ for brevity. Then, the following is obtained:

$$\begin{aligned} -\frac{\mathbf{p}_d^\top}{|\mathbf{p}_d - \mathbf{p}_o|}\mathbf{p}_d^s \dot{\mathbf{s}}_s &\leq \frac{1}{T_b}B \\ -\frac{\mathbf{p}_d^\top}{|\mathbf{p}_d - \mathbf{p}_o|}\mathbf{p}_d^s (\dot{\mathbf{s}}_s - \dot{\mathbf{s}}_d) &\leq \frac{1}{T_b}B + \frac{\mathbf{p}_d^\top}{|\mathbf{p}_d - \mathbf{p}_o|}\mathbf{p}_d^s \dot{\mathbf{s}}_d \\ \mathbf{A}\mathbf{x} &\leq \mathbf{b}, \end{aligned} \tag{6.12}$$

and thus $\mathbf{A}$ and $\mathbf{b}$ is defined as

$$\mathbf{A} = -\frac{\mathbf{p}_d^\top}{|\mathbf{p}_d - \mathbf{p}_o|}\mathbf{p}_d^s, \qquad \mathbf{b} = \frac{1}{T_b}B + \frac{\mathbf{p}_d^\top}{|\mathbf{p}_d - \mathbf{p}_o|}\mathbf{p}_d^s \dot{\mathbf{s}}_d. \tag{6.13}$$

The safe path derivative vector can then be found from the solution of the QP problem as $\dot{\mathbf{s}}_s = \mathbf{x} + \dot{\mathbf{s}}_d$. This ensures that s_2 is activated when necessary to deviate from the nominal path to avoid obstacles. For the controller that should be used in this mode, it is also necessary to compute the derivative of $\mathbf{p}_d$ with respect to $\mathbf{s}$. Differentiating the expression in Equation 6.1 gives

$$\mathbf{p}_d^s = L \begin{bmatrix} \mathbf{T} & \mathbf{N} \end{bmatrix}. \tag{6.14}$$

The second derivative is set to $\mathbf{p}_d^{s^2} = \mathbf{0}_{2\times 2}$ since $\mathbf{p}_d$ is a linear function of $\mathbf{s}$.

When given the waypoints and the path derivatives, the desired heading can be computed. The desired heading is set to be tangential to the combined path, and is the sum of two terms:

$$\psi_d = \psi_T + \sigma_{psi}\psi_N. \tag{6.15}$$

Here, the first term is the heading tangential to the straight-line path. The second term is a heading correction representing the change in heading because of the deviation from the straight line, multiplied with an activation function $\sigma_\psi : \mathbb{R}_{\geq 0} \to \{0, 1\}$. This is active until the vessel gets close to $\mathbf{p}_2$, where it is deactivated to obtain only the heading of the straight-line path. This is set according to

$$\sigma_{psi} = \begin{cases} 1 & s_1 \leq 0.95 \\ 0 & s_1 > 0.95 \end{cases}. \tag{6.16}$$

The heading terms are computed according to

$$\psi_T = \text{atan2}(p_{t,y} - p_{0,y}, p_{t,x} - p_{0,y}), \tag{6.17}$$

$$\psi_N = \text{atan2}\left(\frac{\dot{s}_2}{\mathbf{T}}, \dot{s}_1\right). \tag{6.18}$$

6.2 Docking

The nominal guidance in the docking phase is an improvement of the guidance function in Moen (2020), which is based on the autonomous docking functionality developed by Gauslaa (2020). The principle here is to divide the docking operation into two phases: the first take the vessel to a position just outside the dock with a correct heading, and the second consists of slowly moving closer until docking is completed by making contact with the dock, or reaching a desired distance from the dock.

For the first phase, two waypoints are placed between the initial position and the position where the final phase should start. This gives a total of 4 waypoints defined as:

$$\mathbf{p}_3 = \mathbf{p}_{dock} + \mathbf{R}_b^n \begin{bmatrix} 0 \\ d_{dock} \end{bmatrix}, \tag{6.19a}$$

$$\mathbf{p}_2 = \mathbf{p}_3 + \mathbf{R}_d^n \begin{bmatrix} 0 \\ 0.5L \end{bmatrix} \tag{6.19b}$$

$$\mathbf{p}_1 = \mathbf{p}_2 + \mathbf{R}_d^n \begin{bmatrix} 0.5\Delta_x \\ 0.5\Delta_y \end{bmatrix} \tag{6.19c}$$

$$\mathbf{p}_0 = \begin{bmatrix} x_0 \\ y_0 \end{bmatrix}. \tag{6.19d}$$

Here $d_{dock} = 1.5L$ is the distance from last waypoint to the dock, which is the desired length of phase two. L is the vessel length. The position at the start of the docking operation is given as $\mathbf{p}_o = \begin{bmatrix} x_0 & y_0 \end{bmatrix}^\top$. The distance differences Δ_x and Δ_y is the distance from $\mathbf{p}_0$ to $\mathbf{p}_3$, and is given by:

$$\begin{bmatrix} \Delta x \\ \Delta y \end{bmatrix} = \mathbf{R}_b^n \mathbf{p}_0 - \mathbf{R}_b^n \mathbf{p}_2. \tag{6.20}$$

Furthermore, waypoints are used to produce desired position and heading. This follows the method of Gauslaa (2020). Here, hybrid path parametrization is used to generate a path from the n WPs, as described by Skjetne (2005). This ensures a sufficiently differentiable and continuous path. The path is parametrized by $s_1 \in \begin{bmatrix} 0, & N \end{bmatrix}$, where $N = n - 1$. This gives N subpaths of the total path. For a given s_1, then the desired position is $\mathbf{p}_{d,1}(s_1)$. The details of this path parametrization are given in Appendix B.

In phase two, the starting position is at $\mathbf{p}_3$, with heading normal to the dock. Then, the vessel should continue straight forward with controlled speed while keeping the heading constant. The desired position for this phase in then computed as:

$$\mathbf{p}_{d_2}(s1, s2) = s_2 \mathbf{T}(s_1), \tag{6.21}$$

where $\mathbf{T}$ is the unit tangent vector of the desired path, and s_2 is a path parameter for phase two. In this phase, the distance sensors of the vessel will be used, as described in Section 2.11. From these, the distances d_1 and d_2 from port and starboard sensors are recieved. In the guidance function the distance $d = min\{d_1, d_2\}$ is used. In the guidance law, two activation functions $\sigma_{dock}, \sigma_\psi : \mathbb{R}_{\geq 0} \to \{0, 1\}$ are used. These are defined in Table 6.2. The combined guidance law of the docking phase is:

Table 6.2: Definition of activation functions for docking phase.

Parameter	Function	Condition for activation	Mathematical condition
σ_ψ	Apply heading correction	Arrived at final waypoint of phase 1	$s_1 > N - 0.01$
σ_{dock}	Start phase two of docking	Heading normal to dock and heading correction applied	$\lvert atan2(d_1 - d_2, y_{d_1} - y_{d_2})\rvert < 2^\circ$ && $\sigma_\psi == 1$

$$\dot{s}_1 = v_{s_1} = \frac{u_a}{|\mathbf{p}_{d_1}(s_1)|} \tanh\left(\frac{N - s_1}{\Delta_u}\right), \tag{6.22a}$$

$$\dot{s}_2 = \sigma_{\text{dock}} v_{s_2} = \sigma_{\text{dock}} u_{\text{dock}} \tanh\left(\frac{\tilde{d}}{\Delta_p}\right), \tag{6.22b}$$

$$\begin{aligned}\psi_d &= \psi_{d_1}(s_1) + \sigma_\psi \psi_{\text{corr}} \\ &= \text{atan2}\left(y^s_{d_1}(s_1), x^s_{d_1}(s_1)\right) + \sigma_\psi \,\text{atan2}(\Delta d, \Delta l),\end{aligned} \tag{6.22c}$$

$$\mathbf{p}_d = \mathbf{p}_{d_1}(s_1) + \mathbf{p}_{\text{dock}}(s_1, s_2) = \mathbf{p}_{d_1}(s_1) + s_2 \mathbf{T}_d(s_1). \tag{6.22d}$$

Table 6.3: Constants for docking guidance

Parameter	Definition	Value
u_a	Desired approach speed	$0.2\,\text{m}\,\text{s}^{-1}$
Δ_u	Slope of v_{s_1} as vessel approaches final WP	0.1
u_{dock}	Desired docking speed	$0.05\,\text{m}\,\text{s}^{-1}$
d_{ref}	Docking distance	$0.2\,\text{m}$
Δ_p	Slope of v_{s_2} as vessel approaches final docking position	0.5

Here, N is the number of waypoints in phase 1, and $\tilde{d} = d - d_{ref}$ is the offset from the desired docking distance. Description of the rest of the parameters is in Table 6.3. (6.22a) is the derivative of the desired position along the path, and represents speed assignment for phase 1. This makes the speed equal to the desired approach speed in normal operation. However, the tanh-component does one of three things, depending on the current position along the path:

1. **Positive speed:** in most cases before the vessel reaches the final waypoint, tanh gives a positive value close to 1.
2. **Slow speed:** when the vessel approaches the final waypoint, i.e when $(N - s_1) \to 0$, tanh goes to zero as well. This means that the desired speed goes to zero.
3. **Negative speed:** if the vessel passes the final waypoint, then tanh turns negative to lead the vessel back.

(6.22b) is the speed assignment for phase two. This is zero as long as the activation signal σ_{dock} is zero. When the docking is activated, then the speed is the desired speed multiplied with a tanh-component which has the same functionality as in the expression of $\dot{s}_1$, but used on $\tilde{d}$, so that speed is reduced if the vessel is closer to the dock than the reference signal.

The desired heading in (6.22c) consists of two parts. The first is the angle tangential to the path, while the second is a heading correction that is applied when σ_{psi} is 1. The measurements from the distance sensors are used to ensure that the desired heading is normal to the dock.

Lastly, (6.22d) calculates the desired position based on the path parameters. With $s_2 = 0$, desired position will move along the path as s_1 increases from 0 to N. As $s_1 = N$, the vessel has reached the final waypoint, and s_2 increases such that the desired position moves from $\mathbf{p}_3$ along the tangent vector towards the dock.

6.3 Guidance in MRC-modes

6.3.1 Evasive maneuver

When this mode is activated, heading-based guidance should be used. The guidance function shall provide a desired heading such that the vessel enters a *turning circle* maneuver, i.e. a maneuver that takes the vessel into a hard turn. This maneuver should last until the vessel has turned $90°$. Additionally, the guidance function should provide a desired speed reference that decreases the speed towards the end of the maneuver.

When the maneuver is initiated, the heading reference is set to $\psi_{ref} = \psi_{init} + q\frac{\pi}{2}$, where ψ_{init} is the heading of the vessel at the start of the maneuver. To account for both starboard and port maneuvers, the variable $q = \{-1, 1\}$ is used to assign the correct turning direction. To generate a smooth reference for the controller, a third-order reference model from Fossen (2021) is used. This has the desired state $\mathbf{x}_d = \begin{bmatrix}\psi_d & r_d & \dot{r}_d\end{bmatrix}^\top$. The state-space representation is

$$\dot{\boldsymbol{x}}_d = \boldsymbol{A}_d \boldsymbol{x}_d + \boldsymbol{B}_d \psi_{ref}, \tag{6.23}$$

where

$$\mathbf{A}_d = \begin{bmatrix} 0 & 1 & 0 \\ 0 & 0 & 1 \\ -\omega_n^3 & -(2\zeta+1)\omega_n & -(2\zeta+1)\omega_n \end{bmatrix} \quad , \quad \mathbf{B}_d = \begin{bmatrix} 0 \\ 0 \\ \omega_n^3 \end{bmatrix}. \tag{6.24}$$

This reference model corresponds to a low-pass filter cascaded with a mass-damper-spring system. It ensures smooth signals for the three elements in $\mathbf{x}_d$. The parameters in the reference model are chosen such that the desired heading changes quickly to give a quick turn. The values used are $\omega_n = 1$ and $\zeta = 1$.

For the speed reference, a second-order reference model is used, again from Fossen (2021). The desired state $\mathbf{x}_{du} = \begin{bmatrix}u_d & \dot{u}_d\end{bmatrix}^\top$ gives the states space representation

$$\dot{\boldsymbol{x}}_{du} = \boldsymbol{A}_{du} \boldsymbol{x}_{du} + \boldsymbol{B}_{du} u_{ref}, \tag{6.25}$$

where

$$\mathbf{A}_{du} = \begin{bmatrix} 0 & 1 \\ -\omega_n^2 & -2\zeta\omega_n \end{bmatrix} \quad , \quad \mathbf{B}_{du} = \begin{bmatrix} 0 \\ \omega_n^2 \end{bmatrix}. \tag{6.26}$$

The parameters in the reference model are the same as for the heading version. This reference model is used with the reference speed $u_{ref} = 0$, so that the reference model provides a smooth transition towards zero speed. However, the reference model is not used until the vessel has avoided the yellow area. Until

this, the desired speed is kept at the same value as the vessel had when starting the maneuver, u_{init}. The risk indicating function R is used to check this, so the desired speed is then:

$$u_d = \begin{cases} u_{init} & R > 0 \\ \mathbf{x}_{du}(1) & R \leq 0 \end{cases}. \tag{6.27}$$

6.3.2 End of emergency maneuver

Since switching from MRC and back to nominal control modes is not considered a task for the autonomous system, both MRC-modes transition to DP-mode when the maneuver is finished. This is defined for both crash stop and evasive maneuvers as when $u < 0.1\,\mathrm{m\,s^{-1}}$. Then, the nominal backstepping controller should be used, and therefore the same parameters as in the CBF-based guidance in Section 6.1 must be provided. When DP-mode is entered, these are defined as

$$\boldsymbol{\eta}_d = \boldsymbol{\eta}_{init}, \qquad \mathbf{p}_d^{\mathbf{s}} = \mathbf{0}_{2\times 2}, \qquad \mathbf{p}_d^{\mathbf{s}^2} = \mathbf{0}_{2\times 2}. \tag{6.28}$$

Here, $\boldsymbol{\eta}$ is the position vector of the vessel when DP-mode is entered. The path derivatives are set to zero matrices because the desired position is kept constant. This position is kept until nominal operation is resumed on a signal from an operator that has ensured that it is safe.

Chapter 7

Control system

In this chapter, the proposed control design will be presented. This will solve the maneuvering control problem presented in Section 4.3. First, the high-level controller which calculates the desired control forces will be presented for both nominal operation and MRC, followed by a thrust limitation function made to maintain realism in the simulation. Similar to the guidance system, there will be different controllers in a hybrid structure, used for different modes.

7.1 Cascade-backstepping

In nominal operation, a cascaded backstepping design is used for the high-level control. It is assumed that the states $\boldsymbol{\eta}$ and $\boldsymbol{\nu}$ are available through an observer. Additionally, it is assumed that the desired pose $\boldsymbol{\eta}_d(\mathbf{s})$ and relevant derivatives are available from the guidance system, as well as the speed assignment on the path variables given by:

$$\mathbf{v}(t,s) := \begin{bmatrix} v_1(t,s_1,s_2) \\ v_2(t,s_1,s_2) \end{bmatrix}. \tag{7.1}$$

The path is parametrized by $\mathbf{s} = col(s_1, s_2)$. The design follows that of Jensen (2020) which also has desired path parametrized by two path parameters. This is based on Skjetne (2020a). The control law is designed for two subsystems: $\boldsymbol{\eta} \to \boldsymbol{\eta}_d$ and $\boldsymbol{\nu} \to \boldsymbol{\alpha}$. This divides the design into two steps, where the second can be done first.

7.1.1 Step 2

The virtual control $\boldsymbol{\alpha}(t,s,\eta)$ and the derivative $\dot{\boldsymbol{\alpha}}$ is assumed to be available. Then the objective is to control the error variable

$$\mathbf{z}_2 = \boldsymbol{\nu} - \boldsymbol{\alpha} \tag{7.2}$$

exponentially to zero. Differentiating this gives, by using Equation 2.1:

$$\mathbf{M}\dot{\mathbf{z}}_2 = \mathbf{M}\dot{\boldsymbol{\nu}} - \mathbf{M}\dot{\boldsymbol{\alpha}} = -\mathbf{D}\boldsymbol{\nu} + \boldsymbol{\tau} + \mathbf{R}(\psi)^\top - \mathbf{M}\dot{\boldsymbol{\alpha}}. \tag{7.3}$$

Let the control Lyapunov function for this step be

$$V_2 = \frac{1}{2}\mathbf{z}_2^\top \mathbf{M}\mathbf{z}_2, \tag{7.4}$$

with derivative

$$\dot{V}_2 = \mathbf{z}_2^\top \mathbf{M}\dot{\mathbf{z}}_2 = \mathbf{z}_2^\top(-\mathbf{D}\boldsymbol{\nu} + \boldsymbol{\tau} + \mathbf{R}(\psi)^\top - \mathbf{M}\dot{\boldsymbol{\alpha}}). \tag{7.5}$$

Then the control law

$$\boldsymbol{\tau} = -\mathbf{K}_2\mathbf{z}_2 + \mathbf{D}\boldsymbol{\nu} + \mathbf{R}(\psi)^\top\mathbf{b} + \mathbf{M}\dot{\boldsymbol{\alpha}}, \quad \mathbf{K}_2 = \mathbf{K}_2^\top > 0 \tag{7.6}$$

yields

$$\dot{V}_2 = -\mathbf{z}_2^\top(\mathbf{D} + \mathbf{K}_2)\dot{\mathbf{z}}_2 \leq 0 \tag{7.7}$$

and

$$\mathbf{M}\dot{\mathbf{z}}_2 = -\mathbf{D}\mathbf{z}_2 - \mathbf{K}_2\mathbf{z}_2. \tag{7.8}$$

This makes the equilibrium point $\mathbf{z}_2 = \mathbf{0}$ for the $\dot{\boldsymbol{z}}_2$-subsystem uniformly globally exponentially stable. Here, $\mathbf{K}_2$ is the control gain for this control step.

7.1.2 Step 1

Next the virtual control $\boldsymbol{\alpha} = col(\boldsymbol{\alpha}_p, \alpha_\psi)$ is designed in step 1 such that the $\boldsymbol{z}_1$-subsystem is stabilized. It is assumed that desired position $\mathbf{p}_d$, desired heading ψ_d and the desired speed assignment $\mathbf{v}$ is available from the guidance module. The error variables are defined as:

$$\mathbf{z}_1 := \begin{bmatrix} \mathbf{z}_{1,p} \\ z_{1.\psi} \end{bmatrix}, \qquad \mathbf{z}_{1,p} := \mathbf{R}_2(\psi)^\top(\mathbf{p} - \mathbf{p}_d), \qquad z_{1,\psi} := \text{ssa}(\psi - \psi_d), \tag{7.9}$$

$$\boldsymbol{z}_2 := \begin{bmatrix} \mathbf{z}_{2,p} \\ z_{2,\psi} \end{bmatrix}, \qquad \mathbf{z}_{2,p} := \mathbf{v} - \boldsymbol{\alpha}_p, \qquad z_{2,\psi} := r - \alpha_\psi. \tag{7.10}$$

Here *ssa()* is the smallest signed angle function, which maps the heading error into the interval $[-\pi, \pi)$. The control design is done individually for position and heading. Starting with position, where a maneuvering design is done. Differentiating the position error variable gives

$$\mathbf{z}_{1,p} = \dot{\mathbf{R}}_2(\psi)^\top(\mathbf{p} - \mathbf{p}_d) + \dot{\mathbf{R}}_2(\dot{\mathbf{p}} - \mathbf{p}_d^{s_1}\dot{s}_1 - \mathbf{p}_d^{s_2}\dot{s}_2) \tag{7.11a}$$

$$= -r\mathbf{S}_2\mathbf{z}_{1,p} + \mathbf{z}_{2,p} + \boldsymbol{\alpha}_p - \dot{\mathbf{R}}_2(\psi)^\top\mathbf{p}_d^{s_1}v_1 - \dot{\mathbf{R}}_2(\psi)^\top\mathbf{p}_d^{s_2}v_2. \tag{7.11b}$$

Then the CLF for position is defined as:

$$\mathbf{V}_{1,p} := \frac{1}{2}\mathbf{z}_{1,p}^\top\mathbf{z}_{1,p} \tag{7.12}$$

with derivative

$$\dot{\mathbf{V}}_{1,p} = \mathbf{z}_{1,p}^\top\dot{\mathbf{z}}_{1,p} = \mathbf{z}_{1,p}^\top\left[-r\mathbf{S}_2 + \mathbf{z}_{2,p} + \boldsymbol{\alpha}_p - \dot{\mathbf{R}}_2(\psi)^\top\mathbf{p}_d^{s_1}v_1 - \dot{\mathbf{R}}_2(\psi)^\top\mathbf{p}_d^{s_2}v_2\right]. \tag{7.13}$$

If the virtual control for position is

$$\boldsymbol{\alpha}_{1,p} = -\mathbf{K}_{1,p}\mathbf{z}_{1,p} + \dot{\mathbf{R}}_2(\psi)^\top\mathbf{p}_d^{s_1}v_1 + \dot{\mathbf{R}}_2(\psi)^\top\mathbf{p}_d^{s_2}v_2, \tag{7.14}$$

then the CLF derivative becomes

$$\dot{\mathbf{V}}_{1,p} = -\mathbf{z}_{1,p}^{\top}\mathbf{K}_{1,p}\mathbf{z}_{1,p} + \mathbf{z}_{1,p}^{\top}\mathbf{z}_{2,p} \tag{7.15}$$

where $\mathbf{K}_{1,p}$ is the control gain for position and must be chosen such that $\mathbf{K}_{1,p} = \mathbf{K}_{1,p}^{\top} > \mathbf{0}$.

By assuming that the time derivative of the desired heading $\dot{\psi}_d$ is available from guidance, then a direct tracking design is done for the heading control. Differentiating the heading error gives

$$\dot{z}_{1,\psi} = \dot{\psi} - \dot{\psi}_d = z_{2,\psi} + \alpha_{\psi} - \dot{\psi}_d. \tag{7.16}$$

With a CLF defined as

$$V_{1,\psi} = \frac{1}{2}z_{1,\psi}^2, \tag{7.17}$$

the derivative is

$$\dot{V}_{1,\psi} = z_{1,\psi}\left[z_{2,\psi} + \alpha_{\psi} - \dot{\psi}_d\right]. \tag{7.18}$$

The virtual control for heading

$$\alpha_{\psi} = -k_{1,\psi}z_{1,\psi} + \dot{\psi}_d, \quad k_{1,\psi} > 0 \tag{7.19}$$

gives

$$\dot{V}_{1,\psi} = -k_{1,\psi}z_{1,\psi}^2 + z_{1,\psi}z_{2,\psi} \tag{7.20}$$

where $k_{1,\psi} > 0$ is the heading gain. This, together with the other control gains $\mathbf{K}_{1,p}$ and $\mathbf{K}_2$, are tuned to obtain the preferred behavior of the system.

7.2 Control in MRCs

When an MRC is entered, the control objective changes. To achieve the new objective, it is desirable to have multiple controllers in a hybrid structure such that the best one can be used to fulfill the control objective with good performance. This section presents a controller for each of the selected MRCs.

7.2.1 Crash stop

As stated in Subsection 3.5.1, the output from the controller in this mode should be maximum thrust in the opposite direction of the vessel's velocity. If on a straight path, this is in negative surge direction. But if the vessel is turning, then force must also be used in sway direction. The following expression achieves this:

$$\boldsymbol{\tau}_{XY} = -\tau_{max}\frac{\boldsymbol{\nu}}{|\boldsymbol{\nu}|}. \tag{7.21}$$

Here τ_{max} is the maximum available thrust from the thrusters. In addition to counteracting the velocity with force in surge and sway, it is desirable to keep the heading constant. If not, unwanted transients can occur during the crash stop. The yaw force is computed from a PD-controller in heading (Fossen, 2021):

$$\tau_N = -K_p\text{ssa}(\tilde{\psi}) - K_d r, \tag{7.22}$$

where $\tilde{\psi} = \psi - \psi_d$ is the heading error. The desired heading angle ψ_d is set to the heading the vessel had when the crash stop maneuver begins. The controller gains K_p and K_d is found by pole placement

as shown Fossen (2021). The result is a system that is tuned by the control bandwidth ω_b and relative damping ζ. If these are set, then

$$\omega_n = \frac{1}{\sqrt{1 - 2\zeta^2 + \sqrt{4\zeta^4 - 4\zeta^2 + 2}}}\omega_b, \tag{7.23}$$

and

$$K_p = m\omega_n \tag{7.24a}$$
$$K_d = 2\zeta\omega_n m. \tag{7.24b}$$

Here, m is the mass in the yaw subsystem, corresponding to m_{33} in the vessel mass matrix. The values used for the tuning parameters are $\omega_b = 0.8$ and $\zeta = 1$. Finally, the total force vector is $\boldsymbol{\tau} = \begin{bmatrix}\boldsymbol{\tau}_{XY}^\top & \tau_N\end{bmatrix}^\top$.

7.2.2 Evasive maneuver

Since this mode uses a heading-based guidance method, then there needs to be a different controller that takes desired heading and velocity as input rather than desired position. The objective is to control the heading towards the desired heading that is computed by the guidance function, in addition to obtaining the desired surge speed u_d. To do this, the yaw force is computed by a PD-controller similar to Equation 7.22. The difference is that the yaw rate r is not controlled to 0, but to a desired rate r_d such that the yaw rate error is $\tilde{r} = r - r_d$. Then, the yaw force is

$$\tau_N = -K_p \text{ssa}(\tilde{\psi}) - K_d\tilde{r}. \tag{7.25}$$

The gains are given by Equation 7.24. At the same time, the surge velocity should be controlled by adjusting the surge force τ_X. For a starboard-port symmetric vessel like milliAmpere, surge is decoupled from sway and yaw. Then, the surge force can be calculated independently, to achieve the desired speed. To simulate a speed controller with good performance, the following expression is used to find the desired force based on the desired velocity vector $\boldsymbol{\nu}_d = \begin{bmatrix}u_d & 0 & 0\end{bmatrix}^\top$. This assumes that the model of the vessel Equation 2.1 is known with satisfactory precision.

$$\boldsymbol{\tau} = \mathbf{M}\dot{\boldsymbol{\nu}}_{\boldsymbol{d}} + (\mathbf{C} + \mathbf{D})\boldsymbol{\nu}_{\boldsymbol{d}} \tag{7.26}$$

From this, the desired surge force can be extracted as the first element in the vector, such that

$$\tau_X = \begin{bmatrix}1 & 0 & 0\\ 0 & 0 & 0\\ 0 & 0 & 0\end{bmatrix}\boldsymbol{\tau}. \tag{7.27}$$

It is worth noting that this is not a method feasible for real control systems as the system matrices, in general, can not be assumed to be known, but for this purpose, it emulates a speed controller with good performance. The total force vector is then $\boldsymbol{\tau} = \begin{bmatrix}\tau_X & 0 & \tau_N\end{bmatrix}^\top$.

7.3 Thrust limitation

As stated in Section 4.4, thruster dynamics and -allocation are not considered in this thesis. Therefore, it is not necessary to do thrust allocation in the sense of calculating individual thruster setpoints. However,

to maintain realism, the body forces that are applied should respect the maximum limits for thrust. Combined, the thrusters can produce $\tau_{f,max} 1000\,\mathrm{N}$ of force and $\tau_{N,max} = 1800\,\mathrm{N\,m}$ of moment. This can not be achieved at the same time. Therefore, the limitation should consider also what the other forces are. First, the desired force can be related to the maximum available in that DOF through *thrust coefficients* defined as following:

$$c_{t,f} = \frac{f_d}{\tau_{f,max}} \quad , \quad c_{t,N} = \frac{\tau_{d,N}}{\tau_{N,max}}. \tag{7.28}$$

Here, τ_d is desired force from the controller, and f_d is the desired linear force computed as $f_d = \sqrt{\tau_{d,X}^2 + \tau_{d,Y}^2}$. Then, a relation can be derived to limit the resulting forces, by saying that the sum of the thrust coefficients squared should satisfy

$$c_{t,f}^2 + c_{t,N}^2 = 1. \tag{7.29}$$

This relation ensures that full surge force and yaw moment can not be applied at the same time, and gives sufficient realism for this purpose. Furthermore, to solve this relation directly, it is necessary to specify one of the thrust coefficients. This is done by making two modes - one where force is prioritized and one where yaw moment is prioritized. This is represented by the variable σ_p which take values 0 and 1 respectively. Then, the maximum allowed thrust coefficients are chosen as:

$$c_{t,N} = \begin{cases} 0.8 & \sigma_p = 1 \\ \sqrt{1 - 0.8^2} = 0.6 & \sigma_p = 0 \end{cases}, \quad c_{t,f} = \begin{cases} \sqrt{1 - 0.8^2} = 0.6 & \sigma_p = 1 \\ 0.8 & \sigma_p = 0 \end{cases}, \tag{7.30}$$

if the thrust coefficient exceeds the allowable limit. This restricts the prioritized force/moment to at most 80% of maximum capacity, while the non-prioritized get the remaining capacity such that Equation 7.29 is respected.

Chapter 8

Simulation setup

8.1 MATLAB simulator

To simulate the behavior of milliAmpere, a MATLAB script that does numerical integration of the model in Equation 2.1 is used. The script was generously supplied by Emil Thyri of the Autoferry project. The hydrodynamic parameters used are the ones identified by Pedersen (2019). These can be viewed in Appendix C. As it was realized that milliAmpere is not directionally stable with the parameters used, the code was modified to simplify the model for this project. Both mass and damping matrices were made diagonal, which meant setting all off-diagonal entries to zero. This made the model easier to work with. The script uses MATLABs *ode45* method to solve the equation of motion for each timestep. The dynamics script can be seen in Appendix A.2.

The simulator is made to emulate the flow presented in Figure 4.1. It consists of a for loop running at a timestep of $h = 0.1\,\mathrm{s}$. The input to the solver is the velocity vector $\boldsymbol{\nu}$, the position vector $\boldsymbol{\eta}$ and the body forces $\boldsymbol{\tau}$. The solver then returns new position and velocity vectors, which are used in the next time step. The pseudocode for the simulator where all relevant calls to subfunctions are done can be seen in Algorithm 2, while the actual MATLAB script is presented in Appendix A.3. This script runs the mode simulator first, to determine the mode. Additionally, a function is made to change parameters during the simulation, to emulate new input from the SA system. After this, guidance and control functions are run, before the vessel dynamics script is used to compute the new position and velocity. Lastly, the data from each timestep is saved to be plotted and analyzed later. Then, the loop is repeated as many times as necessary to achieve the specified simulation time.

The implementation of all relevant functions is done in MATLAB. The code is available at GitHub[1]. The different subsystems interact as shown in Figure 4.1. In the following, the specifics of each simulation are presented. The simulations are run by running the *init_simX.m* script, where X is the simulation number. This script runs the simulation and plots the results.

[1] https://github.com/jonmmo/Automatic-control-of-passenger-ferry-with-risk-contingencies

Algorithm 2: Simulator pseudocode

```
initialization;
for each timestep do
    Determine mode by running mode supervisor;
    Change parameters according to simulation specification if needed;
    Compute the desired position by using the correct guidance function;
    Compute control forces by using correct control function;
    Obtain new position and velocity from vessel dynamics;
    Save results;
end
```

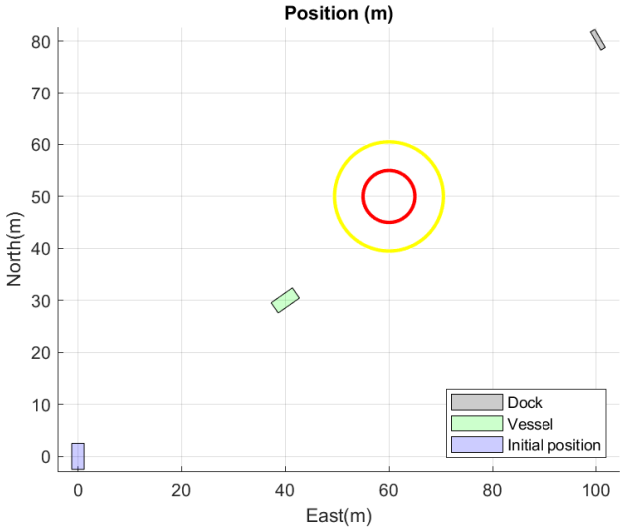

Figure 8.1: Simulation environment. Yellow and red circles represent obstacle regions.

8.2 Simulation specifications

The simulations presented in this section aim to test the performance of the proposed control system. Together, all the simulations should show strengths and weaknesses with this solution. The first few simulations are aimed at showing specific parts of the system, while the rest are to show the performance of the combined system in more complex situations. The simulations share some commonalities, which are presented first before the details of each simulation are presented. Firstly, the simulation environment is made to simulate a crossing similar to the one described in Section 2.11. It has a crossing length of $128\,\mathrm{m}$. The vessel starts at the origin with a heading of $\psi = 0°$, and arrives at a dock at $p_d = \begin{bmatrix} 80 & 100 \end{bmatrix}^\top$, with orientation $\psi_{dock} = 150°$. The environment can be seen in Figure 8.1. In many of the simulations, obstacles are placed in the way of the vessel. The obstacles are represented as stated in Section 5.3 with a yellow region to be avoided by the nominal control system and a red region to be avoided if an MRC is entered. The radiuses are set to $r_r = 5\,\mathrm{m}$ and $r_y = 10.5\,\mathrm{m}$, based on the stop length in crash stop mode.

8.2.1 Simulation 1 - nominal control system

The first simulation shall simulate a nominal crossing, i.e. no MRC-situations. Two obstacles are placed in the way of the straight-line path, and their position is known from the start such that the CBF can

react in due time. The expected behavior from the vessel is to perform a controlled undocking before a seamless switching to crossing mode is done. Here, it should be able to avoid the obstacles by turning around them and keeping a safe distance to the yellow region. Subsequently, the vessel should arrive outside the target dock close to the end waypoint. Here, the speed should be low, and switching to docking mode can be done. Then, a feasible docking path should be computed and the docking should be performed in a controlled fashion. The obstacles are placed at $\mathbf{p}_{o1} = \begin{bmatrix} 20 & 20 \end{bmatrix}^\top$ and $\mathbf{p}_{o1} = \begin{bmatrix} 50 & 62 \end{bmatrix}^\top$.

8.2.2 Simulation 2 - crash stop

Here, the objective is to show the performance of the crash stop maneuver. An obstacle is placed directly in front of the vessel at a time such that it is detected just as the vessel enters the risk zone. As the obstacle is directly in front of the vessel, the mode supervisor should choose the crash stop mode. This simulation is also used to determine the parameters of the maneuver, i.e. stop length, stop time, etc. The obstacles is placed at $\mathbf{p}_o = \begin{bmatrix} 31 & 38 \end{bmatrix}^\top$. The expected behavior is that the vessel initiates a crash stop maneuver and can stop before the red region.

8.2.3 Simulation 3 - evasive maneuver

Similar to simulation 2, this simulation is done to show the performance of the evasive maneuver control modes. Both a maneuver to port and starboard will be done. Then, the turning rate and other relevant data can be extracted, which is used in the design of the switching algorithms. The parameters to be found are similar to that of a turning circle test as seen in Figure 8.2, as described in IMO (2002). Here, the advance and transfer are the most important. The obstacle is placed at $\mathbf{p}_o = \begin{bmatrix} 33 & 35 \end{bmatrix}^\top$, and the starting point of the vessel is varied such that both the port and starboard version is tested.

8.2.4 Simulation 4 - variable detection distance

This simulation is intended to show how detection distance affects the performance of the system. The detection distance is the distance to an obstacle when the obstacle is detected. In a nominal situation, this distance is large enough such that the vessel can plan a route around the obstacle using the nominal guidance function. But if the obstacle ”suddenly” appears, such that the detection distance is shorter than the distance needed to perform a safe maneuver around, the vessel will likely enter the yellow area where an MRC is activated. In this simulation, the detection will vary such that it is possible to see how it affects the choice of MRC. For all the, the obstacle will be placed at $\mathbf{p_o} = \begin{bmatrix} 31 & 38 \end{bmatrix}^\top$. Then, the obstacle will ”appear” in the SA system at the following timings:

- At $t = 0\,\mathrm{s}$: the obstacle is visible from the beginning, so the detection distance is big enough such that the system should behave nominally.
- At $t = 48\,\mathrm{s}$: the obstacle is detected at a distance that should be enough to be able to perform a nominal maneuver around the obstacle.
- At $t = 52\,\mathrm{s}$: here, the obstacle is detected just before the vessel enters the risk zone. Thus, there is a short time where the nominal control system will try to avoid the obstacle before an MRC must be used.

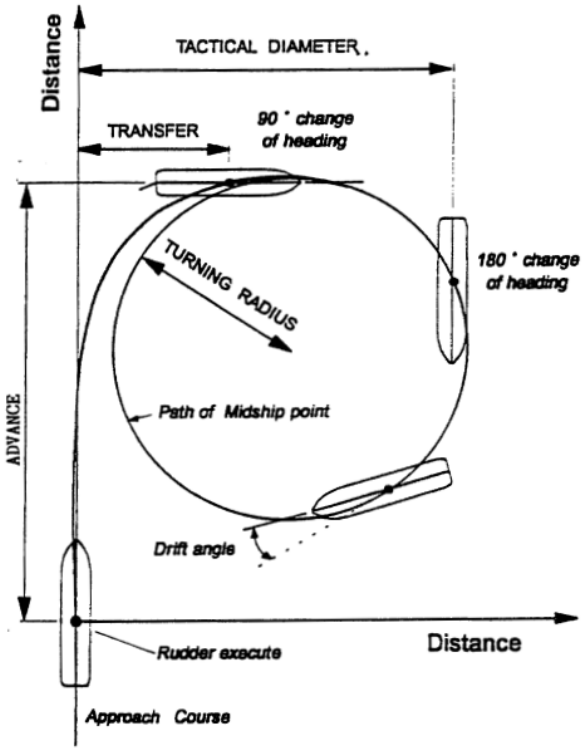

Figure 8.2: Turning circle procedure, as in IMO (2020)

- At $t = 54\,\mathrm{s}$: the obstacle is detected just as the vessel enters the risk region, and an MRC must be used straight away.

This simulation is to be done for both versions of the indicator functions, to examine if there are any differences between them in which maneuver is chosen.

8.2.5 Simulation 5 - variable intersection points

The point of this simulation is to show how the switching algorithms are affected by how and where the vessel enters the risk region. It is expected that the preferred mode is more likely to be an evasive maneuver if the vessel is headed farther to the side of the obstacle. Correspondingly, the highest probability of choosing crash stop will be when the vessel is heading straight towards the center of the obstacle. The parameters in this simulation were determined by trial and error, to get the desired behavior. The obstacle is placed at $\mathbf{p}_o = \begin{bmatrix} 33 & 35 \end{bmatrix}^\top$, and the detection time and initial position for the four different runs are given in Table 8.1, together with a description of each case.

8.2.6 Simulation 6 - multiple obstacles

The previous simulations only contain one obstacle, so the supervisor algorithm only needs to account for this. In this simulation, more obstacles are added to complicate the operation. Firstly, an obstacle is placed such that it blocks the area of the first transit waypoint to test the system's ability to replan its route and switch to crossing even if it is in the process of avoiding an obstacle. Secondly, emergency

Table 8.1: Definition of parameters for simulation 5

Run	Detection time	Initial position	Description
1	$t = 53\,\mathrm{s}$	$\boldsymbol{\eta}_I = \begin{bmatrix} 0 & 0 & 0 \end{bmatrix}^\top$	Course towards starboard side of obstacle
2	$t = 50.5\,\mathrm{s}$	$\boldsymbol{\eta}_I = \begin{bmatrix} 5 & 0 & 0 \end{bmatrix}^\top$	Course a bit starboard of the obstacle center
3	$t = 50\,\mathrm{s}$	$\boldsymbol{\eta}_I = \begin{bmatrix} 8 & 0 & 0 \end{bmatrix}^\top$	Course a bit port of the obstacle
4	$t = 48\,\mathrm{s}$	$\boldsymbol{\eta}_I = \begin{bmatrix} 13 & 0 & 0 \end{bmatrix}^\top$	Course towards port side of obstacle

switching is complicated by two obstacles placed close to each other. The first one is placed such that the best action should have been an evasive maneuver. However, the second is placed in the path where the evasive maneuver should have taken place, to check the ability to account for two obstacles in the algorithm. The expected behavior is that the vessel avoids the first obstacle and then returns to the nominal path until it encounters the two last obstacles. Here, the best mode to avoid both obstacles should be chosen.

Chapter 9

Results

In this chapter, the results from the simulations specified in Section 8.2 are presented. The results are presented through plots. For each simulation, comments about the performance are made, and the performance is compared to the expected performance.

9.1 Simulation 1

The results from this simulation are shown in Figure 9.1 and 9.2. First and foremost, one can see from the North-East plot that the vessel is able to successfully navigate from the initial position to the dock while keeping a safe distance to the yellow risk region. The vessel follows the desired position with little error. The velocity plots show that the surge velocity is increased towards transit speed, but has two ”dips”. At the same time, one can notice fluctuations in sway velocity, meaning that there has been some sideslip during the maneuver around the obstacles. The surge velocity is decreased down to a full stop before the docking phase starts, which is executed with low speed.

This simulation also illustrates some of the shortcomings of the nominal control system. Firstly, the resulting path that the vessel takes is not optimal, as it is not the shortest way from start to finish around the obstacles. The ideal behavior here would be that the vessel continued on a straight path after alternating its path to avoid the first obstacle, before returning toward the dock after avoiding the second obstacle as well. However, this has not been implemented, so the performance is as expected. Secondly, it is evident from Figure 9.2 that the guidance/control combination does not perform optimally. The heading angle cannot follow the desired heading angle reference if it has not been constant for long periods of time. This means that the vessel has been going sideways during the maneuver.

9.2 Simulation 2

The North-East plot and the various time series data for the crash stop test can be seen in Figure 9.3 and 9.4. From these, it can be seen that the vessel follows a straight path toward the waypoint by the dock up until the point where the obstacle is detected. Then, a crash stop maneuver is initiated and completed, and the vessel stop before (the center) reaches the critical region. From the time series, it is clear that

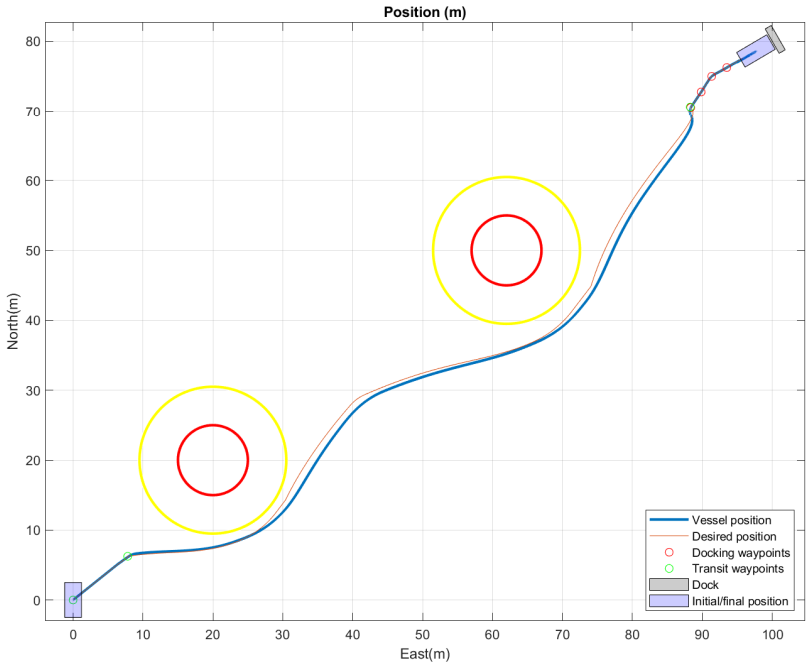

Figure 9.1: North-East plot of simulation 1. Obstacle regions in yellow and red.

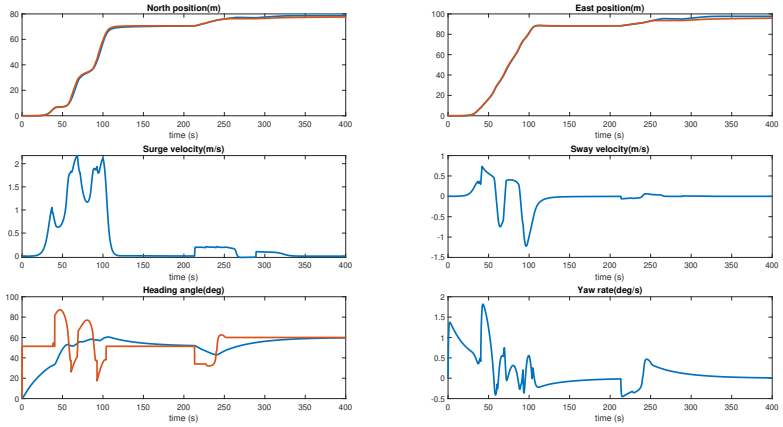

Figure 9.2: Time series data for simulation 1

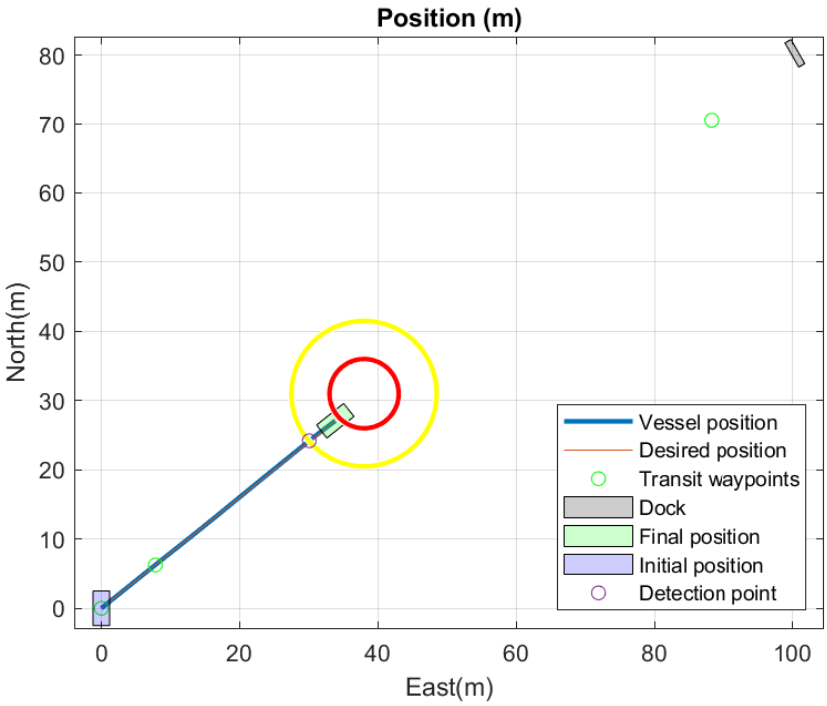

Figure 9.3: North-East plot of simulation 2. Obstacle regions in yellow and red.

the vessel reduces its velocity in both surge and sway, and the heading angle is kept at the same value as when the maneuver was initiated. The resulting stop length and -time was $l_s = 4.4\,\mathrm{m}$ and $t_s = 5.5\,\mathrm{s}$, respectively. The average acceleration from the start of the maneuver until DP-mode was entered, was $a_{avg} = 0.42\,\mathrm{m\,s^{-2}}$. The crash stop is performed just as expected.

9.3 Simulation 3

In simulation 3, the evasive maneuvers were tested. The resulting North-East plots for both versions are shown in Figure 9.5. The time series data for the two maneuvers can be seen in Appendix D.1. From the North-East plot, it is observed that the vessel enters the yellow region shortly after the obstacle is detected. In both cases, the course is towards the edge of the critical region, and an evasive maneuver is started. The vessel then uses some time before the turn has any effect. This is because of sideslip, i.e. the vessel goes sideways after it has changed heading. The resulting parameters of the maneuvers can be found in Table 9.1. Here, one can see that the numbers are similar between the two maneuvers, except for the advance. This is likely because of differences in the state of the vessel when the maneuver was started, for example slightly different initial speed. It is also worth noting that the turning rate is significantly lower than what is used in the indicator function, which implies that this implementation of an evasive maneuver does not get the most out of the vessel.

9.4 Simulation 4

First, this simulation was performed with the dynamic indicator function from Subsection 5.3.1. The resulting plot can be seen in Figure 9.6a. Here, it can be seen that in the two first runs, the obstacle is

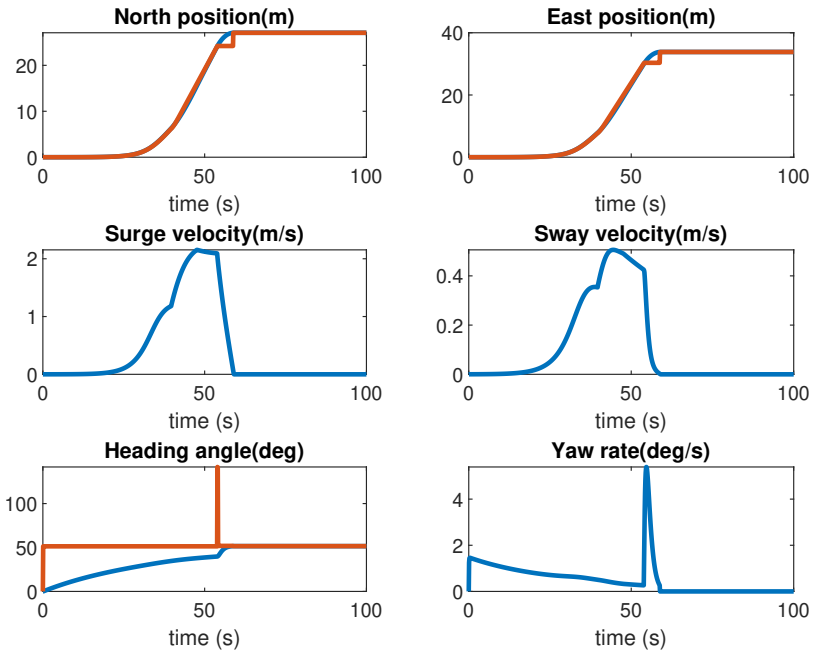

Figure 9.4: Time series data for simulation 2

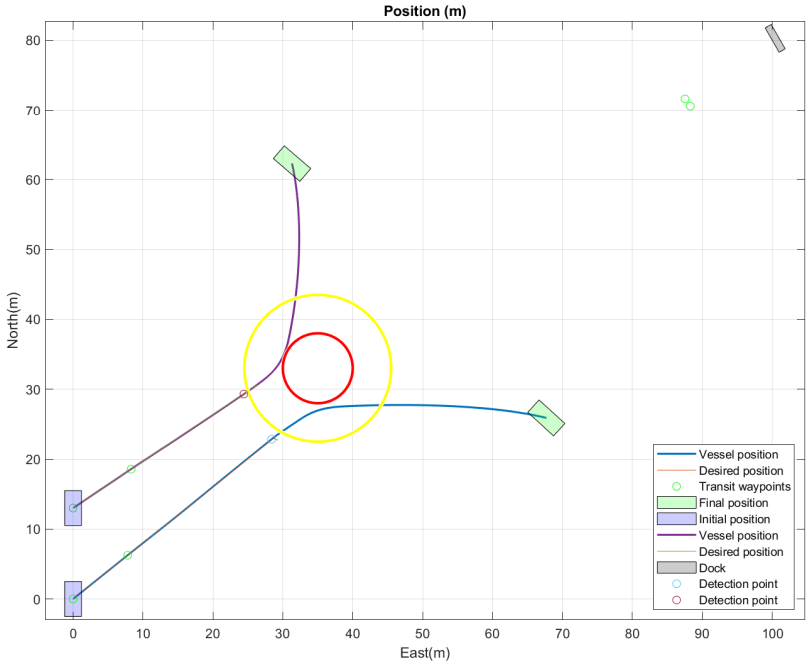

Figure 9.5: North-East plot of simulation 3. Obstacle regions in yellow and red.

Table 9.1: Parameters for evasive maneuver

Parameter	Symbol	Value SB	Value P	Description
Advance	A	$32.6\,\mathrm{m}$	$24.1\,\mathrm{m}$	Longitudinal distance from execution point to $90°$ heading change
Transfer	T	$22.1\,\mathrm{m}$	$23.5\,\mathrm{m}$	Lateral distance from execution point to $90°$ heading change
Max turning rate	r_{max}	$0.48\,\mathrm{rad\,s^{-1}}$	$-0.47\,\mathrm{rad\,s^{-1}}$	Maximum value of turning rate during maneuver
Stop time	t_s	$91\,\mathrm{s}$	$78.9\,\mathrm{s}$	Time from execution to DP-mode

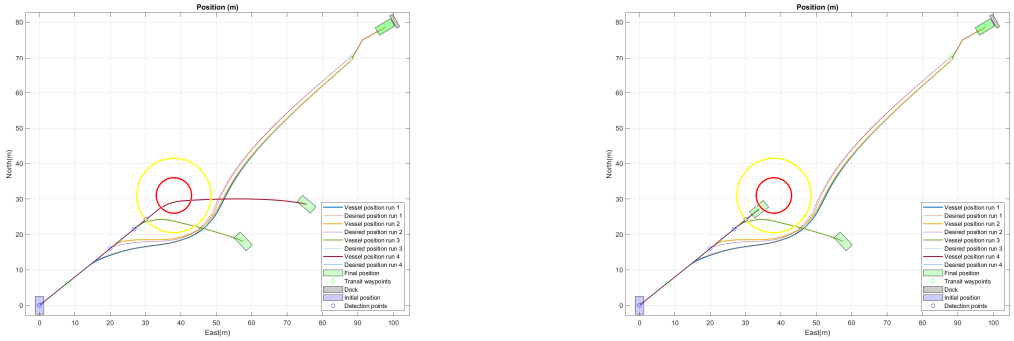

(a) Dynamics-based indicator function.

(b) Indicator function based on a RF

Figure 9.6: North-East plots for simulation 4.

detected with enough distance remaining, such that the obstacle is avoided using the nominal control system. However, the distance from the desired position is larger in the second run. In the third run, the nominal control systems attempt to avoid the obstacle as seen by the blue line representing the desired position near the detection point. When the vessel enters the risk zone, a successful evasive maneuver is performed. This is done even though the vessel is heading almost straight towards the center of the obstacle. The reason that a crash stop is not used, is most likely because a heading change already has been done by the nominal control such that a smaller heading change is necessary to avoid the critical area. Therefore, an evasive maneuver is more feasible. For run 4, the system performs an evasive maneuver that is not successful, as the path continues straight through the critical area. This is an obvious flaw with this indicator function, as a crash stop would be more feasible in this situation.

The same simulation done with the RF is shown in Figure 9.6b. For runs 1-3, the performance is the same as with a dynamic-based indicator function, but not in run 4. Here, the crash stop is selected as the best mode, which is performed successfully. Thus, the use of this indicator function results in a safe state for all runs in this simulation. The remaining two simulations are therefore only run with the RF as indicator function.

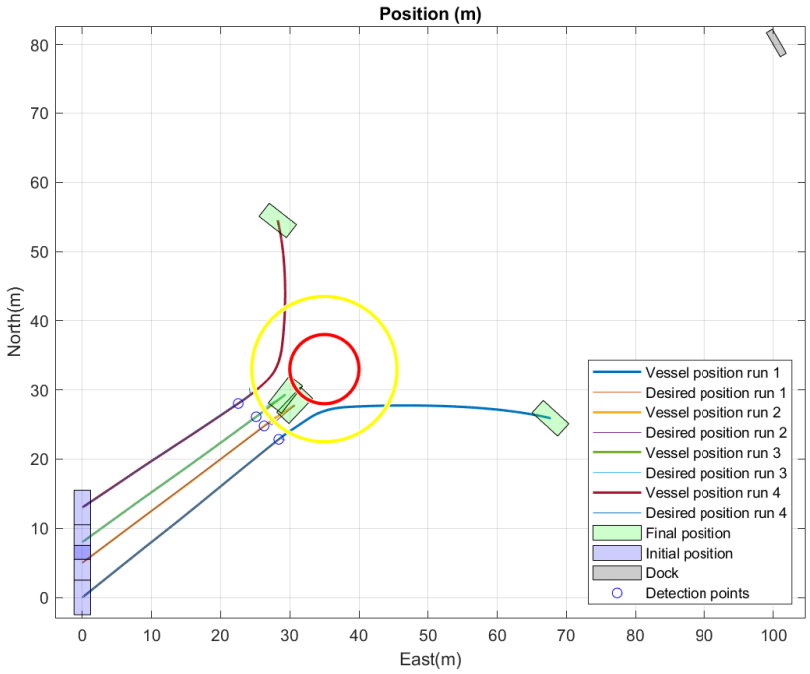

Figure 9.7: North-East plot of simulation 5. Obstacle regions in yellow and red.

9.5 Simulation 5

In this simulation, the vessel starts in a different initial position for each run, as can be seen in Figure 9.7. The result is that when the obstacle is detected, the position is different relative to the center of the obstacle. The resulting maneuvers are as expected - the two which are farthest to the side take an evasive maneuver, while the two which are directed more to the center of the obstacle perform a crash stop. All the runs result in a safe state outside the critical region.

9.6 Simulation 6

In this simulation, multiple obstacles are present. The resulting North-East plot is in Figure 9.8a. This shows that the vessel avoids the first obstacle before returning to the straight line towards the docking WP. It is also seen that the avoidance maneuver around the obstacle is started in the undocking phase. When the two other obstacles are detected, crash stop is selected as the best mode, and it is safely executed. In comparison, when the same simulation is run with only the obstacle directly in the way present, an evasive maneuver to port is selected as the best. This can be seen in Figure 9.8b. Figures D.3 and D.4 show the time series data for the two simulations. This simulation shows that the system can account for multiple obstacles and prioritize the closest one.

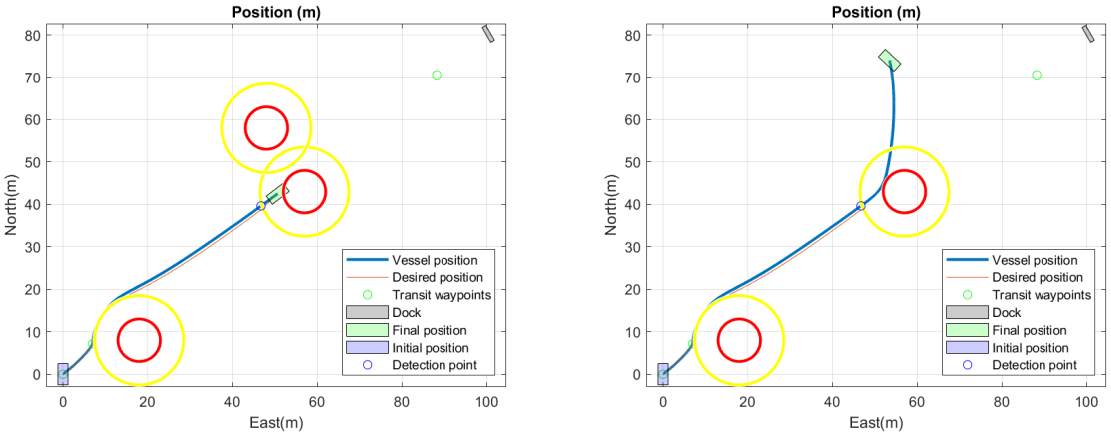

(a) Three obstacles

(b) Two obstacles

Figure 9.8: North-East plots for simulation 6

Chapter 10

Discussion

This chapter discusses the findings of this thesis. In Section 3.2, a set of MRCs is proposed for the autonomous operation of milliAmpere. In connection with this, relevant situations where an MRC is needed are presented, as well as a discussion on risk influencing factors that may lead to these. These findings are all based on brainstorming and inspiration from other sources on the subject. Therefore, it is no guarantee that the proposed set covers all possible situations, but it may serve as a good starting point. As stated in Section 2.8, an autonomous ship system must still go through a FMEA to document that the requirements for MRCs are met.

The results presented in Chapter 9 show both strengths and weaknesses with the proposed solution. In this chapter, the results will be interpreted and the factors that impact performance will be identified. The overall automatic control system has shown to be able to operate nominally while avoiding obstacles. In emergency situations where an obstacle is close by, the mode supervisor can evaluate which emergency maneuver to execute, based on the state of the system.

Although the nominal operation was successful in simulation 1, there are issues with nominal performance. This has not been the main focus during the work with this thesis, so optimal performance was not expected. The behavior might be improved considerably by tuning the backstepping controller better. The tuning was only done to achieve satisfactory performance, and thus there might be better alternatives. The controller performs well at tracking the desired position but struggles more with getting the heading equal to the desired heading, resulting in behavior where the vessel moves sideways more than normal. Small attempts at correcting this were made, but this resulted in lower precision in tracking the desired position. It was decided that for this thesis, better tracking was more important than keeping the correct heading, so more tuning was not done. Another aspect of the nominal control system is that for real operation, it is most likely to have to be COLREG-compliant. The proposed system is not that, and for this specific formulation, it seems like a lot of work. However, Thyri et al. (2020) presents a COLREG-compliant CBF formulation that works and that is tested with simulations of milliAmpere that can be of interest.

The main focus of the work with this thesis has been to develop a supervisor that can switch modes seamlessly and that includes both nominal control modes and minimum risk conditions. This has been achieved, and the indicator function using a risk function based on a CBF-formulation like presented in Subsection 5.3.2 showed to be the best. It can decide which of the emergency maneuvers is the best one, depending on which reduces the risk the most. An important aspect to consider when discussing this indicator function is that it is a momentary method. The decision on what action to execute is taken

based only on which of the actions reduces the RF most. This seems to work fine, but situations might arise where a more predictive method will be better suited. It is possible that this may be achieved through the simulation-based method discussed in Section 5.4. The dynamics-based indicator function performs worse than the RF-based one and gives a result in simulation 4 where the vessel moves through the red region. This may be because this method has oversimplified the problem slightly by not taking the advance as the heading is changed properly into account.

When it comes to the execution of the three MRC-modes treated in this thesis, this showed to be satisfactory during the simulations. The crash stop mode worked as intended. In crash stop mode it was decided to maintain a constant heading. While avoiding spin of the vessel is desired, maintaining a specific heading may not be important. It must also be noted that this maneuver becomes more complicated when thruster dynamics are considered. Regarding the evasive maneuver, there might be room for improvement. Simulation 3 shows how this mode works. From the plot, one can see that it is able to avoid the critical region, but only barely. And this is even when the vessel is heading towards the edge of the critical region. From the time series in Appendix D.1 one can see that the heading quickly goes to the desired value, but at the same time, the sway velocity increases. This means that the vessel moves sideways for a period. There might be room for improvement here, but as this is mainly to show the capabilities of the supervisor, this was not focused on.

Another factor that may have affected the performance of the evasive maneuver and led to the fact that it got so close to the critical region, is the size of the yellow region. The radius of this is set according to the crash stop length. If one wished to make the evasive maneuver available no matter where the vessel enters the yellow region, this radius could be increased up to a size where it was possible to avoid the critical region before hitting it. In the case of a small passenger ferry, this distance would likely become unnecessarily high and complicate operation. But for larger ships, it would be closer to the crash stop distance, or even smaller, such that the radius of the yellow region should be set based on the evasive maneuver parameters and not the parameters for crash stop. The most important here is that the yellow region is set such that at least one MRC is available when the region is entered.

The discussion in the last paragraph underlines the fact that the methodology for a mode supervisor like this is strongly connected to the properties of the ship. Whichever method is used for determining the most suited mode, must take into account the abilities of the ship. This has shown to be true for the MRCs involving obstacles and collision as here, but will also apply for other types of MRCs like when thrust is reduced (how is the performance with reduced thrust?) or if an anchor should be dropped (how long does it take to anchor and how much movement will it allow?). This is important, as the mode supervisor uses this data to determine which mode is best. Thus, bad estimates of the ship's properties may lead to dangerous situations.

Lastly, it is worth noting that the simplifications done during this thesis have made the problem simpler to work with than a real-world application. If measurement noise was considered, functionality for filtering out this would have to be added, and one would have to take the precision of the measurements into account, which is not done here. Thruster dynamics are not considered either. If this was modeled, the maneuvers would likely take more time since a change in thrust magnitude and direction would take some time. This could also introduce some unwanted transients that should be accounted for. When it comes to obstacle avoidance, obstacles are assumed to be stationary and only the position of the center of the vessel is considered when checking where it is relative to the obstacle. For a real application, moving obstacles must be considered, and instead of the vessel center, the edges of the vessel must be accounted for.

Chapter 11

Conclusion

This thesis set out with the objective to develop an automatic control system with risk contingencies for an autonomous passenger ferry. To do this, the use of MRCs for safe operation of autonomous ships has been investigated. Then, a set of 9 MRCs was proposed for the case study vessel milliAmpere. In connection to this, risk influencing factors and causes for using MRCs were discussed. Of the 9 MRCs, two were selected for implementation and testing: evasive maneuver and crash stop. These MRCs are both used for situations where close proximity to an obstacle is causing a dangerous situation. Together with 3 normal control modes, they are used in a proposed control system that completes the objective of the thesis.

The modes are managed automatically by a novel mode supervisor. This function takes in relevant measurements and data from other parts of the system to determine which mode to operate in. For nominal operation, this is done based on the distance to the origin and destination. In the case where an MRC needs to be used, the mode supervisor utilizes an indicator function that quantifies an estimate of the risk associated with an action. Two such indicator functions are proposed; one that is based on dynamical constraints of the vessel and one that is based on a risk function. The first compares the maneuver that is necessary to avoid the obstacle with the max capability of the vessel and chooses the one that is most probable to be successful. The second uses a risk function based on a CBF-formulation that quantifies the risk directly based on the position and velocity of vessel and obstacle. The maneuver chosen is then the one that reduces the risk the most.

Both NCMs and MRCs are detailed into guidance- and control functions. Here, the design follows that of other similar applications. The undocking and crossing phases use a two-parameter guidance method that includes the use of a CBF to avoid obstacles. In the docking phase, path planning is done by placing waypoints in such a fashion that the vessel approaches the dock with a heading normal to the dock. This is combined with a hybrid path parametrization to generate the desired position. In all 3 NCMs, a cascaded backstepping controller is used. In MRC-modes, PID controllers are used. A guidance function is only needed for one of the MRCs - the evasive maneuver. This guidance function provides a heading reference that takes the vessel into a hard turn to either port or starboard.

To test and show the performance of the system, 6 simulations were performed. The tests uncovered both strengths and weaknesses of the system. The indicator function based on dynamical constraints performed worse than the one based on a risk function, which performed well in all situations that were tested. However, more testing is necessary before such a system can be deemed safe. Also, the system must be tested without the simplifications done in this thesis. In general, the system showed satisfactory performance in the simulations, but areas of improvement were also identified that can make the system better and more suited for real-world applications.

11.1 Further work

This thesis shows that designing a control system for an autonomous passenger ferry including risk contingencies is not a small task. Adding the constraint on time faced while working with a master thesis, the result is that there are several things to be improved upon to make the proposed solution better. Therefore, this section will shed light on some of the most important factors that should be focused on if this line of research is to be continued in the future.

In this thesis, only two MRCs are formulated into detailed guidance- and control functions. For a more general and realistic autonomous system, other MRCs must also be detailed and tested together with the mode supervisor. The set of relevant MRCs for the operation of an autonomous passenger ferry is given in Section 3.2. Some of the MRCs are quite different than the ones considered here. This means that other components than just the motion control and SA system must be considered when implementing these modes. Examples are anchors, fault detection functionality, and fire suppression system. The diversity of the conditions also mean that the mode supervisor must consider more information than what is considered here. Additionally, no switching to MRC is done in the docking phase with the current implementation. This was not done due to time constraints. On that subject, it is possible to take inspiration from Gauslaa (2020), which has implemented some situational reactiveness based on jumps in the measurements from distance sensors in phase 2 of docking.

The other aspect of the automatic control system is the nominal control modes. As highlighted in the discussion, there is room for improvement here. This mainly has to do with tuning the guidance- and control functions and the interaction between them. Then, one can aim for a system with better tracking performance and smoother transition. However, this is not unique to this application and it should be possible to take advantage of work done by others in the field. Here, COLREG compliance should eventually be a goal.

A central part of the theme treated in this thesis is obstacles. However, the obstacles used have been restricted to stationary obstacles with a set size of the obstacle region. In reality, many obstacles are of course moving. This can be other boats, persons, kayaks, or debris adrift in the water. Therefore, for a system ready for real life, obstacles that move must be accounted for. Also, to have more efficiency and robustness in the COLAV system, it would be beneficial to have the obstacle regions be dynamic and based on the size and velocity of the obstacle. For small obstacles, this would lead to smaller regions, giving the vessel more room to move and require less of a deviation from the nominal path. For bigger obstacles, it would make the system safer by ensuring that the entire obstacle is included in the critical region. In connection to this, it would be natural to explore the possibility of changing the obstacle regions to ellipses or other shapes, as proposed in Section 5.4.

The simulations presented here can hardly be called thorough testing. Therefore, if more research is done on this subject, it will be important to do proper testing of the system. Here, efforts must be made to ensure that as many different scenarios as possible are tested, to best simulate real life. As the regulations are now, this will be crucial to be able to realize a system like this. While doing this, a lot of the simplifications done in this thesis must be removed. For example, environmental forces must be accounted for in the simulation, and thruster dynamics must be included in the model.

To summarize, further work should focus on increasing the scenarios covered by the MRCs in the system, improve performance and expand the complexity of the situations that the system is able to handle autonomously. This will result in a bigger and more complex integrated system, likely with more control and guidance modes. To achieve assurance of the system, testing is also important and must be done in a way that proves that the technical safety is on a sufficient level for the operational domain of the system.

Bibliography

Ames, A.D., Coogan, S., Egerstedt, M., Notomista, G., Sreenath, K., Tabuada, P., 2019. Control barrier functions: Theory and applications. 2019 18th European Control Conference, ECC 2019 , 3420–3431doi:10.23919/ECC.2019.8796030, arXiv:1903.11199.

Austin, C., 2020. Norwegian ferry completes world's first fully automatic journey. URL: https://safetyatsea.net/news/2020/norwegian-ferry-completes-worlds-first-fully-automatic-journey/.

Bennett, S., 1996. A brief history of automatic control. IEEE Control Systems Magazine 16, 17–25. doi:10.1109/37.506394.

Bitar, G., Martinsen, A.B., Lekkas, A.M., Breivik, M., 2020. Trajectory planning and control for automatic docking of asvs with full-scale experiments. IFAC ArXiv:2004.07793.

Blanke, M., Kinnaert, M., Lunze, J., Staroswiecki, M., 2016. Diagnosis and Fault-Tolerant Control, Third edition. Springer.

Blanke, M., Nguyen, D.T., 2018. Fault tolerant position-mooring control for offshore vessels. Ocean Engineering 148, 426–441. URL: https://www.sciencedirect.com/science/article/pii/S0029801817307114, doi:https://doi.org/10.1016/j.oceaneng.2017.11.042.

DNV-GL, 2018. Class guideline: Autonomous and remotely operated ships. URL: https://rules.dnvgl.com/docs/pdf/DNVGL/CG/2018-09/DNVGL-CG-0264.pdf.

Dubins, L.E., 1957. On curves of minimal length with a constraint on average curvature, and with prescribed initial and terminal positions and tangents. American Journal of Mathematics 79, 497–516. URL: http://www.jstor.org/stable/2372560.

Fleischer, C., 2020. Optimal Path-Planning on a Bio-Inspired Neural Network Guidance Model for Autonomous Surface Vessels. Master's thesis. Norwegian University of Science and Technology. Trondheim.

Formela, K., Gil, M., Śniegocki, H., 2015. Comparison of the efficiency of williamson and anderson turn manoeuvre. TransNav, the International Journal on Marine Navigation and Safety of Sea Transportation 9, 565–569. doi:10.12716/1001.09.04.14.

Fossen, T., 2021. Marine craft hydrodynamics and motion control, DRAFT MANUSCRIPT. John Wiley & Sons.

Gauslaa, E., 2020. Navigation, guidance, and control for autonomous docking of ships. Master's thesis. Norwegian University of Science and Technology. Trondheim.

IMO, 1972. COLREG: Convention on the International Regulations for Preventing Collisions at Sea. IMO.

IMO, 2002. Explanatory notes to the standards for ship manoeuvrability.

IMO, 2019. Msc.1/circ.1604: Interim guidelines for mass trials.

IMO, 2020. Autonomous shipping. URL: http://www.imo.org/en/MediaCentre/HotTopics/Pages/Autonomous-shipping.aspx.

Jensen, J.S., 2020. Reactive path-planning for autonomous harbor maneuvering. Master's thesis. Norwegian University of Science and Technology. Trondheim.

Knædal, M., 2020. Autonomous Path Planning and Maneuvering of a Surface Vessel. Master's thesis. Norwegian University of Science and Technology. Trondheim.

Koushan, K., 2017. Lecture notes: TMR4220 Naval Hydrodynamics. Department of Marine Technology, NTNU.

Lekkas, A.M., 2014. Guidance and Path-Planning Systems for Autonomous Vehicles. Ph.D. thesis. Norwegian University of Science and Technology. Trondheim.

Marley, M., 2021. Technical note Maneuvering control design using two path variables Revision B .

Marley, M., Skjetne, R., Breivik, M., Fleischer, C., 2020. A hybrid kinematic controller for resilient obstacle avoidance of autonomous ships. IOP Conference Series: Materials Science and Engineering 929. doi:10.1088/1757-899X/929/1/012022.

Marley, M., Skjetne, R., Teel, A.R., 2021. Synergistic control barrier functions with application to obstacle avoidance for nonholonomic vehicles, in: American Control Conference (ACC), New Orleans, USA. pp. 242–248.

Moen, J.M., 2020. Prestudy on autonomous control system for passenger ferry. Specialisation project. Master's thesis. Norwegian University of Science and Technology. Trondheim.

Murdoch, E., Dand, I.W., Clarke, C., 2012. A Master's Guide to Berthing, 2nd edn,. London: Standard House.

Nguyen, T.D., Sørensen, A.J., Tong Quek, S., 2007. Design of hybrid controller for dynamic positioning from calm to extreme sea conditions. Automatica 43, 768–785. URL: https://www.sciencedirect.com/science/article/pii/S0005109807000301, doi:https://doi.org/10.1016/j.automatica.2006.11.017.

NHTSA, N.D. Automated driving systems 2.0: a vision for safety. URL: https://www.nhtsa.gov/sites/nhtsa.dot.gov/files/documents/13069a-ads2.0_090617_v9a_tag.pdf.

Norwegian Maritime Authority, 2020. Føringer i forbindelse med bygging eller installering av automatisert funksjonalitet, med hensikt å kunne utføre ubemannet eller delvis ubemannet drift. URL: https://www.sdir.no/sjofart/regelverk/rundskriv/foringer-i-forbindelse-med-bygging-eller-installering-av-automatisert-funksjonalitet-med-hensikt-a-kunne-utfore-ubemannet-eller-delvis-ubemannet-drift2/.

Nowicki, J., 2014. Stopping of Ships Equipped with Azipods. TransNav, the International Journal on Marine Navigation and Safety of Sea Transportation 8, 373–376. doi:10.12716/1001.08.03.07.

NTNU, N.D. Autoferry. URL: https://www.ntnu.edu/autoferry.

Park, J.y., Oh, P., Kim, T., Lee, J.h., 2020. Study on Stopping Ability of a Ship Equipped with Azimuth Propeller. Journal of Ocean Engineering and Technology 34, 13–18.

Paulsen, G., 2019. Alltid rabiat - Jens Glad Balchen og den kybernetiske tenkemåten. Fagbokforlaget. p. 252.

Pedersen, A.A., 2019. Optimization Based System Identification for the milliAmpere Ferry. Master's thesis. Norwegian University of Science and Technology. Trondheim.

Porathe, T., 2019. Safety of autonomous shipping: Colregs and interaction between manned and unmanned ships, in: Proceedings of the 29th European Safety and Reliability Conference, Hannover, Germany.

Reilly, C., 2020. Hidden Markov Models. Statistics in Human Genetics and Molecular Biology , 151–162doi:10.1201/b16380-13.

Rødseth, Ø.J., 2018. Defining ship autonomy by characteristic factors. Proceedings of the 1st International Conference on Maritime Autonomous Surface Ships , 19–26.

Skjetne, R., 2005. The Maneuvering Problem. Ph.D. thesis. Norwegian University of Science and Technology. Trondheim.

Skjetne, R., 2020a. Notes on: Guidance and maneuvering design for docking Revision A (Draft). NTNU.

Skjetne, R., 2020b. Technical note: Maneuvering-based guidance design for dynamic positioning Revision B (Draft), NTNU. NTNU.

Skjetne, R., 2020c. Technical note: Maneuvering control design of a low-speed fully actuated vessel with stepwise path generation Revision E, NTNU. NTNU.

SNAME, 1950. Nomenclature for Treating the Motion of a Submerged Body Through a Fluid. Technical and Research Bulletin No.1-5. .

Sæther, B., 2019. Development and Testing of Navigation and Motion Control Systems for milliAmpere. Master's thesis. Norwegian University of Science and Technology. Trondheim.

Thyri, E.H., 2019. A Path-Velocity Decomposition Approach to Collision Avoidance for Autonomous Passenger Ferries. Master's thesis. Norwegian University of Science and Technology. Trondheim.

Thyri, E.H., Basso, E.A., Breivik, M., Pettersen, K.Y., Skjetne, R., Lekkas, A.M., 2020. Reactive collision avoidance for ASVs based on control barrier functions. CCTA 2020 - 4th IEEE Conference on Control Technology and Applications , 380–387doi:10.1109/CCTA41146.2020.9206340.

Torben, T.R., Brodtkorb, A.H., Sørensen, A.J., 2019. Control allocation for double-ended ferries with full-scale experimental results. IFAC PapersOnLine 52, 45–50.

Utne, I., Sørensen, A., Schjølberg, I., 2017. Risk management of autonomous marine systems and operations, in: Proceedings of the 36th International Conference on Ocean, Offshore & Arctic Engineering, Trondheim, Norway.

Wärtsilä, 2018. Look, ma, no hands! auto-docking ferry successfully tested in norway. URL: https://www.wartsila.com/insights/article/look-ma-no-hands-auto-docking-ferry-successfully-tested-in-norway.

Yang, H., Jiang, B., Cocquempot, V., Lu, L., 2012. Supervisory fault tolerant control with integrated fault detection and isolation: A switched system approach. International Journal of Applied Mathematics and Computer Science 22, 87–97. doi:10.2478/v10006-012-0006-9.

Zang, S., Ding, M., Smith, D., Tyler, P., Rakotoarivelo, T., Kaafar, M.A., 2019. The impact of adverse weather conditions on autonomous vehicles: How rain, snow, fog, and hail affect the performance of a self-driving car. IEEE Vehicular Technology Magazine 14, 103–111. doi:10.1109/MVT.2019.2892497.

Zeabuz, 2020. Fully autonomus test of milliampere. URL: https://www.linkedin.com/posts/zeabuz_autonomous-ferry-operation-test-with-milliampere-activity-6762998437114859520-00ux.

Zeabuz, N.D.a. Home - zeabuz. URL: https://zeabuz.com/.

Zeabuz, N.D.b. milliampere - zeabuz. URL: https://zeabuz.com/miliampere/.

Åsheim, N., 2021. Collision Avoidance. Master's thesis. Norwegian University of Science and Technology. Trondheim.

Appendix A

MATLAB-files

A.1 Supervisor function

```
function [mode, WP_out] = supervisor(dock_pos, init_pos, mode, ...
    eta, nu, COLAV_index, alpha_d, p_o, indicator)
% Supervisor function to determine operation mode
% Takes in all data available and decides on mode based on an indicator
% function.

persistent flag WP
d_undock = 10;  %distance from start dock to first WP
d_dock =15;     %distance from target dock to start docking  from crossing
d_dock_direct = 25; % distance to go directly to docking from undocking

u = nu(1);


%% Calculate transit waypoints
if isempty(flag)
    WP = zeros(2,3);
    WP(:,1) = init_pos;
    L = norm(dock_pos - init_pos);
    T = (dock_pos - init_pos)/L;
    WP(:,2) = init_pos + d_undock*T;
    WP(:,3) = dock_pos - d_dock*T;
    flag = 1;
end


%% Determine mode, different depending on current mode
% squared distance to origin and target dock
d2_init = (eta(1)-init_pos(1))^2 + (eta(2)-init_pos(2))^2;
d2_target = (eta(1)-dock_pos(1))^2 + (eta(2)-dock_pos(2))^2;

```

```
if mode == 1    % undocking
    if COLAV_index ~= 0
        mode = 4;   % only crash stop available in undocking phase
    elseif d2_init > d_undock^2 && d2_target > d_dock_direct^2
        %switch to crossing
        mode = 2;
        clear guidance_CBF
        if norm(eta(1:2) - WP(:,2)) > 0.2
            WP(:,2) = eta(1:2);
        end
    elseif d2_init > d_undock^2 && d2_target < d_dock_direct^2
        mode = 3;
    end
elseif mode == 2    % crossing
    if  COLAV_index == -1     % distance from p_d too large
        mode = 4;
    elseif COLAV_index ~= 0    % COLAV failed
        if indicator == 0
            mode = collision_indicator(eta, nu, alpha_d, ...
                p_o(:,COLAV_index));  %dynamic constraints
        else
            mode = collision_indicator2(eta, nu, p_o);          %RIF
        end
    elseif d2_target < d_dock^2
        mode = 3;
    end
elseif mode == 3    % docking

elseif mode == 4    % crash stop
    if u < 0.1
        mode = 7;
    end
elseif mode == 5 || mode == 6   % evasive maneuver
    if u < 0.1
        mode = 7;
    end
end

WP_out = WP;

end
```

A.2 Vessel dynamics

```
function dxdt = milliAmpere_vessel_dynamics_surge_decopuled_no_thrusters(t,x)
% x is a vector of vessel states;
% x(1:3,1) are the body velocities (nu) : [surge, sway, yaw_rate]'
% x(4:6,1) are the position/pose (eta) : [north, east, heading]'
```

```
% x(7:9,1) are are the forces acting on the vessel: [X,Y,N]'
dxdt = zeros(9,1);
% nu_dynamics, dxdt(1:3,1)
[M,C,D] = comp_matrices_surge_decoupled_mod(x(1:3,1));
dxdt(1:3,1) = M\(x(7:9,1) - (C+D)*x(1:3,1));

% eta_dynamics dxdt(4:6,1);
dxdt(4:6,1) = [cos(x(6,1)),-sin(x(6,1)), 0;...
               sin(x(6,1)), cos(x(6,1)), 0;...
               0          , 0          , 1]*x(1:3,1);
end
```

A.3 Simulator script

```
for i=2:iteration
    %% Supervisor function
    [mode, WP] = supervisor(eta_dock(1:2), eta_0(1:2), mode, x(4:6,i-1), ...
    x(1:3, i-1), COLAV_index, alpha_d, p_o, indicator);

     %% Change parameters for simulation
    [mode, p_o] = change_params(sim, mode, p_o, i);

    %% Guidance
    if mode == 1        % undocking
        WP = WP(:,1:2); % undocking waypoints
        [eta_d, v, pd_s, pd_ss, COLAV_index, alpha_d] = guidance_CBF(WP, h, ...
        p_o, 1, x(4:6, i-1), x(1:3,i-1));
    elseif mode == 2    % crossing
        WP = WP(:,2:3); % crossing waypoints
        [eta_d, v, pd_s, pd_ss, COLAV_index, alpha_d] = guidance_CBF(WP, h, ...
        p_o, 2, x(4:6, i-1), x(1:3,i-1));
    elseif mode == 3    % docking
        if isempty(dWP)
            dWP = docking_wps(x(4:6,i-1), eta_dock, p);
        end
        [~, ~, d1_pos, d2_pos, d1, d2] = distance_sensors(2.4, 2.4, 0.7, ...
        -0.7, eta_dock, x(4:6,i-1));
        [eta_d, v, pd_s, pd_ss] = dock_guidance(dWP, h, d1, d2, d_const);
    elseif mode == 5   % evasive maneuver starboard
        [psi_d, r_d, u_d, ud_dot] = guidance_turning_circle(x(4:6, i-1), ...
        x(1:3,i-1), h, p_o(:, COLAV_index), 1);
    elseif mode == 6   % evasive maneuver port
        [psi_d, r_d, u_d, ud_dot] = guidance_turning_circle(x(4:6, i-1), ...
        x(1:3,i-1), h, p_o(:, COLAV_index), -1);
    elseif mode == 7
        if DP_flag == 0
            eta_d = x(4:6, i-1); % set desired DP position
            DP_flag = 1;
```

```
        end
    end

    %% Control
    if mode == 4 % crash stop
        if cs_flag == 0
            psi_d = x(6, i-1) + atan(x(2,i-1)/ x(1,i-1));
            %atan2(x(2,i-1), x(1,i-1));
            % set desired heading to course angle when entering crash stop
            cs_flag = 1;
            start_time = i;
        end
        x(7:9,i-1) = crash_stop_control(x(1:3,i-1), x(4:6, i-1), psi_d, ...
        hc_const);
    elseif mode == 5 || mode == 6 % evasive maneuver
        x(7:9,i-1) = heading_control(x(4:6,i-1), x(1:3,i-1), psi_d, r_d, u_d, ..
        ud_dot, hc_const);
    elseif mode == 7 % DP
        x(7:9,i-1) = backstepping(x(4:6,i-1), x(1:3,i-1), eta_d, [0, 0]', ...
        zeros(2,2), zeros(2,2), c_const);
    else % nominal control
        x(7:9,i-1) = backstepping(x(4:6,i-1), x(1:3,i-1), eta_d, v, pd_s, ...
        pd_ss, c_const);
    end

    %% Vessel dynamics
    [t, x_out] = ode45(@milliAmpere_vessel_dynamics_surge_decopuled_no_thrusters
    [0,h],x(1:9,i-1));
    x(1:9,i) = x_out(end,:)';

    %% Write to desired position
    if mode == 5 || mode == 6 % evasive manuever - only desired heading
        x(12, i) = psi_d;
        ud(i) = u_d;
    elseif mode == 4          % crash stop - p_d = p_d_last
        x(10:11, i) = x(10:11, i-1);
        x(12, i) = psi_d;
    else                      % nominal control and DP.
        x(10:12, i) = eta_d;
        % too far from p_d, enter MRC. Not used.
%         if norm(eta_d(1:2) - x(4:5, i)) > d_safe
%             COLAV_index = -1;
%         end
    end

end
```

Appendix B

Hybrid path parametrization

The docking path is computed from a set of WPs. For the generation of a path, a hybrid path parametrization as presented in Skjetne (2005) is used. The explanation that follows is based on the presentation of hybrid path parametrization in Gauslaa (2020). The method constructs a number of path segments that have order k. Each path segment goes between two WPs, and they are concatenated at each WP in a way such that the overall path is continuous and sufficiently differentiable.

B.1 A $\mathcal{C}^r$ path generated from waypoints

The desired path $\mathbf{p}_d(s)$ is divided into subpaths between waypoints, which are polynomials as a function of s, of a chosen order k. Call the polynomials $p_{d,i}$, with $i = 1, 2, \ldots, N$. To ensure that each subpath is connected with $\mathcal{C}^r$ continuity, the following must be true:

$$\begin{array}{ll} \lim_{s\nearrow i-1} x_{d,i-1}(s) = \lim_{s\searrow i-1} x_{d,i}(s), & \lim_{s\nearrow i-1} y_{d,i-1}(s) = \lim_{s\searrow i-1} y_{d,i}(s), \\ \lim_{s\nearrow i-1} x^s_{d,i-1}(s) = \lim_{s\searrow i-1} x^s_{d,i}(s), & \lim_{s\nearrow i-1} y^s_{d,i-1}(s) = \lim_{s\searrow i-1} y^s_{d,i}(s), \\ \vdots & \vdots \\ \lim_{s^i-1} x^{r^r}_{d,i-1}(s) = \lim_{s\searrow i-1} x^{s^r}_{d,i}(s), & \lim_{s\nearrow i-1} y^{s^r}_{d,i-1}(s) = \lim_{s\searrow i-1} y^{s^r}_{d,i}(s), \end{array} \tag{B.1}$$

for $i \in \mathcal{I} \setminus \{1\}$. The subpaths are given by polynomials order k:

$$x_{d,i}(s) = a_{k,i}s^k + \ldots + a_{1,i}s + a_{0,i}, \tag{B.2a}$$

$$y_{d,i}(s) = b_{k,i}s^k + \ldots + b_{1,i}s + b_{0,i}, \tag{B.2b}$$

where the coefficients $\{a_{i,j}, b_{i,j}\}$ are found by solving a set of linear equations. In total, there are $(k + 1)2n$ coefficients to find. The coefficients can be found for each subpath independently. To ensure continuity at the WPs, numerical values for neighboring subpaths must be assigned. This is done by hybrid parametrization, as presented in Skjetne (2005).

B.2 Hybrid parametrization of a $\mathcal{C}^r$ path

Each subpath is parametrized in an interval $\theta = s - \lfloor s \rfloor \in [0, 1)$. A subpath is identified by the index $i = \lfloor s \rfloor + 1$. The floor operator $\lfloor s \rfloor$ rounds s down to the nearest integer. The coefficients for each

subpath are calculated according the linear equations given by the following criteria:

$\mathcal{C}^0$: continuity at the waypoints for $i \in \mathcal{I}$:

$$\begin{array}{ll} x_{d,i}(0) = x_i, & y_{d,i}(0) = y_i \\ x_{d,i}(1) = x_{i+1}, & y_{d,i}(1) = y_{i+1}. \end{array} \tag{B.3}$$

$\mathcal{C}^1$: the slopes at the first and last waypoints are chosen to be:

$$\begin{array}{ll} x^{\theta}_{d,1}(0) = x_2 - x_1, & y^{\theta}_{d,1}(0) = y_2 - y_1, \\ x^{\theta}_{d,n}(1) = x_{n+1} - x_n, & y^{\theta}_{d,n}(1) = y_{n+1} - y_n. \end{array} \tag{B.4}$$

The slopes at the intermediate waypoints are given by:

$$\left.\begin{array}{ll} x^{\theta}_{d,1}(0) & = \lambda\left(x_{i+1} - x_{i-1}\right) \\ y^{\theta}_{d,1}(0) & = \lambda\left(y_{i+1} - y_{i-1}\right) \end{array}\right\} \quad i = 2, \ldots, n \tag{B.5a}$$

$$\left.\begin{array}{ll} x^{\theta}_{d,1}(1) & = \lambda\left(x_{i+2} - x_i\right) \\ y^{\theta}_{d,1}(1) & = \lambda\left(y_{i+2} - y_i\right) \end{array}\right\} \quad i = 1, \ldots, n-1 \tag{B.5b}$$

where λ is a design constant that affects how the slope is at the waypoints.

$\mathcal{C}^j$: setting derivatives of order $j \geq 2$ to zero:

$$\begin{array}{ll} x^{\theta^j}_{d,i}(0) = 0, & y^{\theta^j}_{d,i}(0) = 0, \\ x^{\theta^j}_{d,i}(1) = 0, & y^{\theta^j}_{d,i}(1) = 0. \end{array} \tag{B.6}$$

To compute the desired heading, the path tangential vector is needed. This gives a differtiability requirement of $\mathcal{C}^3$. This, in turn, require that the polynmoials are of order $k = 7$. The result is hybrid path parametrization where each subpath i is parametrized by θ, such that

$$\overline{\mathbf{p}}_d(i, \theta) = \left[\begin{array}{c} x_{d,i}(\theta) \\ y_{d,i}(\theta) \end{array}\right] \tag{B.7}$$

where $i \in \mathcal{I}$ and $\theta \in [0, 1)$. The desired $\mathcal{C}^r$ map is then a continious parametrization by s (Skjetne, 2005):

$$s \mapsto \mathbf{p}_d(s) := \overline{\mathbf{p}}_{\mathbf{d}}(i(s), \theta(s)). \tag{B.8}$$

Appendix C

Hydrodynamic parameters

Table C.1: Hydrodynamic parameters for MilliAmpere, identified by Pedersen (2019)

Parameter	Estimated Value	Unit
m_{11}	2389.657	kg
m_{22}	2533.911	kg
m_{23}	62.386	kg
m_{32}	28.141	kg
m_{33}	5068.910	$\mathrm{kg\,m^2}$
X_u	-27.632	$\mathrm{kg\,s^{-1}}$
$X_{\|u\|u}$	-110.064	$\mathrm{kg\,s^{-1}}$
X_{uuu}	-13.965	$\mathrm{kg\,s^{-1}}$
Y_v	-52.947	$\mathrm{kg\,s^{-1}}$
$Y_{\|v\|v}$	-116.486	$\mathrm{kg\,s^{-1}}$
Y_{vvv}	-24.313	$\mathrm{kg\,s^{-1}}$
$Y_{\|r\|v}$	-1540.383	$\mathrm{kg\,s^{-1}}$
Y_r	24.732	$\mathrm{kg\,s^{-1}}$
$Y_{\|v\|r}$	572.141	$\mathrm{kg\,s^{-1}}$
$Y_{\|r\|r}$	-115.457	$\mathrm{kg\,s^{-1}}$
N_v	3.524	$\mathrm{kg\,s^{-1}}$
$N_{\|v\|v}$	-0.832	$\mathrm{kg\,s^{-1}}$
$N_{\|r\|v}$	336.827	$\mathrm{kg\,s^{-1}}$
N_r	-122.860	$\mathrm{kg\,s^{-1}}$
$N_{\|r\|r}$	-874.428	$\mathrm{kg\,s^{-1}}$
N_{rrr}	0.000	$\mathrm{kg\,s^{-1}}$
$N_{\|v\|r}$	-121.957	$\mathrm{kg\,s^{-1}}$

Appendix D

Simulation data

D.1 Simulation 3

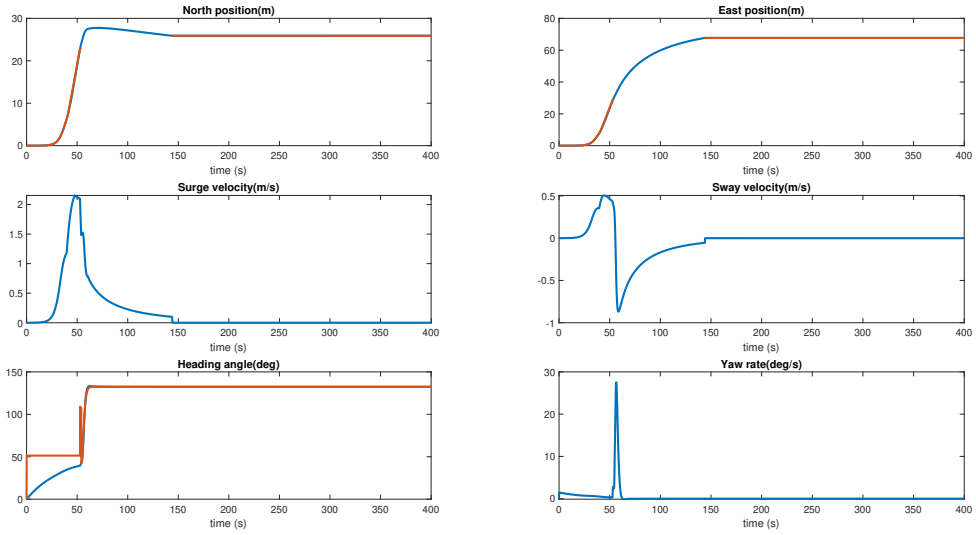

Figure D.1: Timeseries data for evasive maneuver towards port from simulation 3

D.2 Simulation 6

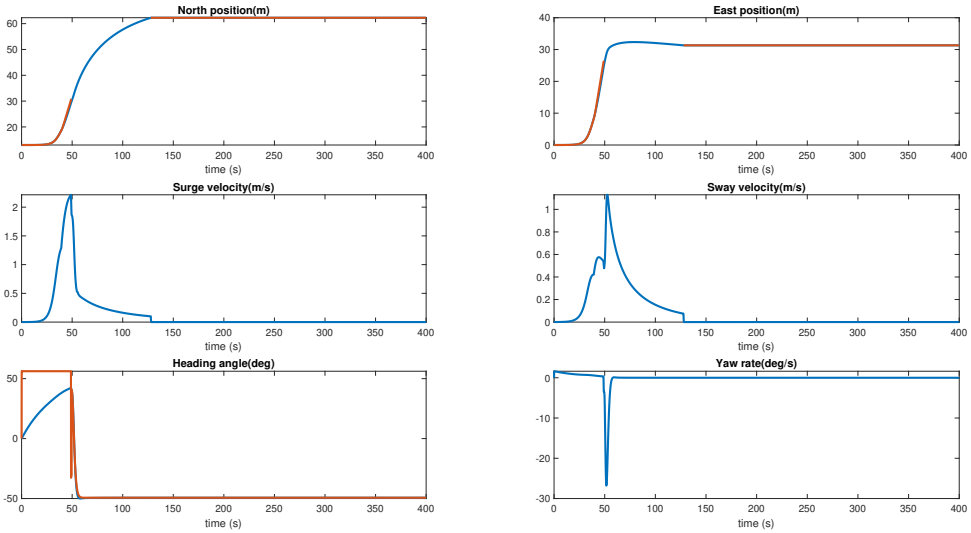

Figure D.2: Timeseries data for evasive maneuver towards starboard from simulation 3

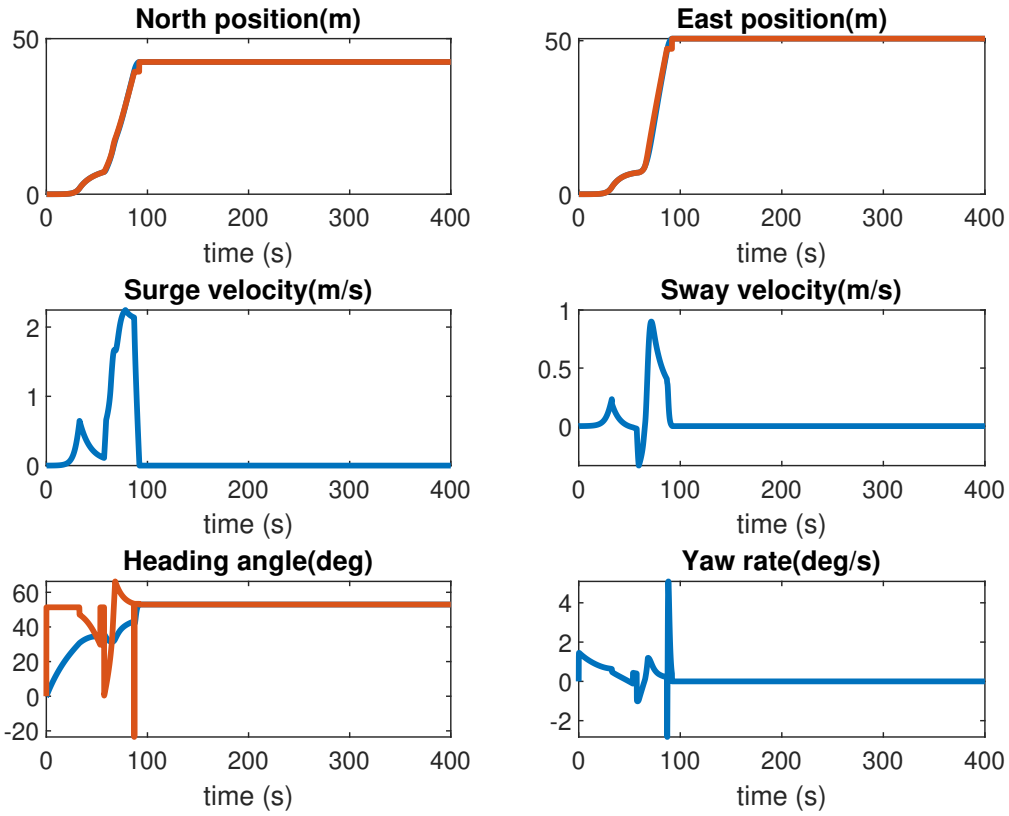

Figure D.3: Timeseries data for simulation 6 with 3 obstacles

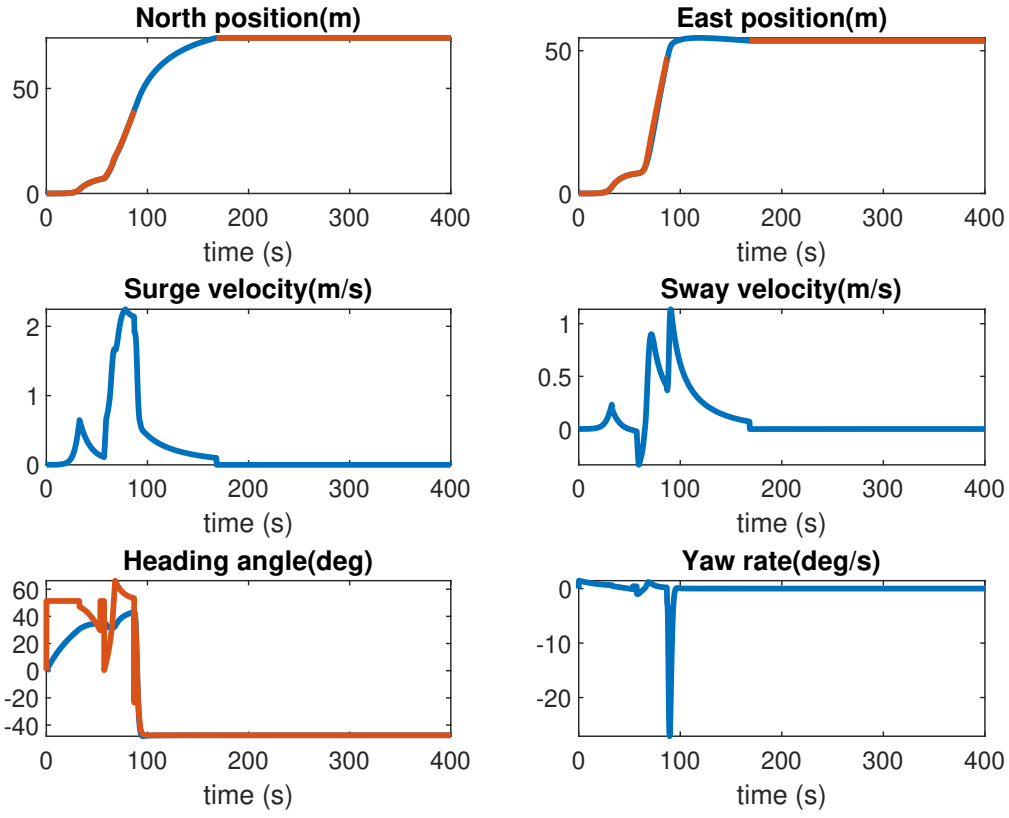

Figure D.4: Timeseries data for simulation 6 with 2 obstacles

NTNU

Norwegian University of
Science and Technology